Structural Engineering Report No. 110

SHEAR STRENGTH OF DEEP REINFORCED CONCRETE CONTINUOUS BEAMS

by

D. M. ROGOWSKY

J. G. MacGREGOR

November, 1983

RECENT STRUCTURAL ENGINEERING REPORTS

Department of Civil Engineering

University of Alberta

80. *Leakage Tests of Wall Segments of Reactor Containments* by S.K. Rizkalla, S.H. Simmonds and J.G. MacGregor, October 1979.

81. *Tests of Wall Segments from Reactor Containments* by S.H. Simmonds, S.K. Rizkalla and J.G. MacGregor, October 1979.

82. *Cracking of Reinforced and Prestressed Concrete Wall Segments* by J.G. MacGregor, S.K. Rizkalla and S.H. Simmonds, October 1979.

83. *Inelastic Behavior of Multistory Steel Frames* by M. El Zanaty, D.W. Murray and R. Bjorhovde, April 1980.

84. *Finite Element Programs for Frame Analysis* by M. El Zanaty and D.W. Murray, April 1980.

85. *Test of a Prestressed Concrete Secondary Containment Structure* by J.G. MacGregor, S.H. Simmonds and S.H. Rizkalla, April 1980.

86. *An Inelastic Analysis of the Gentilly-2 Secondary Containment Structure* by D.W. Murray, C. Wong, S.H. Simmonds and J.G. MacGregor, April 1980.

87. *Nonlinear Analysis of Axisymmetric Reinforced Concrete Structures* by A.A. Elwi and D.W. Murray, May 1980.

88. *Behavior of Prestressed Concrete Containment Structures - A Summary of Findings* by J.G. MacGregor, D.W. Murray, S.H. Simmonds, April 1980.

89. *Deflection of Composite Beams at Service Load* by L. Samantaraya and J. Longworth, June 1980.

90. *Analysis and Design of Stub-Girders* by T.J.E. Zimmerman and R. Bjorhovde, August 1980.

91. *An Investigation of Reinforced Concrete Block Masonry Columns* by G.R. Sturgeon, J. Longworth and J. Warwaruk, September 1980.

92. *An Investigation of Concrete Masonry Wall and Concrete Slab Interaction* by R.M. Pacholok, J. Warwaruk and J. Longworth, October 1980.

93. *FEPARCS5 - A Finite Element Program for the Analysis of Axisymmetric Reinforced Concrete Structures - Users Manual* by A. Elwi and D.W. Murray, November 1980.

Structural Engineering Report No. 110

SHEAR STRENGTH OF DEEP REINFORCED CONCRETE CONTINUOUS BEAMS

by

David M. Rogowsky

and

James G. MacGregor

Department of Civil Engineering
University of Alberta
Edmonton, Alberta
Canada T6G 2G7

November 1983

ABSTRACT

The objective of this research was to develop behavior models for the design of deep reinforced concrete beams with particular reference to shear in continuous beams. A series of beam tests was performed to aid in the development of this objective.

The experimental program consisted of 6 simple span beams and 17 two span continuous beams, each span being 2 m in length. The shear span to depth ratios ranged from 1 to 2.5. Various arrangements and amounts of web reinforcement were used including: no web reinforcement, minimum and maximum horizontal web reinforcement, and minimum and maximum vertical web reinforcement. The beams were supported and loaded by columns cast monolithically with the beams. The loads were applied through columns to the top of the beams at midspan.

Measurements made during each test included applied loads and reactions, midspan deflections, and concrete and steel strains. The strains were measured over 2 to 5 inch gage lengths. Cracks were marked and photographed at each load step.

The beams generally failed in shear, exhibiting a wide range of behavior, ranging from very brittle to very ductile, depending on the amount and arrangement of the web reinforcement, and the shear span to depth ratio. Within the range of parameters tested, horizontal web reinforcement

was found to be ineffective. Vertical stirrups when used in sufficient numbers increased the beam strength and greatly improved the ductility. Beams with this amount of vertical web reinforcement (about ACI maximum stirrups) did not exhibit typical deep beam behavior in that they did not show an increase in shear strength with a decrease in shear span to depth ratio.

The test specimens behaved as "trusses" or "tied arches" after the formation of cracks. It was found that the plastic truss model gave good predictions of stresses as well as ultimate strength provided that appropriate models were used. The effective concrete strength was found to be less important than the current concrete plasticity literature suggests. The choice of an appropriate plastic truss was found to be very important, especially for the statically indeterminate beams where several different plastic trusses are plausible.

Design recommendations based on plastic truss models of behavior are presented for simply supported and continuous deep beams.

ACKNOWLEDGEMENTS

I am indebted to Professor J.G. MacGregor for his guidance and patience throughout this project.

The assistance and cooperation of the many staff of the I.F. Morrison Laboratory, University of Alberta, in conducting the experimental program is gratefully acknowledged. I would like to particularly thank: L. Burden and R. Helfrich for their skill and craftsmanship in fabricating and testing the specimens, D. Barth, J. Monney, and V.J. Parmar for their assistance in various stages of testing and data reduction.

I am indebted to A. Dunbar and T. Casey for their help in programming and operating various computing systems and programs.

My thanks are extended to Professor P. Marti at the University of Toronto for his tutoring on the subject of plasticity.

My appreciation is extended to Ms. N. Shaw for typing this text.

This study was made possible by Grant A1673 from the Natural Science and Engineering Research Council of Canada.

Finally, I am very grateful to my wife for her continued support and encouragement. This project could not have been completed without her forbearance and understanding during the long and sometimes inconvenient hours required in the laboratory.

Table of Contents

List of Tables

List of Figures

List of Symbols

a shear span measured from face of support to centre of load, unless otherwise noted

b width of beam

d effective depth

f'_c concrete compressive strength

f^*_c effective concrete compressive strength

f_y yield strength of reinforcement

f^*_y effective yield strength of reinforcement

h overall beam depth

M bending moment at a section

T force in tension reinforcement

V shear at a section

ν concrete efficiency factor, f^*_c/f'_c

θ slope of inclined truss members, measured from the horizontal

ρ main steel ratio, A_s/bd

ρ_h ratio of horizontal web reinforcement area to gross concrete area of a vertical section

ρ_v ratio of vertical web reinforcement area to gross concrete area of a horizontal section

ϕ internal angle of friction

ϕ_c performance factor for concrete

ϕ_m performance factor for truss model

ϕ_s performance factor for steel

1. INTRODUCTION

1.1 Problem Statement

This work considers shear in deep reinforced concrete beams, with particular reference to continuous beams. Such members typically occur as transfer girders, pile caps and foundation walls, for example. A deep beam for the purposes of this thesis is defined as a directly loaded beam with a shear span to depth ratio, a/d, between 0.5 and 2.5.

A distinguishing feature of deep beams is that after the formation of inclined cracks, "tied arch" behavior may develop which in turn provides for considerable reserve "shear" capacity. Shallow beams, that is beams with a/d greater than about 2.5, do not develop significant arching behavior, and generally fail shortly after the formation of inclined cracking unless web reinforcement is provided. On the other hand, very deep beams with a/d less than about 0.5 fall into the category of brackets or corbels. They may not even develop inclined cracking and may fail with a sliding, or shear friction type of mechanism.

The deep beam can be considered as the transition between a slender beam and a bracket or corbel. Current concrete design codes, such as the American Concrete Institute (ACI) Building Code (ACI, 1977), do not provide for a smooth transition in shear capacity between slender beams and deep beams, and between deep beams and corbels. A second problem with current design procedures is that they

are empirically based on data from simple span beams. As a result, the ACI Code design equations "blow up" for continuous deep beams. When the critical section for shear is near the point of inflection, which it frequently is, the ACI design equations require division by zero.

1.2 Research Objectives

The general objective of this research was to develop design procedures for continuous deep beams. Specifically, however, the objective was to develop a rational physical model which would explain the ultimate strength behavior of deep beams. The physical model should:

1) adequately predict ultimate strength,
2) provide a smooth transition in capacity from slender beams through to corbels,
3) clearly explain the function of concrete, longitudinal and transverse steel,
4) account for different types of loading and support conditions,
5) provide a clear understanding of the "flow of forces" through the member,
6) result in correctly detailed reinforcement.

Once derived, such a model can form the basis of design rules.

1.3 Outline of Problem Solution

As with all research, the search for a solution started with a review of the existing literature on deep beams. This review is presented in Chapter 2. Its purpose was to identify pertinent experimental data, establish the prime variables and the range of interest for each variable, critically examine existing problem formulations with a view to identifying defects or "gaps" in the formulations, and to determine areas which require further experimentation. Each of the existing theories required calibration to test data in some form or another. This led to the development of an experimental program designed to provide the necessary data.

The experimental program is described in Chapter 3. The program consisted of 23 beams, simply supported and continuous, with various arrangements of web reinforcement and various shear span to depth ratios. The tests provided quantitative information on concrete strains, steel strains and load deflection behavior as well as qualitative behavioral observations.

Chapter 4 consists of an interpretation of the data and a synthesis of the problem in light of the data. This results in the development of a simple conceptual model of behavior.

The simple conceptual model is developed into a detailed computational model in Chapter 5. The model is calibrated against the available data and its limits of application are examined.

A calibrated, simplified, but rational design model is presented in Chapter 6. The model is an explicit plasticity model, and as such it is presented in a manner which is more or less compatible with design procedures currently being proposed for the Canadian concrete design code.

A summary of the proposed design provisions and significant observations and conclusions are presented in Chapter 7.

Design examples are given in Appendix B.

2. LITERATURE REVIEW

2.1 Introduction

The existing literature on deep beams was reviewed. First, general background, or overview papers were considered. Although these works do not present original findings they do attempt to collect and synthesize the data available at the time they were written. From these references, the important parameters which affect deep beams can be identified.

The next area examined was major research papers on deep beams. These papers present original experimental data along with empirical or semi-empirical analyses of the results. They represent the major works leading to the Canadian, American, British and European design recommendations, along with some papers which have not found their way into design codes yet. These works are examined to see how they consider or account for the important parameters which influence deep beam behavior.

The growing literature on plasticity in reinforced concrete was examined. While most of this literature does not deal specifically with deep beams, deep beams do fall within the scope of most plasticity methods. The various plasticity solutions are examined to see how they consider each of the important parameters which influence deep beam behavior.

2.2 General Background

The Joint ASCE-ACI Task Committee 426 "Shear and Diagonal Tension" (ACI-ASCE, 1973) produced a benchmark paper on shear in reinforced concrete members in 1973. The basic mechanisms of shear transfer in slender concrete beams were identified as:

V_s shear force transferred by stirrups

V_{cz} shear force transferred by the compression zone

V_d shear force transferred by dowel action of longitudinal steel

V_{ay} shear force transferred by aggregate interlock along the diagonal tension crack.

The total shear capacity V_T is given as:

$$V_T = V_s + V_{cz} + V_d + V_{ay} \tag{2.1}$$

It was recognized that in deep beams, arch action can provide an additional method for transmitting the loads to the supports. This is true provided that the reinforcement is detailed such that the beam can act as a tied arch. Five failure modes for deep beams were identified. These are illustrated in Fig. 2.1. The anchorage and bearing failures relate to inadequate detailing. Once adequate details are used, these premature failures will not develop, and the strength of the beam will then depend on the strength of the tension tie (flexural failure) or the strength of the concrete arch or strut (arch rib failure). Hence, the main

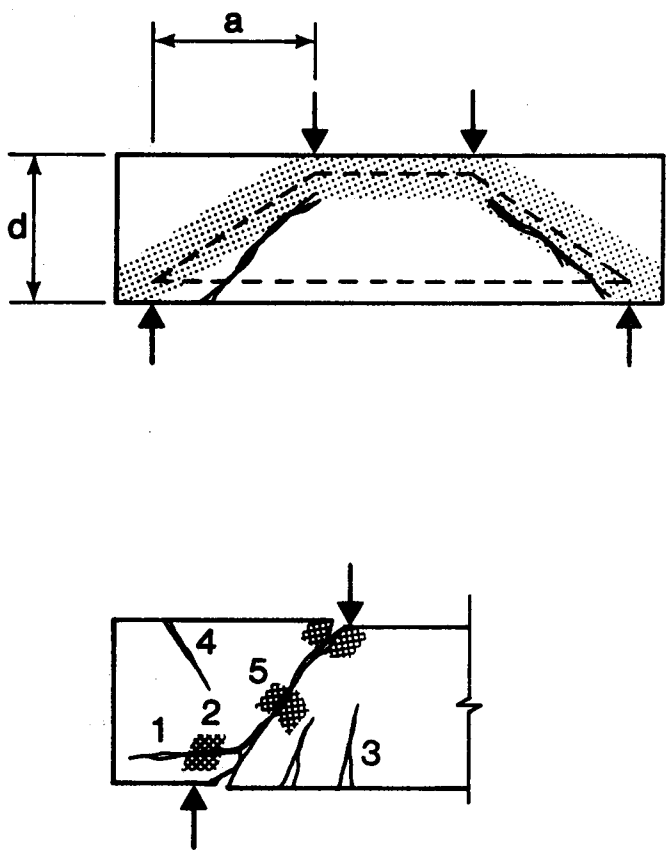

Type of Failure

1. Anchorage failure
2. Bearing failure
3. Flexural failure
4. & 5. Arch-rib failure

Figure 2.1. Modes of Failure of Deep Beams From ACI-ASCE, 1973

steel ratio ρ and the concrete strength f'_c are important variables which affect the behavior of deep beams.

The type of tied arch or truss which can form depends on the method of load application. For example, the beam shown in Fig. 2.1 would mobilize a different truss geometry if the point loads were moved closer to midspan. The slope of the inclined truss members, approximately equal to d/a, would change. A marked increase in shear capacity occurs in beams with a/d less than about 2.5. If the point loads were replaced with an equivalent uniformly distributed load, the truss or tied-arch geometry would be different again and the strength would change. If the loads were 'hung' from the bottom of the beam, it is not possible to visualize a truss or tied arch which would carry this type of loading unless large amounts of 'hanger' reinforcement are used to 'lift' the applied forces to the top of the beam. As a result, only beams with direct loading exhibit shear strength increases associated with deep beams. Hence the type of loading and a/d are important parameters which affect the behavior of deep beams.

It is worth noting that much of the literature considers M/Vd, the ratio of moment to the shear times the effective depth, to be a very important parameter. For simply supported, point loaded beams, M/Vd reduces to a/d since M = aV. Most of the data available on deep beams relates to such simply supported beams so that empirical correlations based on M/Vd can be rewritten with a/d as the

parameter. For uniformly loaded simply supported beams, M/Vd and a/d can be related but the relationship depends to a large extent on the definitions of M, V, a and d. The real difficulty with using M/Vd as a parameter occurs in continuous beams. In this case M/Vd is highly dependent on definitions and dimensions. Still worse, it no longer relates to the slope of the inclined members of the tied arch which develops after inclined cracking. As a result, a/d will be considered the prime parameter rather than M/Vd.

The type of shear reinforcement can have an effect on the shear capacity. Reinforcement may be vertical (perpendicular to the longitudinal axis of the beam) or horizontal (parallel to the longitudinal axis of the beam). As a beam becomes deeper or shorter, the inclined cracks become more vertical, and vertical stirrups become less effective while horizontal web reinforcement is believed to become more effective as shear friction reinforcement across the inclined crack. Inclined web reinforcement is a possibility but it usually is not practical due to placing difficulties. As a result, only vertical web reinforcement and horizontal web reinforcement will be considered in this review. This reinforcement may be dealt with quantitatively through the parameters ρ_v the ratio of vertical web reinforcement area to gross concrete area of a horizontal section, and ρ_h the ratio of horizontal web reinforcement area to gross concrete area of a vertical section.

The nature of the loading is an important issue if the loading causes reversals of shear. In the case of wind loading, reversals do occur, but the main requirement is that the member develop its design ultimate strength. Earthquake loading on the other hand requires several cycles of inelastic load reversal. The inclined cracks and the associated truss which develops must change as the direction of the loading changes. The extensive cross-inclined-cracking which develops raises doubts about the contribution of the concrete to the shear capacity of the member. Paulay (1969) has examined this problem, which is a question of ductility as well as strength. This thesis will deal with the development of the design ultimate strength under monotonic loading only, earthquake loading and inelastic load reversals will not be considered.

A parameter not adequately discussed in the literature, but which significantly affects the strength of deep beams is the 'statical condition'. That is, whether the member is simply supported or continuous. In the continuous case a point of inflection occurs within the shear span. At this point the top and bottom flexural steel are both in tension. This has a considerable effect on the cracking of the beam web, as it tends to pull the concrete apart, reducing the effective strength of the concrete compression members of the truss or tied arch which develops after inclined cracking.

In summary, the parameters of interest which affect the

behavior of deep beams are

1) the shear span to depth ratio, a/d,
2) the compressive strength of the concrete, f'_c
3) the geometrical ratio of flexural steel area to concrete area, ρ
4) the geometrical ratio of vertical web reinforcement area to concrete area, ρ_v
5) the geometrical ratio of horizontal web reinforcement area to concrete area, ρ_h
6) type of load
7) statical condition.

2.3 Major Deep Beam Literature

The purpose of this section is to review a few major papers on deep beams and examine how each considers the important parameters listed in the previous section.

Dischinger (1932) provided an elastic analysis of deep reinforced concrete beams. This analysis clearly illustrated that in an elastic deep beam, sections that are plane before bending do not necessarily remain plane after bending. Information on the extent and magnitude of the tensile zones was used in determining the necessary flexural reinforcement on a working stress design basis. The Portland Cement Association (1980) still produces a publication based on Dischinger's work. There have been several other elastic solutions for deep beams (Chow, Conway, and Winter, 1952; Geer, 1960 for example). All of

these, Dishinger's included, suffer from the fact that they are not valid after cracking has occurred in the beam, and that they do not provide any information on the ultimate strength of deep beams.

Leonhardt and Walther (1966) conducted a major analytical and experimental investigation of the behavior of deep beams. It was found that while elastic solutions provide a good description of behavior before cracking, the stresses measured after cracking differed significantly from the theoretical elastic stresses. In particular, the actual stresses in the reinforcement of the tensile chord were much smaller than those values predicted from elastic solutions. All of the test beams developed a marked 'strut frame action', that is, a truss developed with inclined concrete compression members and horizontal steel tension members. The stresses in the tension chord reinforcement decreased much less towards the end of the girder than the moments, implying that the steel acted as a tension tie with approximately constant force from one end of the beam to the other. It was recommended that the main flexural reinforcement be carried straight to the supports without cutoffs, and that it be adequately anchored there. Leonhardt and Walther suggested that this could best be accomplished with 180° hooks lying in a horizontal plane since the vertical bearing stress helps clamp the reinforcement, improving its pull out resistance. Vertical hooks do not benefit as much from the bearing pressure and

the vertical extensions tend to straighten out and push the cover off the end of the beam rendering the extension useless.

The distribution of bending moment in the continuous beams tested by Leonhardt and Walther was found to correspond to that obtained from an elastic analysis which included shear deformations. In a deep continuous beam, the shear deformations reduce the interior support moment, and increase the midspan moments, and thus should not be neglectd. (It might be argued in hindsight that since the reinforcement in the specimens was proportioned on the basis of a linear elastic solution including shear deformation, plastic redistribution of internal forces would ensure agreement with this solution.) The principal compressive stress in the concrete in the support regions was greater than predicted by theory, and was often critical. A grid of reinforcement in these regions was recommended to help resist these stresses. For bottom and indirect loading, web reinforcement was required to prevent a shear failure, while there was no danger of a shear failure in top loaded beams.

For beams loaded on top and supported on the bottom so that compression struts could develop, vertical or inclined web reinforcement was of no benefit. Leonhardt and Walther concluded that, "For deep beams with $L/d < 2$, one should not speak of shear and shear reinforcement. Such beams always fail because the concrete crushes near the bearing where the principal compression stresses become critical and give the

upper limit of the carrying capacity, if the tie bars are well anchored and distributed." It should be pointed out that the test specimens were very deep beams, generally with $a/d < 0.5$. As a result, the results may not be directly applicable in the range of a/d values studied in this report. In addition, the beams were supported on steel bearing plates which may have contributed to the failure of the concrete near the supports.

The CEB design recommendations for deep beams (Comité Européan du Béton, 1970) are based primarily on the work of Leonhardt and Walther. In summary, they provide recommendations for the distribution and detailing of main reinforcement which encourages and ensures tied arch behavior. The design recommendations recognize the effects of ρ, type of loading, the statical condition, and to some extend a/d. The effect of effective concrete strength (f_c^*) is dealt with by requiring an additional grid of reinforcement in the region of point loads and point supports so that the stress becomes less important. Finally web reinforcement (ρ_v and ρ_h) is only required for temperature and shrinkage. The CEB recommendations apply to very deep beams, and thus are only applicable to the low a/d end of the range of beams investigated in this thesis.

De Paiva and Siess (1965) conducted a series of tests on 19 deep beams with L/d ratios between 2 and 4. The specimens all had a span of 24 in. with overall heights ranging from 7 in. to 13 in. The beams were loaded with 2

point loads giving a/d ratios ranging from 0.67 to 1.33. Although these beams are shallower than those of Leonhardt and Walther, they still exhibited tied arch behavior. Empirical equations fitted to the data considered the effects of f'_c, ρ, and a/d. It was found that vertical and inclined stirrups had no effect on the formation of the inclined cracks and seemed to have little effect on the ultimate strength of beams failing in either flexure or shear. The results of this study have limited application because:

1) Almost half, (9 out of 19) the specimens failed in flexure. This makes the population of shear failures rather small, and leads to questions of confidence in the empirical equations.
2) The small size of the specimens may have introduced scale effects. In tests of slender beams the shear strength tends to increase as the specimen size decreases (Chana, 1981). Size induced shear strength increases of 20% to 50% could exist in these tests.

Crist (1971) conducted static tests on nine large scale deep beams with span-to-depth ratios between 1.6 and 3.8. The loading consisted of 7 point loads which represented an almost uniformly distributed load. The observed behavior of the specimens was similar to that already described. Equations for the static shear strength of deep beams were derived using the lower boundary of the data for these and other tests. Some 73 tests were considered. Crist's

semirational derivation of design equations is important as it is the basis for the ACI code recommendations for deep beams. It starts with the premise that:

Total shear capacity = shear capacity of the concrete + shear capacity of the web reinforcment

$$V_u = V_c + V_s \tag{2.2}$$

The shear capacity of the concrete V_c is assumed to be:

$$V_c = \left[3.5 - \frac{4}{3}\left(\frac{M}{V}\right)\frac{1}{d}\right]\left[1.9\sqrt{f'_c} + 2500\left(\frac{V}{M}\right)\rho d\right] bd \tag{2.3}$$

The second term represents the inclined cracking load of a slender beam (ACI 1977) while the first term reflects the reserve shear capacity of deep beams after the development of inclined cracking. The critical section is assumed to occur at the midlength of the inclined crack. For uniformly distributed loads, this was found to occur at:

$$\frac{x_c}{d} = 0.2\,\frac{L}{d} \quad \text{when} \quad \frac{L}{d} < 5 \tag{2.4}$$

The ACI recommendations differ slightly in that:

$$V_c = \left[3.5 - 2.5 \frac{M_u}{V_u d}\right] \left[1.9 \sqrt{f'_c} + 2500 \rho_w \frac{V_u}{M_u} d\right] b_w d \quad (2.5)$$

with the critical section taken at $0.15\ell_n$ for uniform loads, and 0.5a for concentrated loads.

The shear capacity of the web reinforcement was developed considering shear friction along the inclined crack as illustrated in Fig. 2.2. The shear friction analogy gives:

$$S = F_{DT} \tan \phi \quad (2.6)$$

where F_{DT} = the normal force on the inclined crack; $\tan \phi$ = the apparent coefficient of friction; and S = the shear along the crack. The vertical component of the shear along the crack is:

$$V_s = S \sin \theta \quad (2.7)$$

The normal force F_{DT} is produced by tension in the reinforcement which results from crack dilation as slip occurs. Assuming that the stirrups are yielded at the ultimate load condition:

$$F_v = A_v f_y \quad (2.8)$$

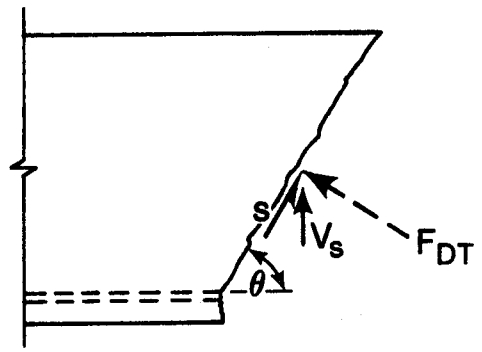

(a) Forces on Inclined Crack Plane

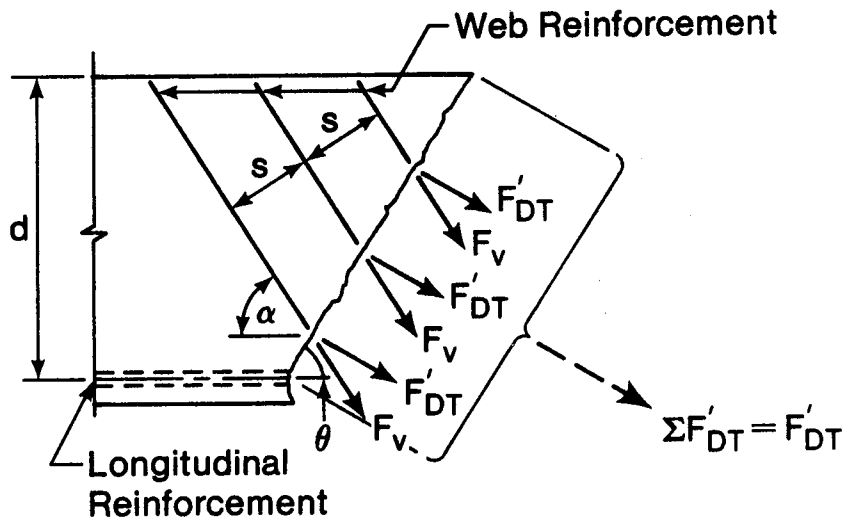

(b) Forces in Stirrups Along Inclined Crack Plane

Figure 2.2. Derivation of Equations for Web Reinforcement in Deep Beams

And from geometry this gives:

$$F_{DT} = \Sigma(F_{DT})_i = \Sigma F_{vi} \sin(\alpha_i + \theta) \tag{2.9}$$

And therefore:

$$V_s = \Sigma F_{vi} \sin(\alpha_i + \theta) \tan\phi \sin\theta \tag{2.10}$$

With further trigonometric and algebraic manipulation for vertical and horizontal web reinforcement

$$V_s = f_y d \tan\phi \left[\frac{A_v}{s} \cos^2\theta + \frac{A_{vh}}{s_h} \sin^2\theta\right] \tag{2.11}$$

where A_v and s refer to vertical web reinforcement and A_{vh} and s_h refer to horizontal web reinforcement. A lower bound to the crack inclination data for uniformly loaded deep beams gives

$$\cos^2\theta = \frac{1}{12}\left(1 + \frac{\ell_n}{d}\right) \tag{2.12}$$

This can be used with Eq. 2.11 to give:

$$V_s = f_y d \tan\phi \left[\frac{A_v}{s} \frac{1}{12}\left(1 + \frac{\ell_n}{d}\right) + \frac{A_{vh}}{s_h} \frac{1}{12}\left(11 - \frac{\ell_n}{d}\right)\right] \tag{2.13}$$

ACI uses this equation assuming that the coefficient of friction, $\tan\phi$, is equal to 1.0 while Crist originally suggested that $\tan\phi = 1.5$. For deep beams, the normal or

clamping stress provided by the reinforcement is quite small. The rock mechanics literature (Barton, 1973) indicates that the coefficient of friction, tan ϕ, for existing crack surfaces and presumably precracked concrete is dependent on the normal stress.

$$\tan \phi = \tan \left[20 \log_{10} \left(\frac{f'_c}{\sigma_n} \right) + 30^0 \right] \qquad (2.14)$$

where σ_n is the clamping stress on the crack surface. Typically f'_c/σ_n is approximately 20 in Crist's beams. For this value Eq. 2.14 gives tan ϕ = 1.48.

The analysis of V_s assumes that failure takes place by sliding along the inclined crack. Because such a failure is a complete failure mechanism in itself, there is no rational basis for adding the capacity V_c to the capacity of this failure mechanism. The sliding hypothesis is an upper bound solution in accordance with the upper bound plasticity theorem. Thus, V_s represents an upper limit to the total shear capacity, and not just the shear capacity of the web reinforcement.

In summary, Crist recognizes the influence of f'_c as it affects the tensile strength of the concrete and the inclined cracking load. He does not consider the compressive strength of the concrete relative to any compressive stress the concrete must carry. The effect of a/d is considered directly in Eq. 2.5 and indirectly in Eq. 2.12. The model does take into account web reinforcement as

shear friction reinforcement, but ignores the effect of the main reinforcement acting in a similar manner. There is no logical reason for ignoring this effect. The shear transmitted across the crack by the vertical component of the stirrup forces is not considered. The statical condition (continuity) of the beam is not considered. For continuous beams Eq. 2.3 and 2.5 present "division by zero" problems when the critical section is near the point of inflection. The Crist model of behavior does not recognize the tied arch or truss which develops after inclined cracking. Finally, on the basis of the upper bound theorem, the superposition of V_c and V_s is not strictly rational.

Kong (1977) has conducted numerous tests on deep beams. His work forms the basis for British practice (CIRIA 1977). On the basis of tests with $0.23 < x/h < 0.70$, where x = the clear shear span, a semi-empirical equation for shear capacity was obtained:

$$V_u = C_1\left(1 - 0.35 \frac{x}{h}\right) f_{ti} bh + C_2 \Sigma A_s \frac{y}{h} \sin^2\beta \qquad (2.15)$$

The first term relates to the shear carried by the concrete while the second term relates to the shear carried by the reinforcement. The geometric symbols are illustrated in Fig. 2.3. C_1 is a coefficient equal to 1.4 for normal weight concrete and 1.0 for lightweight concrete, C_2 is a coefficient equal to 130 MPa for plain round bars and 300 MPa for deformed bars, and f_{ti} is the split cylinder tensile

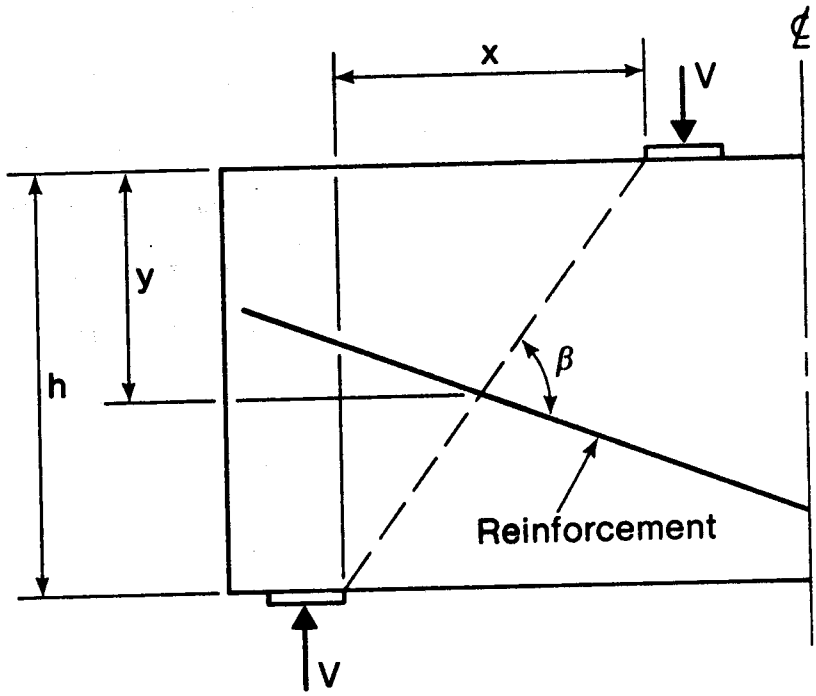

Figure 2.3. Kong's Symbol Definitions

strength of the concrete. The test specimens were loaded with concentrated loads rather than uniformly distributed loads. This accounts for some of the differences between the recommendations of Kong and those of Crist. The second term of Eq. 2.15 is almost identical to the Eq. 2.10, however, the area of the main reinforcement is included in Eq. 2.15 while it is ignored in Eq. 2.10.

The comments on Crist's work are also valid for Kong's results. It should be pointed out that Kong's tests had very deep shear spans with a/d ranging between about 0.25 and 0.8. Again, Eq. 2.15 does not seem to reflect the tied-arch behavior described by Leonhardt.

There are many other minor deep beam studies. They will not be discussed specifically since they contain results and conclusions similar to those already considered. The significant conclusions are:

1) Current design recommendations are semi-empirical and are based on tests simply supported deep beams which are at the deep end of the range of a/d of interest.
2) Current design recommendations do not attempt to predict the strength of the tied-arch or truss which forms after inclined cracking.
3) There is strong disagreement about the effectiveness of web reinforcement, particularly horizontal web reinforcement.

2.4 Plasticity Literature

During the last two decades, the growing literature of plasticity in reinforced concrete has developed to the extent that it forms the basis for shear design in some reinforced concrete design codes (CEB, 1978; SIA, 1976). Generally, a modified Mohr-Coulomb failure criterion with a zero or small tension cut-off and an associated flow rule are used in conjunction with the upper and lower bound plasticity theorems. The lower bound solutions generally take the form of truss models while the upper bound solutions relate to the various possible failure mechanisms. Most of the published solutions are 'exact' in the plasticity sense in that the upper and lower bounds for the collapse load are identical. The lower bound solutions are particularly useful in design since they give the designer an understanding of the 'flow of forces' through the member, and if the failure criteria are adequate, the solutions will always be safe estimates for member capacity. Only lower bound solutions will be discussed here. For a more complete discussion of plasticity in reinforced concrete, see Appendix A.

Two typical simple truss models are presented in Fig. 2.4 (Marti, 1980; Jensen, 1979). The essential features of these models are:

1) The concrete only resists compression and has an effective compressive strength $f_c^* = \nu f_c'$ where $\nu < 1.0$,

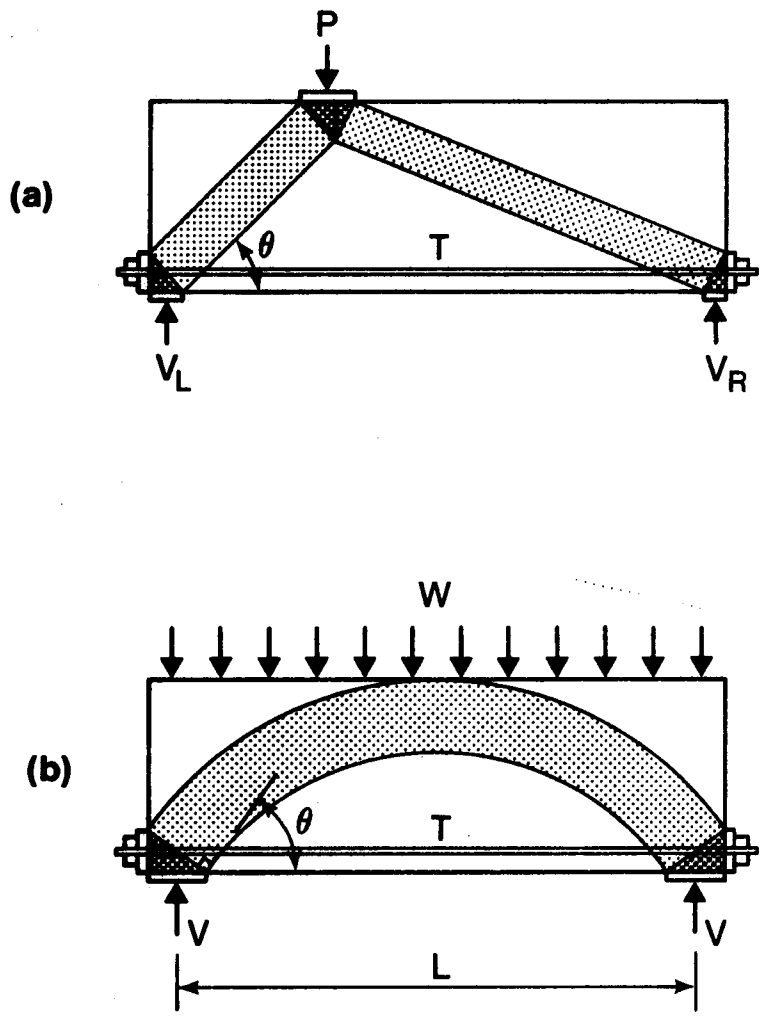

Figure 2.4. Plastic Trusses for Beams Without Web Reinforcement

2) Steel is required to resist all tensile forces,

3) The centroids of each truss member and the lines of action of all externally applied loads at a joint must coincide.

4) Joints are accommodated by using hydrostatic stress elements (wedges of concrete shown with dark shading in Fig. 2.4) in which both principal stresses are equal to f_c^*.

5) Bearing plates, support conditions, and details must be such that local bearing failures in the concrete do not occur.

Provided that the conditions in item 5 are satisfied, simple equilibrium gives:

$$V = T \tan \theta \tag{2.16}$$

where T is the yield force in the steel member of the truss. Closed form expressions based on Eq. 2.16 are available for some simple cases, but if a suitable truss can be drawn, the angle θ can be scaled from the drawing, and Eq. 2.16 can be used directly. Some examples are illustrated in Fig. 2.5.

A simple span beam with horizontal web reinforcement is shown in Fig. 2.5(a). The load is carried by two trusses - an upper truss utilizing the web bar, and a lower truss utilizing the main reinforcement. The capacity of each truss may be determined with Eq. 2.16 and added together.

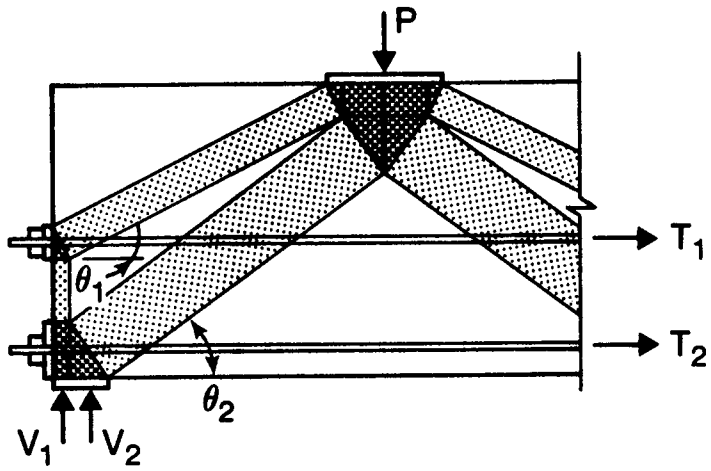

(a) Beam with Horizontal Web Reinforcement

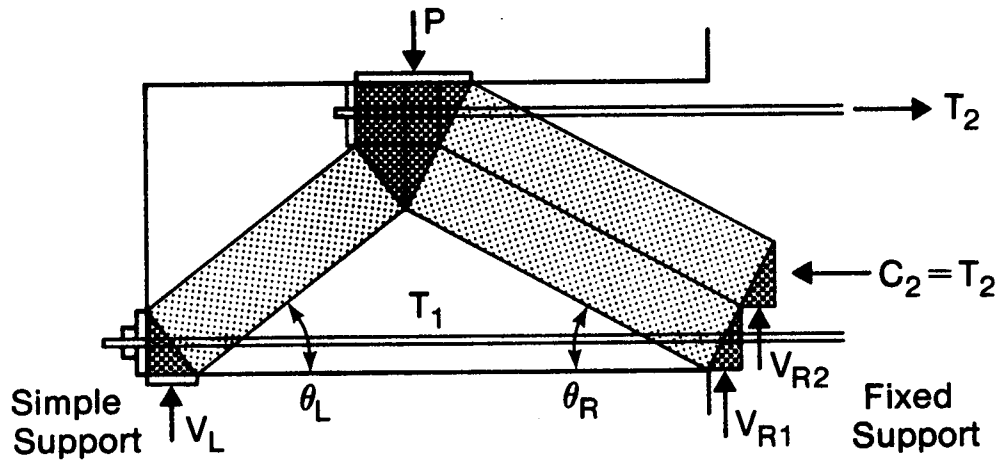

(b) Fixed-Simple Support Conditions

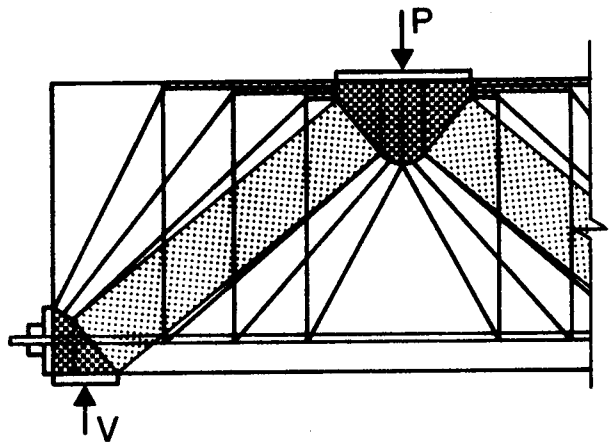

(c) Beam With Vertical Web Reinforcement

Figure 2.5. Applications of Plastic Trusses

Figure 2.5(b) illustrates a beam with fixed-simple support conditions. At the fixed support, two trusses carry the load - an upper truss utilizing the top reinforcement with force T_2, and a lower truss utilizing the bottom reinforcement with force T_1. Again, the capacity of each truss may be determined with Eq. 2.16 and added together. A simple span beam with vertical web reinforcement is shown in Fig. 2.5(c). The plastic truss uses the stirrups as vertical web members. This case will be discussed in detail in Chapter 5.

The plasticity trusses consider each of the 7 important parameters listed in Section 2.2 in an explicit manner. The shear span to depth ratio a/d as well as other geometric considerations are reflected in θ. The concrete strength f_c^* governs the joint details and these, in turn, govern θ. The type of loading and statical condition govern the geometry of the plastic truss.

Apparently the most important parameter in the plastic truss models is the effective concrete strength. This relates to the strain softening behavior of concrete. Often, portions of the concrete will be stressed beyond peak strength and begin to soften before other portions of the concrete begin to mobilize full strength. Hence one cannot rely on mobilizing the full strength of the concrete over the entire section. In addition, local effects often give rise to local complicated stress distributions which are oversimplified in the plasticity model (Thürlimann, 1979).

This leads to the introduction of an effective concrete strength $\nu f'_c$, where $\nu < 1.0$ is an efficiency factor. While Exner (1979) employs theoretical means to evaluate the efficiency factor, values of ν are usually back calculated from test data, and thus depend upon the plasticity model used in predicting the member capacity. At present, different ν factors are suggested for beam shear, punching shear, anchorage, etc.

There are other forms of plasticity solutions for deep beams. Manuel (1974), Kumar (1976) etc. present less rigorous versions of the models already discussed. Collins and Mitchel (1980) have presented a somewhat more rigorous solution in that they attempt to describe the entire nonlinear response of the concrete in a beam web. Their work is based on an empirically obtained constitutive relationship for reinforced concrete under uniform plane stress conditions. The method has yet to be fully developed and verified for problems with nonuniform stress fields such as those in point loaded deep beams where compression struts develop. In Collin's analysis, the design "problem" in a typical deep beam is not shear, rather it is one of excessive bearing stress at the support.

2.5 Unresolved Issues

This brief literature review has brought to light a number of unresolved issues. The problems start with an inadequate data base for a/d between 1.0 and 2.5, especially

when spans are continuous. The current semi-empirical design recommendations must be extrapolated for the range of parameters of interest. This extrapolation may not be appropriate, for there is considerable disagreement about the effectiveness of web reinforcement, particularly horizontal web reinforcement. The plasticity solutions which attempt to predict the strength of the tied-arch or truss which forms after inclined cracking rely on a concrete efficiency factor ν. Appropriate truss models and efficiency factors for the type of deep beams under consideration in this thesis have yet to be determined due to the lack of sufficient test data.

In light of the above, an experimental test series was designed to provide data on the effects of statical condition, ρ_v, ρ_h, and f'_c for a/d between 1.0 and 2.5.

3. EXPERIMENTAL PROGRAM

3.1 Overview of Experimental Program

The experimental program consisted of tests of 23 specimens, 4 of which were tested by Ong (1982). This chapter is a brief summary of the testing program. The detailed documentation for the tests can be found in a report by Rogowsky, MacGregor and Ong (1983). The specimens included 6 simple span beams and 17 two span continuous beams, each span being 2 m in length. The shear span to depth ratios ranged from 1 to 2.5. Various arrangements and amounts of web reinforcement were used including: no web reinforcement, "minimum" and "maximum" horizontal web reinforcement, and "minimum" and "maximum" vertical web reinforcement. The beams were supported and loaded by columns cast monolithically with the beams. The loads were applied through columns to the top of the beams at midspan.

Measurements made during each test included applied loads and reactions, midspan deflections, and concrete and steel strains. The strains were measured mechanically over 2 to 5 inch gage lengths. Cracks were marked and photographed at each load step.

The beams generally failed in shear, exhibiting a wide range of behavior, ranging from very brittle to very ductile depending on the amount and arrangement of the web reinforcement, and the shear span to depth ratio.

3.2 Test Specimens

The standard series of specimens at each shear span to depth ratio consisted of 7 beams shown schematically in Fig. 3.1. Beams 1 and 2 in each series were simply supported and contained identical flexural reinforcement. Stirrups were provided at only one end of each of these beams giving a total of 4 different web reinforcement conditions in the 4 simply supported shear spans. The remaining beams in the series were two-span continuous beams which had the geometry of two simple spans end to end. All of the continuous beams in a series had the same main flexural reinforcement, and were symmetrical so that 5 different web reinforcement conditions were considered in the continuous shear spans.

The identification number for each beam consists of an integer number corresponding to its place in the test series as shown in Fig. 3.1, followed by a '/' and a real number which indicates the nominal shear span to depth ratio, followed by 'N', or 'S' indicating the north and south shear span. Hence, BM 2/1.0N conceptually has the same basic type of reinforcement, and is directly comparable to BM 2/1.5N and BM 2/2.0N. A suffix of 'T1' indicates that the data is for the first loading of the beam leading to failure of one of the shear spans (virgin test), while a suffix of 'T2' indicates that the data is for the retest of the beam after the initial failure had been reinforced externally. The second test series, shear span to depth ratio of 1.5, had 8

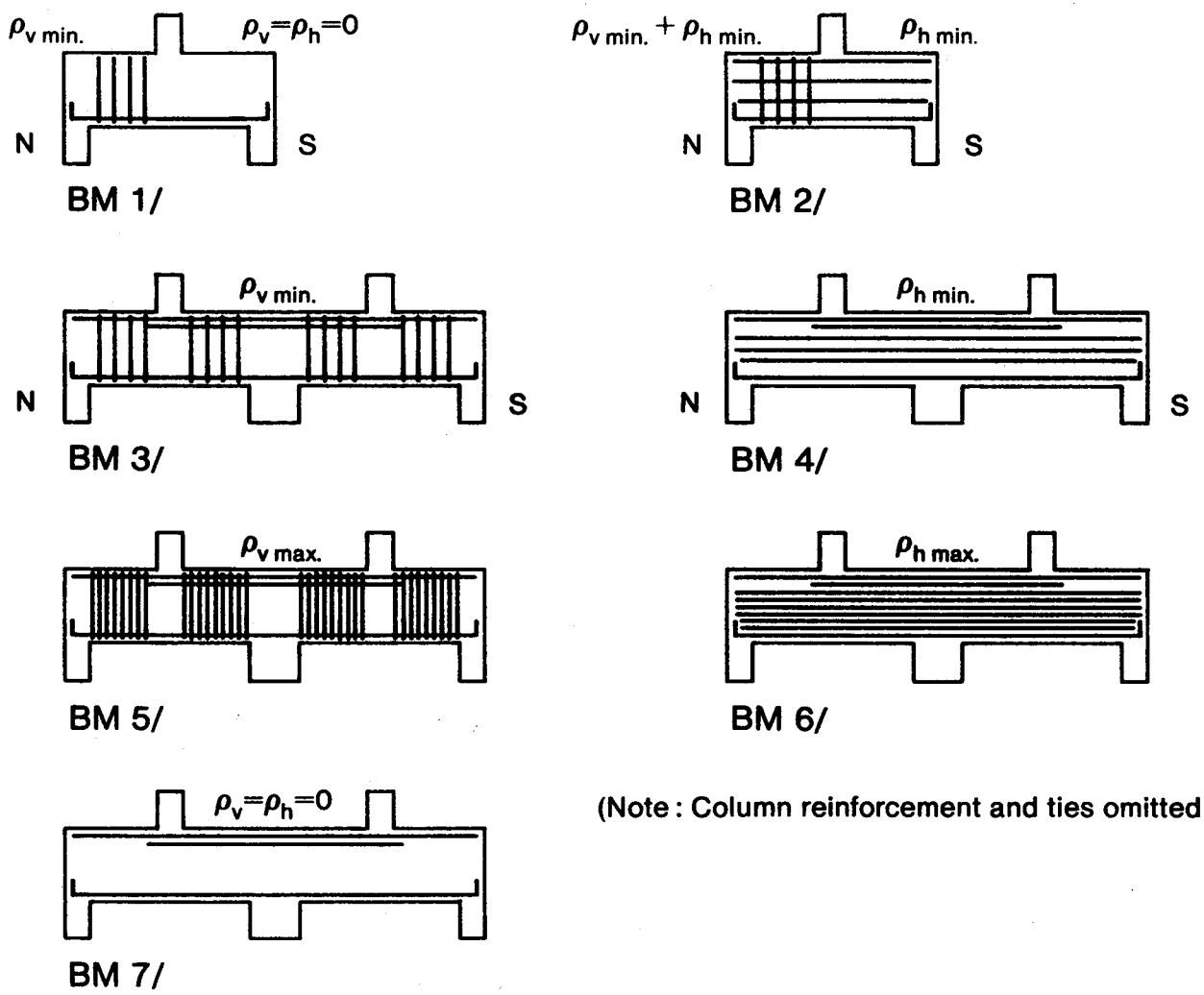

(Note : Column reinforcement and ties omitted for clarity).

Figure 3.1 Typical Test Series

beams. Beam 8/1.5 had minimum vertical and minimum horizontal web reinforcement.

The locations of the centre lines of the loads and reactions were the same for all beams tested. Only the beam depth and size of loading column were varied to obtain the desired shear span to depth ratios. The beams were loaded and supported through column stubs cast integrally with the beam to load and support the beam in a realistic manner.

All specimens were concreted in a vertical position in the same set of forms and differed only in overall depths and number of spans. The overall dimensions are given in Fig. 3.2. The details of the reinforcement for each beam are given in Tables 3.1 and 3.2. Typical details are illustrated in Figs. 3.3 and 3.4. In all cases the beam reinforcement passed inside the vertical column bars. The clear cover to the column ties and the top and bottom of the stirrups was 10 mm. The clear side cover to the stirrups was 25 mm. The side clear cover to the outside longitudinal bars was 35 mm except in beams 1, 2, 3, and 4 of the x/1.0 series in which it was 45 mm. All bottom flexural reinforcement extended the full length of the beam. Both ends of the bars had standard hooks located within the exterior column cages. All column steel extended at least one compression development length into the beam. Horizontal stirrups were anchored at each end with standard hooks. All vertical stirrups were closed stirrups anchored at the top with 135 degree hooks around a main flexural bar

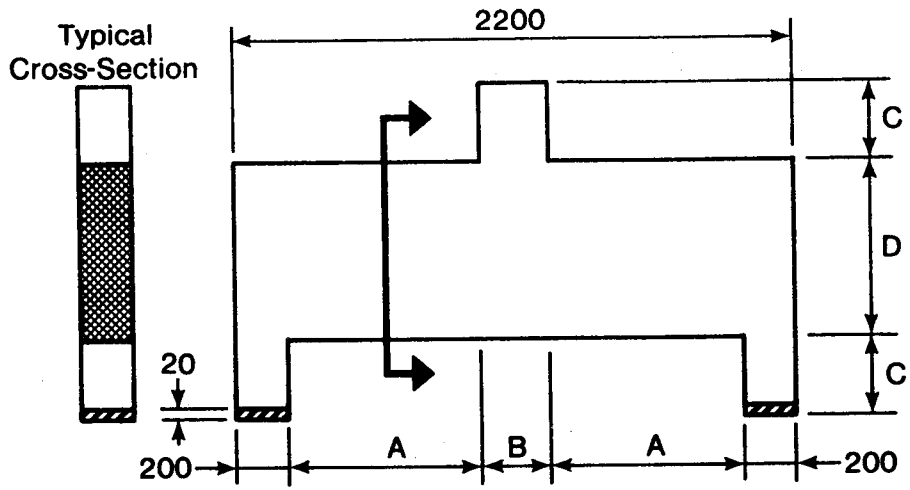

(a) Simple Span Specimens

Series	A	B	C	D
/ 1.0	750	300	450	1000
/ 1.5	750	300	300	600
/ 2.0	800	200	300	500
/ 2.5	800	200	300	400

Note : All Dimensions in mm.

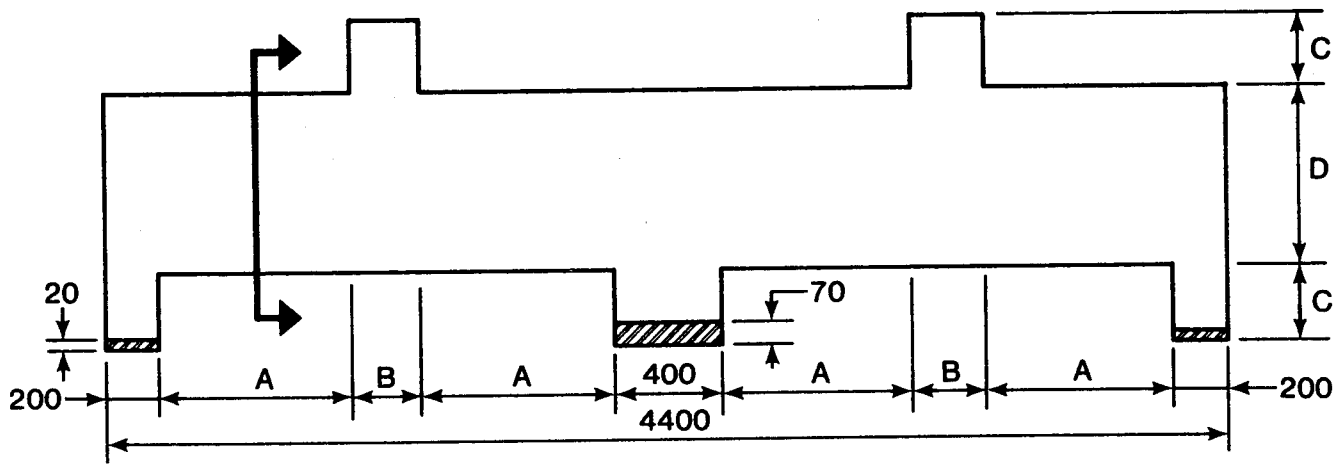

(b) Two Span Specimens

Figure 3.2 Overall Dimensions of Specimens.

Table 3.1 Reinforcement Details of Specimens

Specimen	Top Steel			Bottom Steel			Web Steel *			
	Bars	$A_s f_y$/Bar (kN)	ρ	Bars	$A_s f_y$/Bar (kN)	ρ	No. of Strips	ρ_v	No. of Horiz. Bars	ρ_h
1/1.0N	-	-	-	6-20M	114	0.0095	4	0.0015	-	-
1/1.0S	-	-	-	6-20M	114	0.0095	-	-	-	-
2/1.0N	2-6mm	16.2	0.0003+	6-20M	114	0.0095	4	0.0015	4	0.0006
2/1.0S	2-6mm	16.2	0.0003+	6-20M	114	0.0095	-	-	4	0.0006
3/1.0	4-20M	114	0.0063	3-20M	114	0.0046	4	0.0015	-	-
4/1.0	4-20M	114	0.0063	3-20M	114	0.0046	-	-	4	0.0006
5/1.0	4-20M	121	0.0063	3-20M	121	0.0046	16	0.0060	-	-
6/1.0	4-20M	121	0.0063	3-20M	121	0.0046	-	-	12	0.0018
7/1.0	4-20M	121	0.0063	3-20M	121	0.0046	-	-	-	-
1/1.5N	-	-	-	6-15M	91	0.0112	5	0.0019	-	-
1/1.5S	-	-	-	6-15M	91	0.0112	-	-	-	-
2/1.5N	2-6mm	16.2	0.0003+	6-15M	91	0.0112	5	0.0019	4	0.0011
2/1.5S	2-6mm	16.2	0.0003+	6-15M	91	0.0112	-	-	4	0.0011
3/1.5	6-15M	91	0.0072**	2-10M 4-15M	46 91	0.0096	5	0.0019	-	-
4/1.5	6-15M	91	0.0072**	2-10M 4-15M	46 91	0.0096	-	-	4	0.0011
5/1.5	6-15M	91	0.0072**	2-10M 4-15M	48 91	0.0096	16	0.0060	-	-
6/1.5	6-15M	91	0.0072**	2-10M 4-15M	48 91	0.0096	-	-	12	0.0032
7/1.5	6-15M	91	0.0072**	2-10M 4-15M	46 91	0.0096	-	-	-	-
8/1.5	6-15M	91	0.0072**	2-10M 4-15M	46 91	0.0096	5	0.0019	4	0.0011
1/2.0N	-	-	-	4-15M	91	0.0088	4	0.0014	-	-
1/2.0S	-	-	-	4-15M	91	0.0088	-	-	-	-
2/2.0N	2-6mm	16.2	0.0003+	4-15M	91	0.0088	4	0.0014	4	0.0012
2/2.0S	2-6mm	16.2	0.0003+	4-15M	91	0.0088	-	-	4	0.0012
3/2.0	4-15M 2-10M	91 48	0.0088**	2-10M 4-15M	48 91	0.0119	4	0.0014	-	-
4/2.0	4-15M 2-10M	91 46	0.0088**	2-10M 4-15M	46 91	0.0119	-	-	4	0.0013
5/2.0	4-15M 2-10M	91 48	0.0088**	2-10M 4-15M	48 91	0.0119	16	0.0057	-	-
6/2.0	4-15M 2-10M	91 46	0.0088**	2-10M 4-15M	46 91	0.0019	-	-	12	0.0039
7/2.0	4-15M 2-10M	91 48	0.0088**	2-10M 4-15M	48 91	0.0019	-	-	-	-
5/2.5	4-15M	91	0.0113	4-15M	91	0.0113	16	0.0057	-	-

* All web steel was 6 mm deformed bars with $A_s f_y$ per bar = 16.2 kN. ρ_v and ρ_h based on average d.

** Due to bar cut offs within the interior shear span, only 4-15M were effectively anchored. The ρ given includes only these bars.

\+ This top steel has been neglected in calculations for simply supported beams.

Table 3.2 Geometric Details of Specimens

Specimen	d(mm)			a* (mm)	a/d**
	*** Top steel	Bot.Steel	Average		
1/1.0	-	950	950	750	0.79
2/1.0	980+	950	950	750	0.79
3/1.0	950	975	963	750	0.78
4/1.0	950	975	963	750	0.78
5/1.0	950	975	963	750	0.78
6/1.0	950	975	963	750	0.78
7/1.0	950	975	963	750	0.78
1/1.5	-	535	535	750	1.40
2/1.5	580+	535	535	750	1.40
3/1.5	555	520	538	750	1.40
4/1.5	555	520	538	750	1.40
5/1.5	555	520	538	750	1.40
6/1.5	555	520	538	750	1.40
7/1.5	555	520	538	750	1.40
8/1.5	555	520	538	750	1.40
1/2.0	-	455	455	800	1.76
2/2.0	480+	455	455	800	1.76
3/2.0	455	420	438	800	1.83
4/2.0	455	420	438	800	1.83
5/2.0	455	420	438	800	1.83
6/2.0	455	420	438	800	1.83
7/2.0	455	420	438	800	1.83
5/2.5	355	355	355	800	2.25

* Clear distance between faces of loading and supporting columns.

** Average d used

*** d for effectively anchored bars only. (see footnote to Table 2.2)

\+ This top steel has been neglected in calculations for simply supported beams.

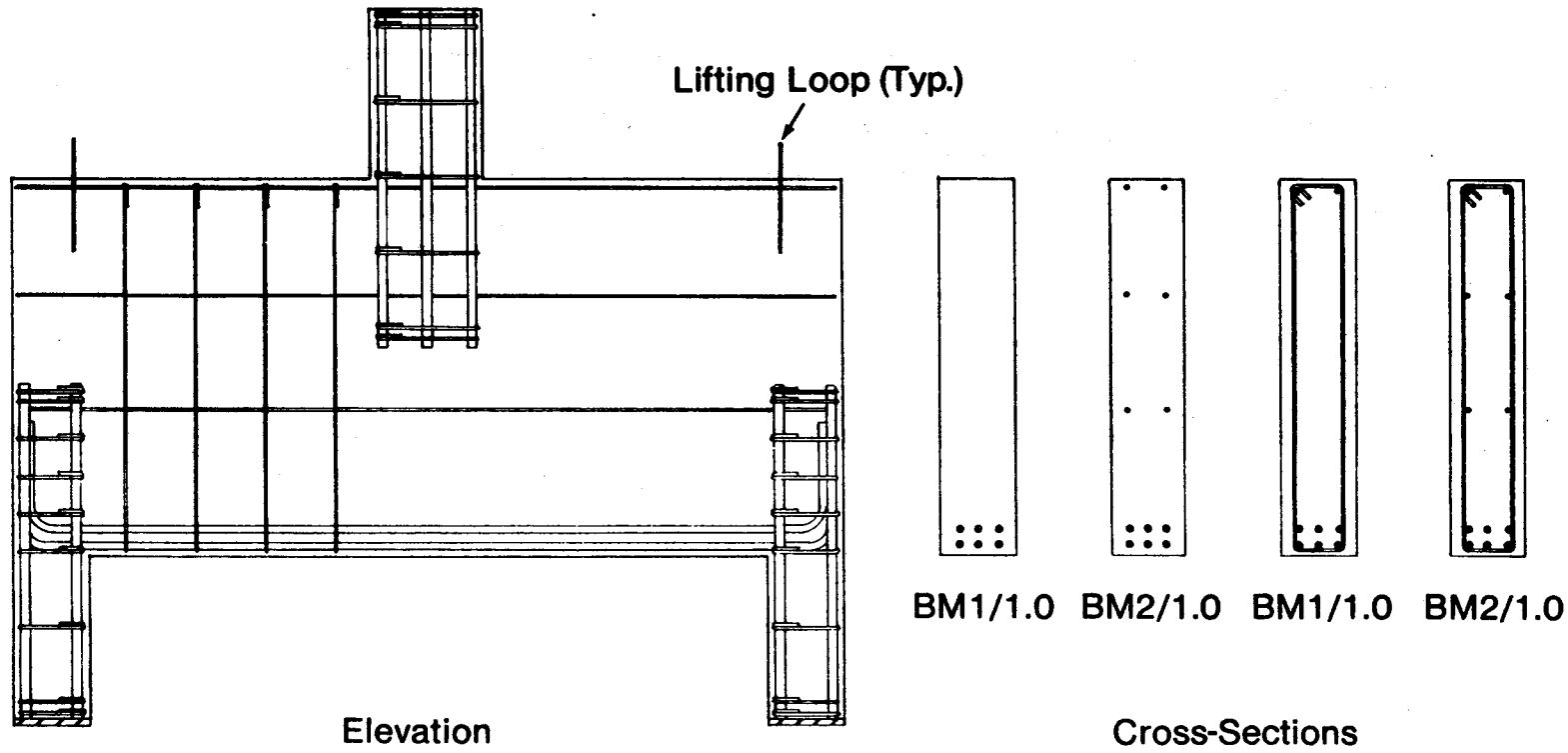

Figure 3.3. Beam 1/1.0 and 2/1.0 Reinforcement Details.

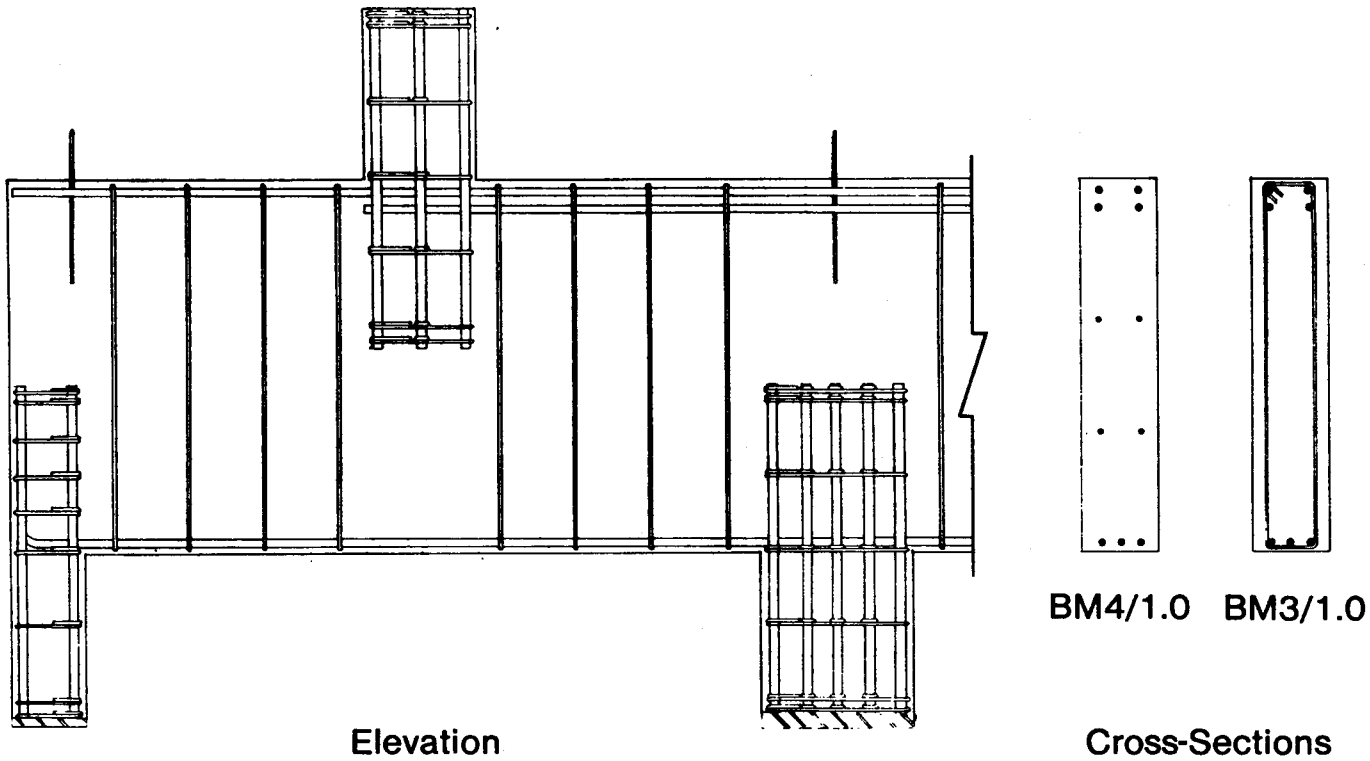

Figure 3.4. Beam 3/1.0 and 4/1.0 Reinforcement Details.

or, in the case of simple spans, around a 6 mm stirrup support bar. The column bars were saw cut square and tack welded to the steel base plates.

Lifting loops were provided at the ends of each beam. The continuous beams were provided with a third lifting loop over the interior support. The lifting loops consisted of 10M bars or 1/2 inch diameter prestressing strand. The bars were abandoned in favor of the prestressing strand because the strand readily and safely accommodated the flexing which occurred during the movement and handling of the specimens. The lifting loops did not appear to influence the behavior of the beams in any way.

All reinforcement, except the column ties consisted of deformed bars. The 6 mm diameter deformed bars were obtained from Sweden while the remaining bars were obtained locally. The reinforcement had a specified yield strength of 400 MPa with measured yield strengths ranging from 380 to 480 MPa. The bar yield forces are given in Table 3.1. The average Young's Modulus for the reinforcement was approximately 204,000 MPa.

The concrete mix was designed to produce a 28 day cylinder strength of about 30 MPa. Normal Type 10 Portland cement and normal weight river washed aggregates were used. The maximum aggregate size was 10 mm and the slump was approximately 100 mm. Owing to variation in the supply of aggregates and cement over the duration of construction and testing (14 months), the inevitable delay in the testing

of individual specimens and the variable curing conditions in the laboratory, there was considerale scatter in the values of concrete strength at the time of testing. The concrete properties at the time each specimen was tested are given in Table 3.3.

The specimens were heavily instrumented to obtain as much information as possible about the behavior of the beams at each stage of loading. All loads and reactions were determined with load cells. The steel and concrete strains were measured using Demec Gages (demountable mechanical extensometers). Displacements were measured with standard dial gauges and linear variable-differential transformers (LVDT's). The data acquisition computer became functional part way through the testing program and was used to record data for the last 15 specimens.

The specimens were tested in the loading frame shown in Fig. 3.5. The loads were applied by hydraulic jacks. The load was applied in increments, with approximately 7 load steps to failure. During each increment, the load was kept constant while cracks were marked and photographed, and loads, displacements, and strains were measured and recorded.

Each beam was tested to failure twice. After the first shear span failed, it was externally reinforced with a yoke above and below the beam and twelve 3/4 in. diameter tie rods acting as stirrups. The external reinforcement is visible in Fig. 3.5. The support reactions of the

Table 3.3 Concrete Properties

Beam	f'c (MPa)	COV* of f'c	fsp (MPa)	Ec (GPa)	Age (Days)	$E_c(f'_c)^{-0.5}$	$f_{sp}(f'_c)^{-0.5}$	$f_{sp}(f'_c)^{-0.7}$
1/1.0	26.1	-	2.28	20.0	72	3915	0.446	0.232
2/1.0	26.8	-	2.65	23.4	106	4520	0.512	0.265
3/1.0	28.9	0.10	2.48	20.8	128	3869	0.461	0.235
4/1.0	28.5	0.03	2.86	-	127	4017	0.536	0.274
5/1.0	36.9	0.04	3.10	24.4	20	4017	0.510	0.248
6/1.0	35.8	0.04	2.97	21.2	20	3543	0.496	0.243
7/1.0	34.5	0.06	2.99	21.6	20	3677	0.510	0.251
1/1.5	42.4	0.04	3.27	21.1	72	3241	0.502	0.237
2/1.5	42.4	0.04	3.27	21.1	72	3240	0.502	0.237
3/1.5	14.5	0.06	-	-	-	-	-	-
4/1.5	32.5	0.04	-	-	-	-	-	-
5/1.5	39.6	0.06	2.98	23.6	66	3750	0.474	0.227
6/1.5	45.0	0.02	3.19	24.6	73	3667	0.476	0.222
7/1.5	30.4	0.06	-	-	-	-	-	-
8/1.5	37.2	0.04	-	-	-	-	-	-
1/2.0	43.2	0.04	3.09	24.8	39	3773	0.470	0.221
2/2.0	43.2	0.04	3.09	24.8	39	3773	0.470	0.221
3/2.0	42.5	0.04	2.34	22.9	58	3513	0.359	0.170
4/2.0	38.3	0.04	2.44	22.4	55	3620	0.394	0.190
5/2.0	41.1	0.03	2.86	22.5	62	3510	0.446	0.212
6/2.0	37.4	0.04	2.41	21.6	30	3532	0.394	0.191
7/2.0	46.8	0.03	2.64	24.0	66	3508	0.386	0.179
5/2.5	34.0	0.05	2.46	20.4	21	3499	0.422	0.204
					Mean	3694	0.461	0.224
					COV	0.08	0.11	0.12

* Coefficient of Variation of the batches making up one beam.

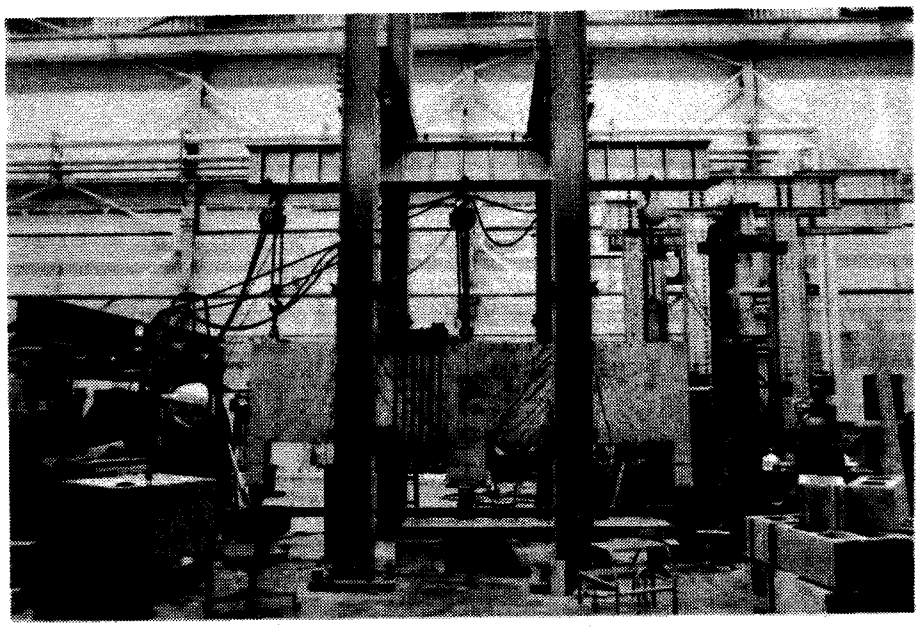

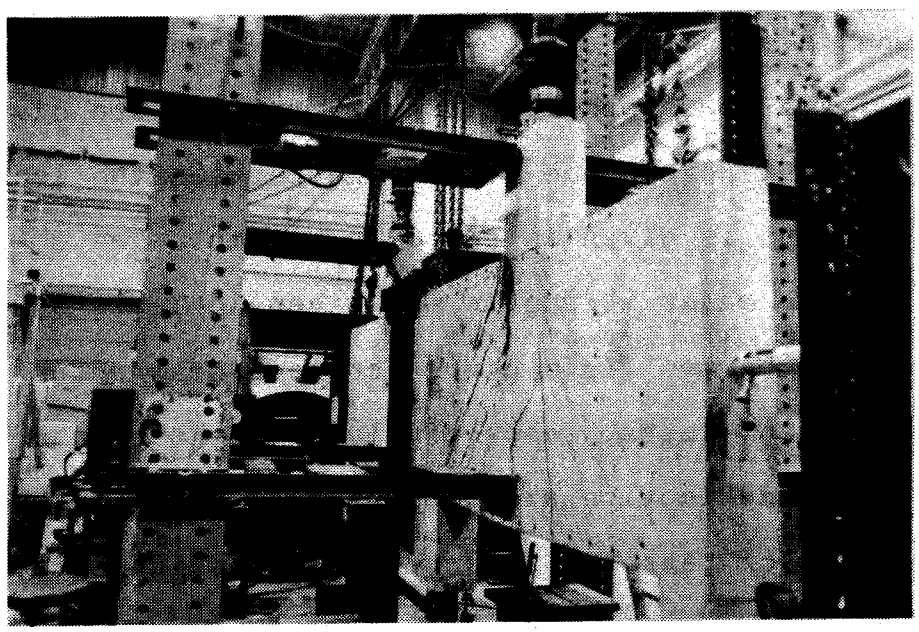

Figure 3.5 Loading Frame and Test Set-up
(Beam 5/1.0 is shown in the testing frame)

continuous beams were then remounted on their bearing plates to allow for any movement due to adding the yokes. The beams were then retested.

3.3 Test Results

This section of the thesis presents a brief summary of the test results with typical results presented where appropriate. Most of the data has been reduced to graphical form for ease of interpretation.

All of the beams were tested spanning in a north-south direction. The figures illustrating the beams always have the north end of the beam shown as the left end. Thus, the drawings of the east face have been reversed. This has been done to allow direct comparison of data from the two faces.

The loads and reactions at failure are given in Table 3.4. The percentage difference between the loads and the reactions is given in the last column. The corresponding ultimate shear strengths are given in Table 3.5. In these tables the two lines given for each beam refer to the first and second tests, respectively. Graphs of the jack load vs. midspan deflection are presented in Figs. 3.6 to 3.13.

Crack patterns, concrete strains, and steel strains have been reported for each beam (Rogowsky et al., 1983). The results for a few typical beams are presented here. The data for each beam consists of a sketch of the crack pattern with shaded areas representing regions that crushed or spalled at failure. The concrete strains are plotted on a

Table 3.4 Loads and Reactions at Ultimate Failure

Beam Mark	Type of Web Reinforcement	R1 N. Support Reaction (kN)	P1 N. Jack Load (kN)	R2 Int. Support Reaction (kN)	P2 S. Jack Load (kN)	R3 S. Support Reaction (kN)	e/ΣP (%)
1/1.0	Min. Vert. None	602* 699	1204 1397			602 699*	1 0
2/1.0	Min. Horiz. Min Vert. + Min. Horiz.	750 750*	1500 1500			750* 750	0 0
3/1.0	Min. Vert. Min. Vert.	400* 400	1085 1176	1385 1540	1082 1150	393 386*	-1 -1
4/1.0	Min. Horiz. Min. Horiz.	420 378	1087 996	1330 1229	1078 979	415* 369	-1 -1
5/1.0	Max. Vert. Max. Vert.	413 304	1288 961	1740 1491	1271 1333	405 499*	-1 -1
6/1.0	Max. Horiz. Max. Horiz.	461 479*	1107 1084	1280 1186	1083 1034	448* 453	-1 0
7/1.0	None None	287 405*	711 1100	842 1377	698 1070	280* 389	-1 -1
1 1.5	None Min. Vert.	303 354*	606 709			303* 354	0 0
2/1.5	Min. Horiz. Min. Vert. + Min. Horiz.	226 348	452 696			226* 348	0 0
3/1.5	Min. Horiz. Min. Vert.	158 181*	401 468	485 572	398 464	156* 179	-2 -1
4/1.5	Min. Horiz. Min. Horiz.	118* 138	324 373	411 467	321 368	116 136*	-2 -2
5/1.5	Max. Vert. Max. Vert.	293* 318	858 888	1126 1136	847 879	287 313*	-1 -1
6/1.5	Max. Horiz. Max. Horiz.	147 150*	407 408	515 514	399 405	143* 148	0 -1
7/1.5	None None	137 220*	360 568	445 693	357 565	135* 219	-1 -1
8/1.5	Min. Vert. + Min. Horiz. Min. Vert. + Min. Horiz.	201 218*	543 600	681 762	537 594	198* 214	-1 -2
1/2.0	None Min. Vert.	177 199*	354 399			177* 199	1 -1
2/2.0	Min. Horiz. Min. Vert. + Min. Horiz.	185 204*	369 407			185* 204	0 0
3/2.0	Min. Vert. Min. Vert.	164* 167	425 447	521 557	422 440	162 163*	-1 -2
4/2.0	Min. Horiz. Min. Horiz.	105* 128	300 373	390 488	297 369	103 126*	-2 -2
5/2.0	Max. Vert. Max. Vert.	224* 242	677 703	899 918	661 693	216 237*	-2 -2
6/2.0	Max. Horiz. Max. Horiz.	113 97*	299 238	372 277	297 228	111* 92	-2 0
7/2.0	None None	108 82	296 232	374 299	291 227	106* 79	-1 -1
5/2.5	Max. Vert. Max. Vert.	156* -	486 -	656 -	478 -	152 -	-2 -

*Indicates end of beam in which failure occurred.

Table 3.5 Ultimate Shear Strengths

Beam Mark	Type of Web Reinforcement	V_u (kN)	v_u (MPa)	f'c (MPa)	$v_u(f'_c)^{-0.5}$ (SI)	$v_u(f'_c)^{-1}$
1/1.0	Min. Vert.	602	3.17	26.1	0.62	0.121
	None	699	3.68	26.1	0.72	0.141
2/1.0	Min. Horiz.	750	3.95	26.8	0.76	0.147
	Min. Vert. + Min. Horiz.	750	3.95	26.8	0.76	0.147
3/1.0	Min. Vert.	685	3.61	28.9	0.67	0.125
	Min. Vert.	764	4.02	28.9	0.75	0.139
4/1.0	Min. Horiz.	663	3.49	28.5	0.65	0.122
	Min. Horiz.	618	3.25	28.5	0.61	0.114
5/1.0	Max. Vert.	875	4.61	36.9	0.76	0.125
	Max. Vert.	834	4.39	36.9	0.72	0.119
6/1.0	Max. Horiz.	635	3.34	35.8	0.56	0.093
	Max. Horiz.	605	3.18	35.8	0.53	0.089
7/1.0	None	418	2.20	34.5	0.37	0.064
	None	695	3.66	34.5	0.62	0.106
1/1.5	None	303	2.86	42.4	0.44	0.067
	Min. Vert.	354	3.34	42.4	0.51	0.079
2/1.5	Min. Horiz.	226	2.13	42.4	0.33	0.050
	Min. Vert. + Min. Horiz.	348	3.28	42.4	0.50	0.077
3.15	Min. Vert.	242	2.30	14.5	0.61	0.159
	Min. Vert.	287	2.73	14.5	0.72	0.188
4/1.5	Min. Horiz.	206	1.96	32.5	0.34	0.060
	Min. Horiz.	232	2.21	32.5	0.39	0.068
5/1.5	Max. Vert.	565	5.38	39.6	0.86	0.136
	Max. Vert.	566	5.39	39.6	0.86	0.136
6/1.5	Max. Horiz.	256	2.44	45.0	0.36	0.054
	Max. Horiz.	258	2.46	45.0	0.37	0.055
7/1.5	None	222	2.11	30.4	0.38	0.069
	None	348	3.31	30.4	0.60	0.109
8/1.5	Min. Vert. + Min. Horiz.	339	3.23	37.2	0.53	0.087
	Min. Vert. + Min. Horiz.	382	3.64	37.2	0.60	0.098
1/2.0	None	177	1.30	43.2	0.20	0.030
	Min. Vert.	199	2.21	43.2	0.34	0.051
2/2.0	Min. Horiz.	185	2.06	43.2	0.31	0.048
	Min. Vert. + Min. Horiz.	204	2.27	43.2	0.34	0.053
3/2.0	Min. Vert.	261	2.97	42.5	0.45	0.070
	Min. Vert.	277	3.15	42.5	0.48	0.074
4/2.0	Min. Horiz.	195	2.22	38.3	0.36	0.058
	Min. Horiz.	243	2.76	38.3	0.45	0.072
5/2.0	Max. Vert.	453	5.15	41.1	0.80	0.125
	Max. Vert.	456	5.18	41.1	0.81	0.126
6/2.0	Max. Horiz.	186	2.11	37.4	0.35	0.056
	Max. Horiz.	141	1.60	37.4	0.26	0.43
7/2.0	None	185	2.10	46.8	0.31	0.045
	None	150	1.70	46.8	0.25	0.036
5/2.5	Max. Vert.	330	4.65	34.0	0.80	0.137
	Max. Vert.	-	-	-	-	-

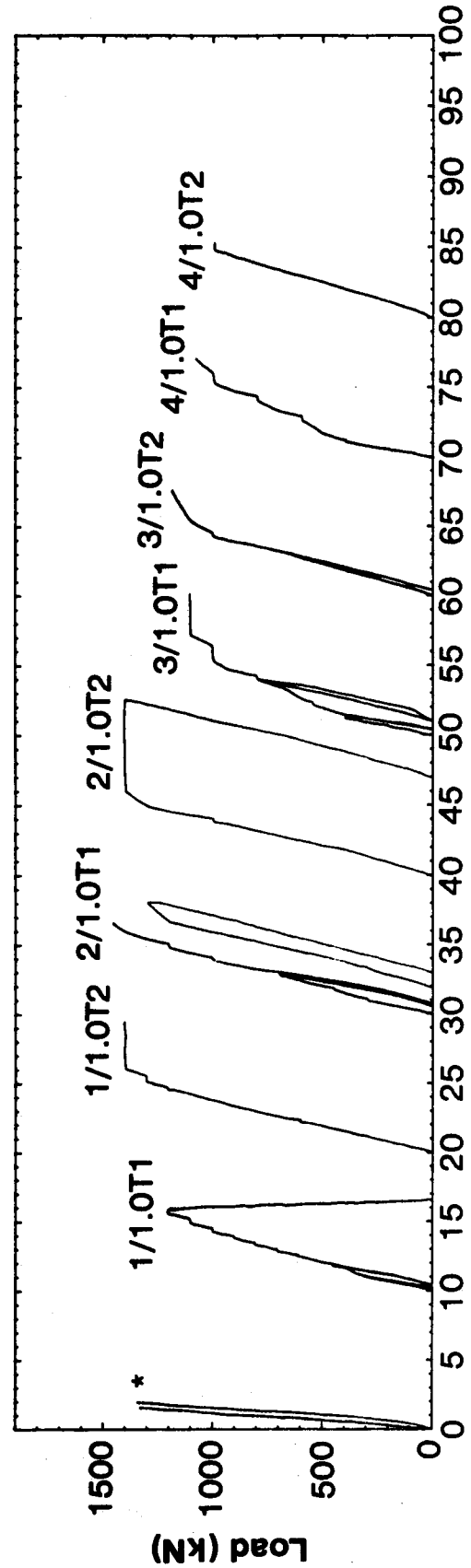

*Range of midspan deflection due to suport settlement

Figure 3.6. Beam 1/1.0, 2/1.0, 3/1.0, and 4/1.0 Load Deflection Curves

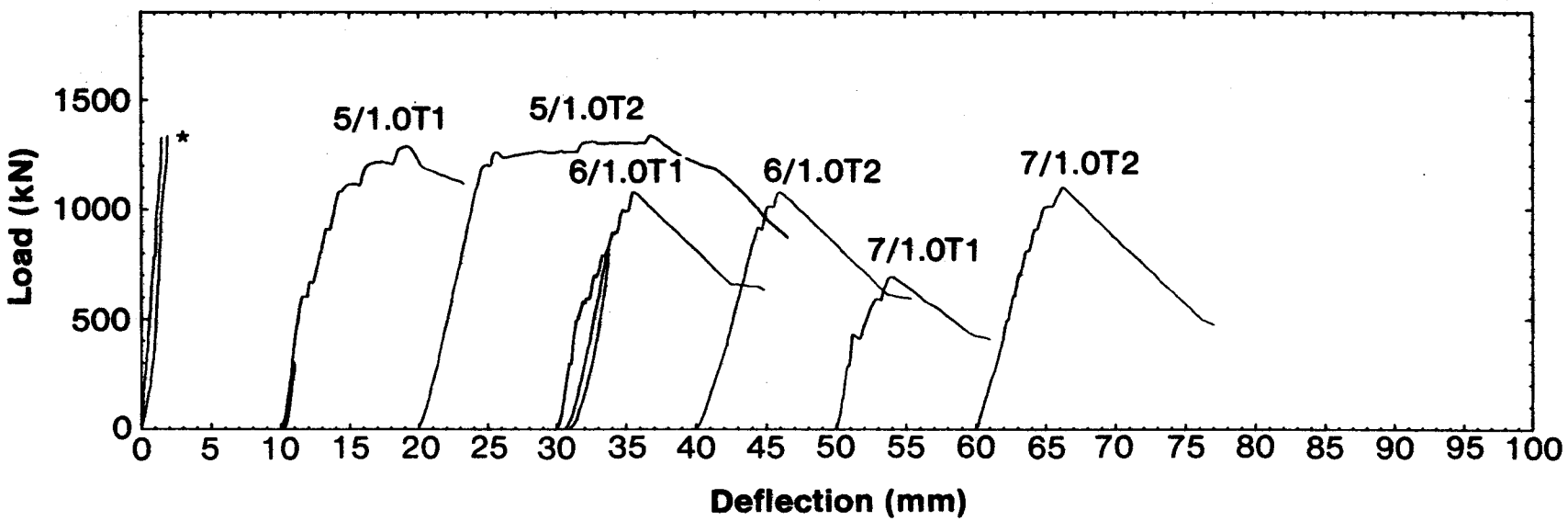

*Range of midspan deflection due to support settlement

Figure 3.7. Beam 5/1.0, 6/1.0, and 7/1.0 Load Deflection Curves

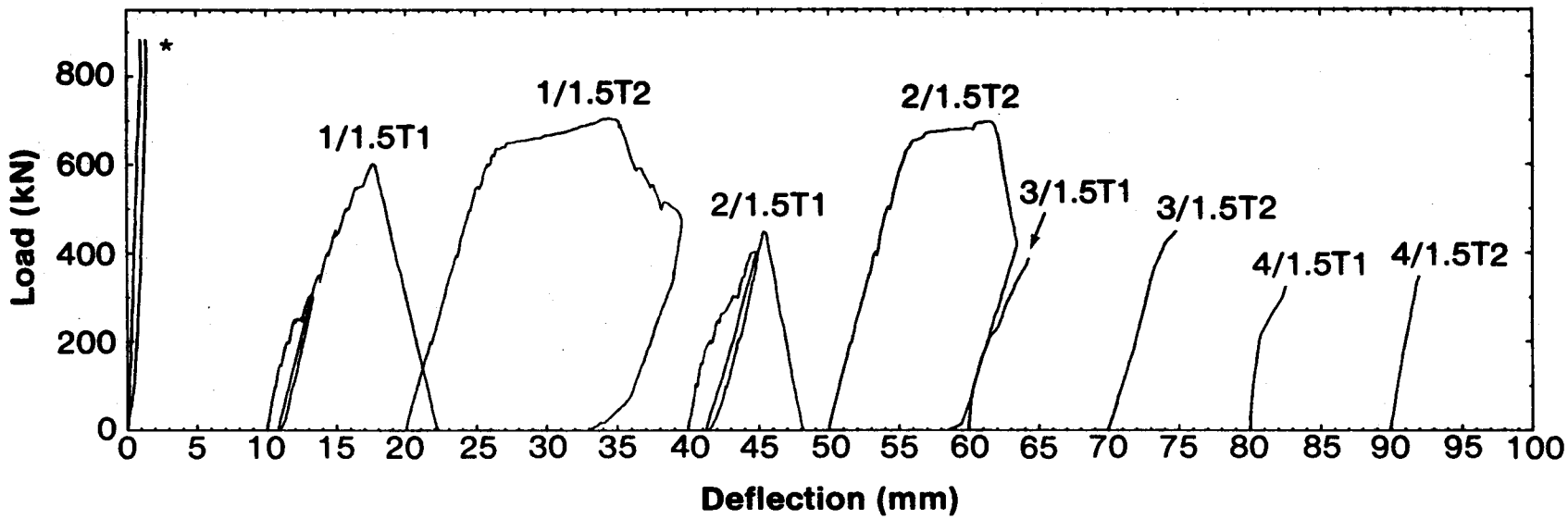

*Range of midspan deflection due to support settlement

Figure 3.8. Beam 1/1.5, 2/1.5, 3/1.5, and 4/1.5 Load-Deflection Curves

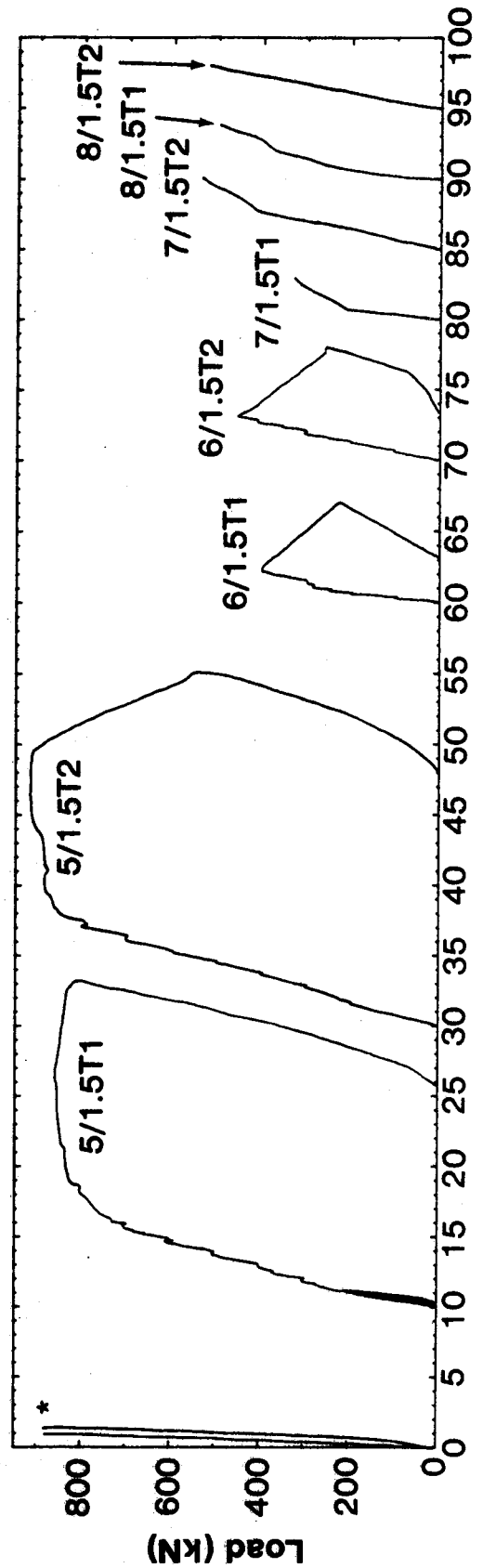

*Range of midspan deflection due to support settlement

Figure 3.9. Beam 5/1.5, 6/1.5, 7/1.5, and 8/1.5 Load-Deflection Curves

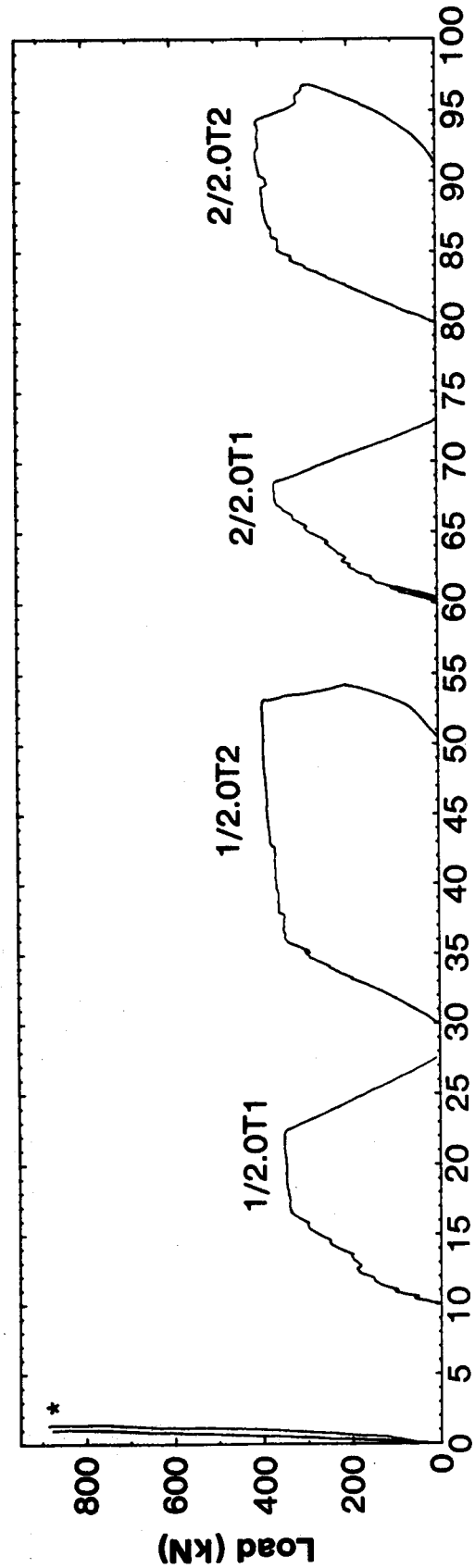

*Range of midspan deflection due to support settlement

Figure 3.10 Beam 1/2.0 and 2/2.0 Load-Deflection Curves

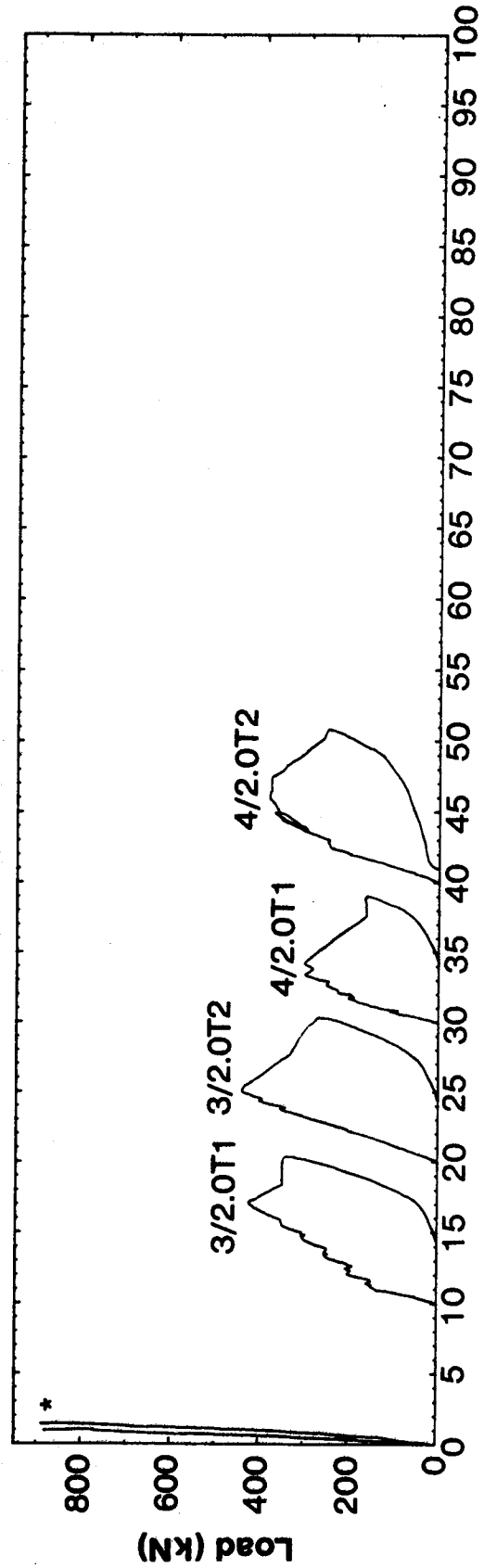

*Range of midspan deflection due to support settlement

Figure 3.11. Beam 3/2.0 and 4/2.0 Load-Deflection Curves

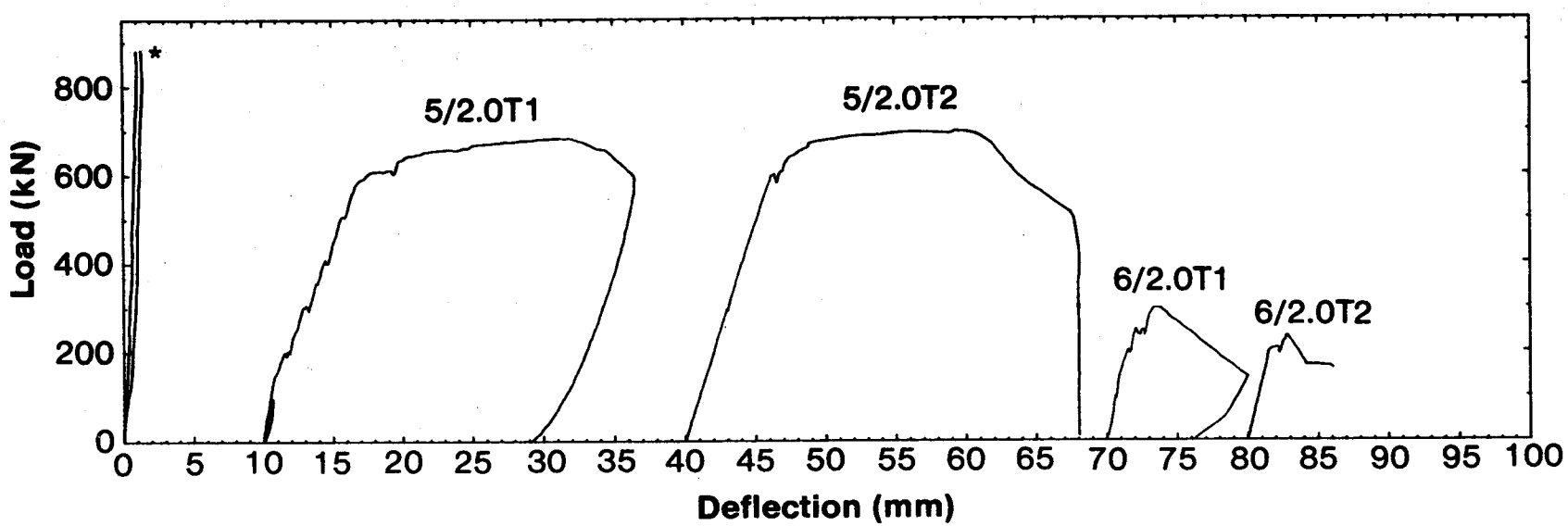

*Range of midspan deflection due to support settlement

Figure 3.12. Beam 5/2.0 and 6/2.0 Load-Deflection Curves

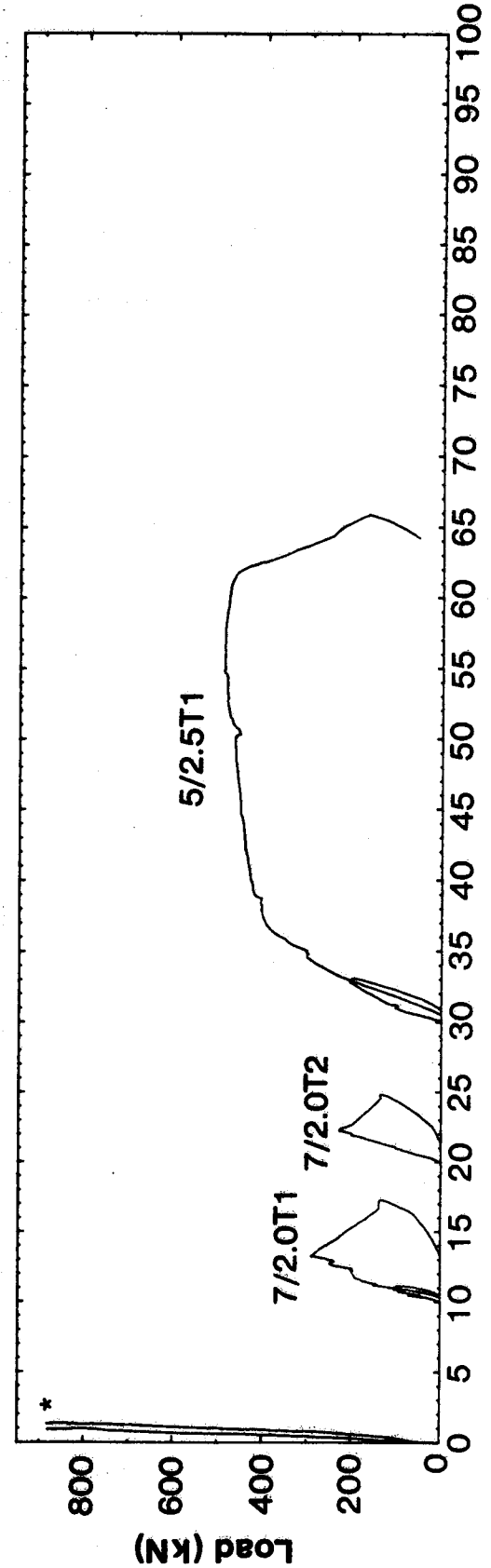

*Range of midspan deflection due to support settlement

Figure 3.13. Beam 7/2.0 and 5/2.5 Load-Deflection Curves

sketch of the beam. Only the principal compressive strains are shown for clarity with a crossing line representing the location of the rosette. Two figures are used to present the steel strain data. The first includes an elevation of the beam showing the location of the reinforcement and Demec targets superimposed on the crack pattern. Directly below this, the steel strains are plotted as a function of the position along the bars. A second plot relates the strain in selected gage locations to the applied jack load. In the latter figures, heavy solid lines are used for bottom main steel, light solid lines are used for top main steel, and broken lines for web steel. Data are presented for the following specimens:

Figure	Beam	Typical of:
3.14(a) to (e)	1/1.0	simple span deep beam
3.15(a) to (d)	5/1.0	continuous deep beam with heavy stirrups
3.16(a) to (d)	6/1.0	continuous deep beam without heavy stirrups

Beam 1/1.0 which is documented in Fig. 3.14(a) to (e) is typical of the behavior of simple span deep beams without stirrups or with light stirrups. Major inclined cracks developed almost instantaneously at a jack load of about 350 kN. The cracks appeared to be very severe even though the load was only about 25% of the eventual failure load. After inclined cracking, the behavior was essentially that of a truss or tied-arch. This is evident in the concrete

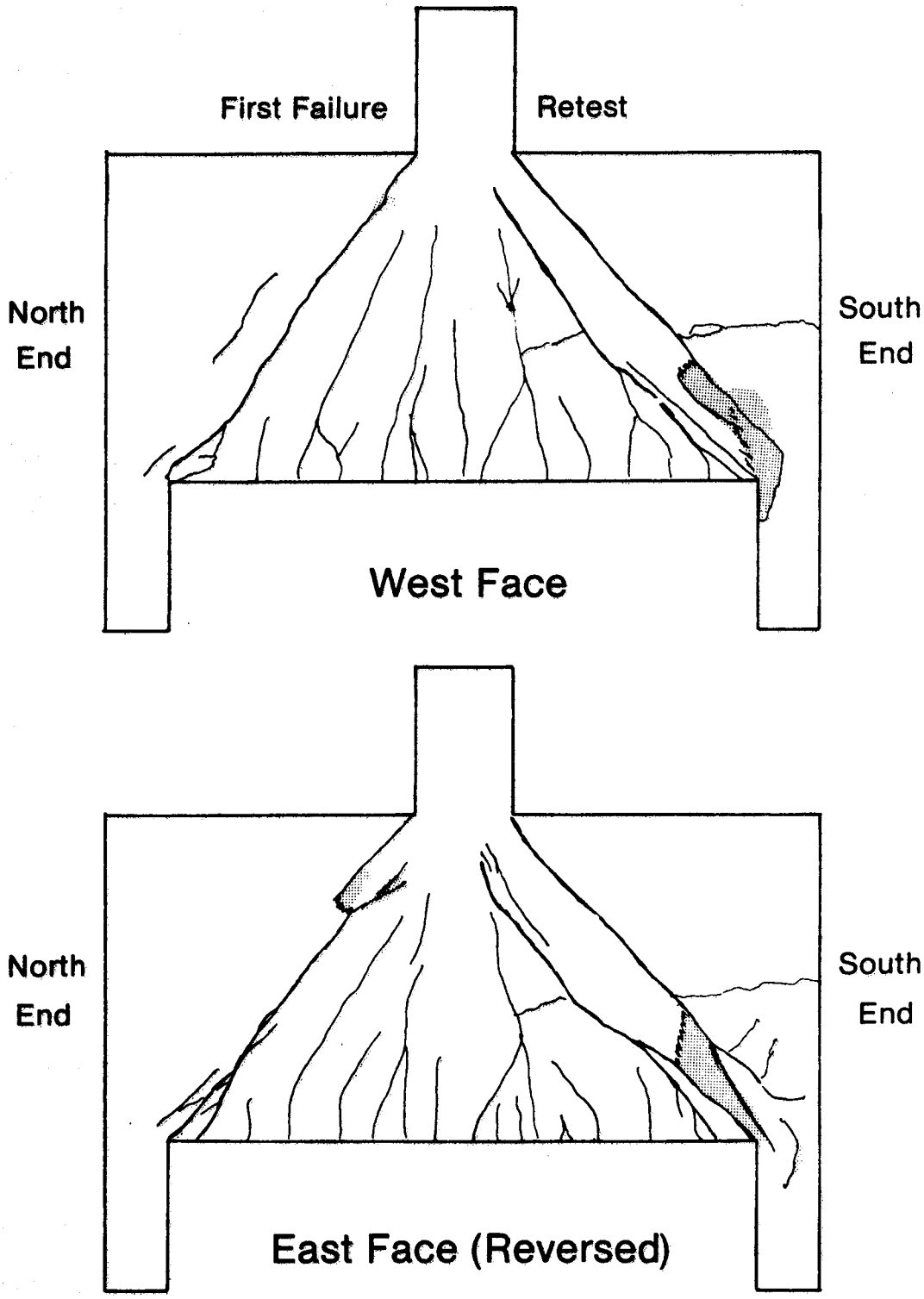

Figure 3.14(a) Beam 1/1.0 Crack Patterns

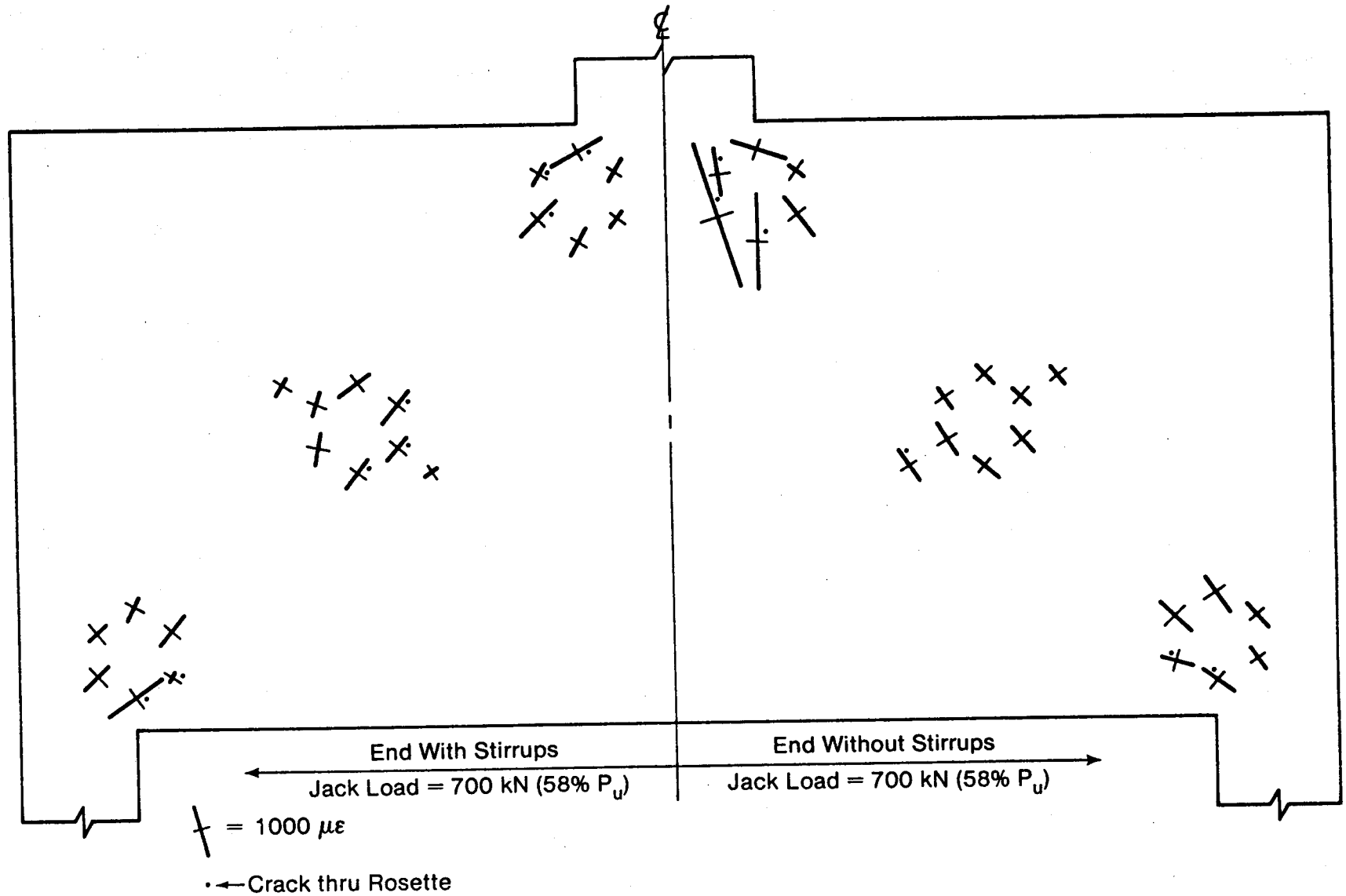

Figure 3.14 (b) Beam 1/1.0 Concrete Compressive Strains

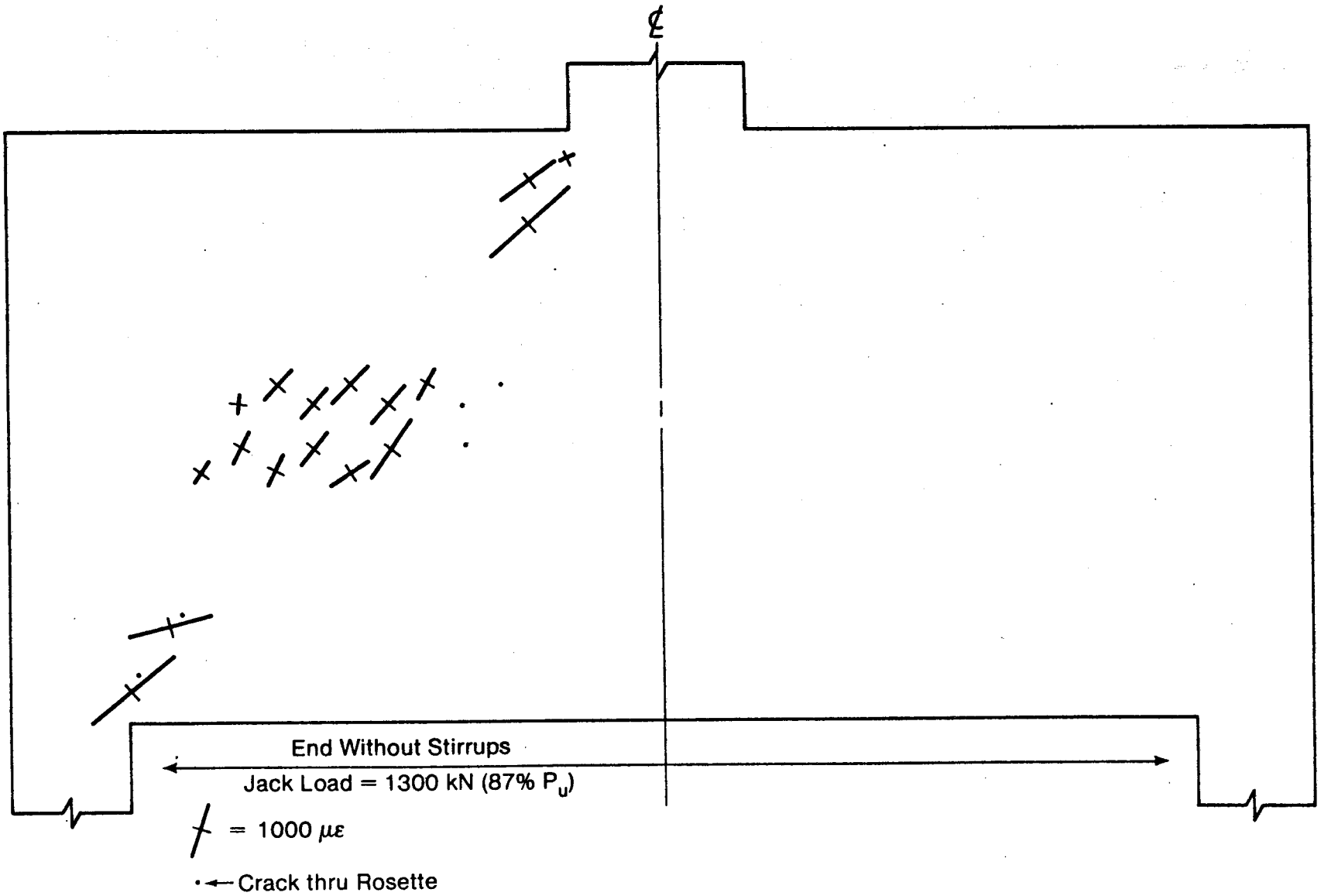

Figure 3.14 (c) Beam 1/1.0 Retest Concrete Compressive Strains

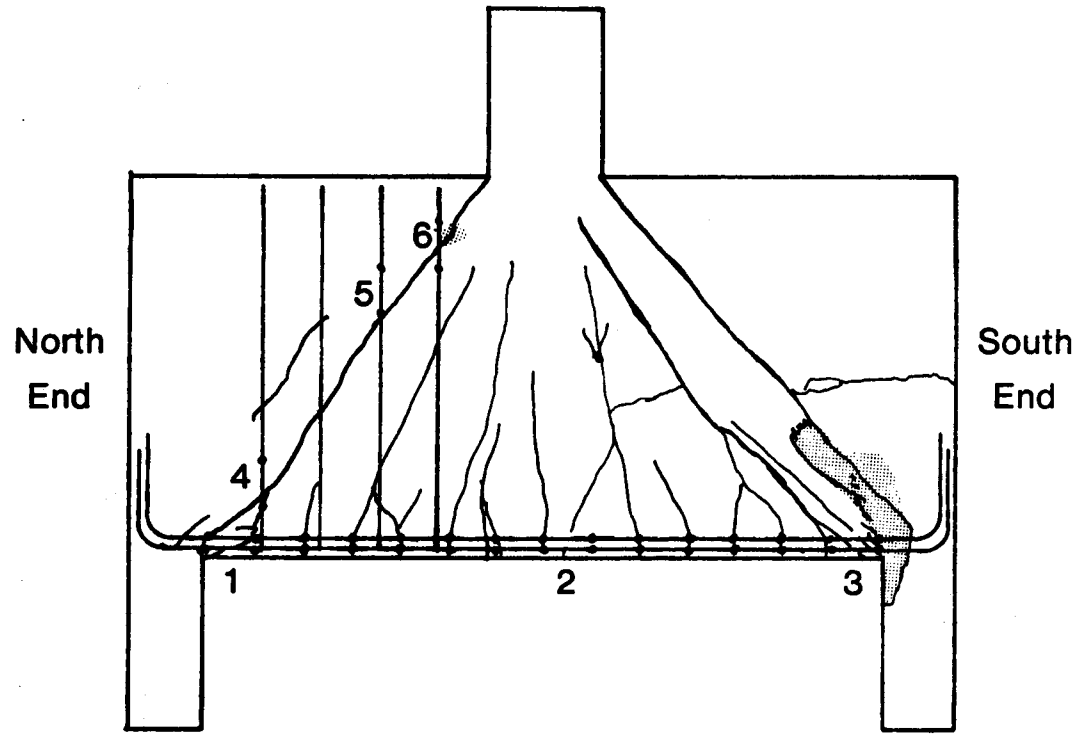

Gage Locations

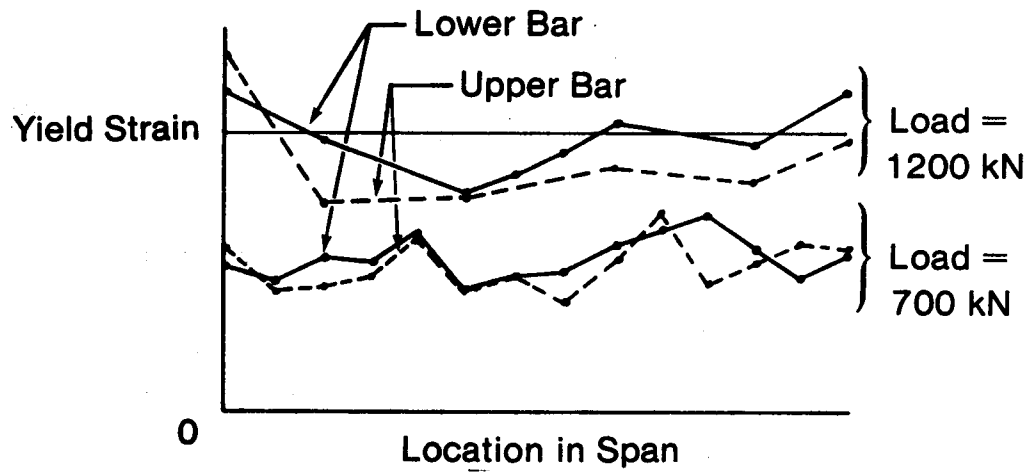

Main Steel Strains

(Strain Scale: 1mm = 50 Micro-Strain)

Figure 3.14 (d) Beam 1/.1.0 Steel Strains.

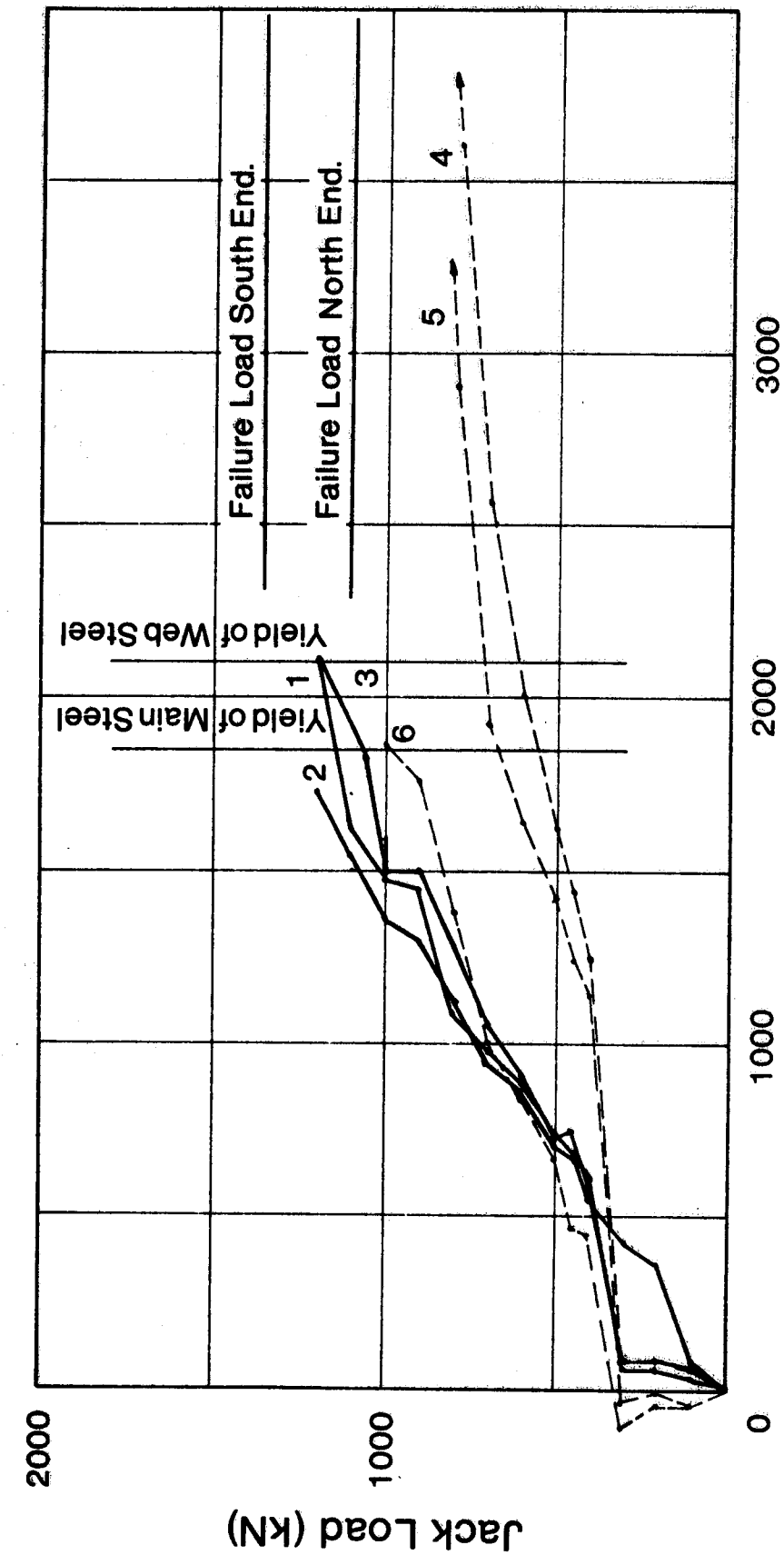

Figure 3.14(e) Beam 1/1.0 Load vs. Steel Strain

strain diagrams (Fig. 3.14(b) and (c)) which show bands of compressed concrete joining the load and reactions and in the steel strain diagrams (Fig. 3.14(d)) which show almost constant steel strains from end to end. The stirrups crossing the major inclined crack in the North shear span were at or near yield at failure. Some of these reached yield at 50 to 60 percent of the failure load. Ultimate failure was due to crushing of the compression strut as shown in Fig. 3.14(a) or (d). Although the north end had stirrups it failed first (T1) at a lower load and deflection than the south end.

Beam 5/1.0 (Fig. 3.15(a) to (c)) was typical of a continuous deep beam with heavy stirrup reinforcement. Even though there were a large number of stirrups present, inclined cracking still occurred with a loud 'thud'. There were crack "fans" over the interior support and under each load. The compression struts formed between the cracks making up these fans and tended to be less well defined than in other continuous beams. The steel strain diagrams in Fig. 3.15(c) resembled the bending moment diagrams shifted away from points of maximum moment rather than being constant as expected in a simple truss as observed in Specimen 1/1.0 (Fig. 3.14(d)). Ultimate failure was due to crushing near the top of the compression strut in the interior shear span. This was often precipitated by vertical opening of the inclined cracks which tended to pull the compression strut apart. The failure was very ductile

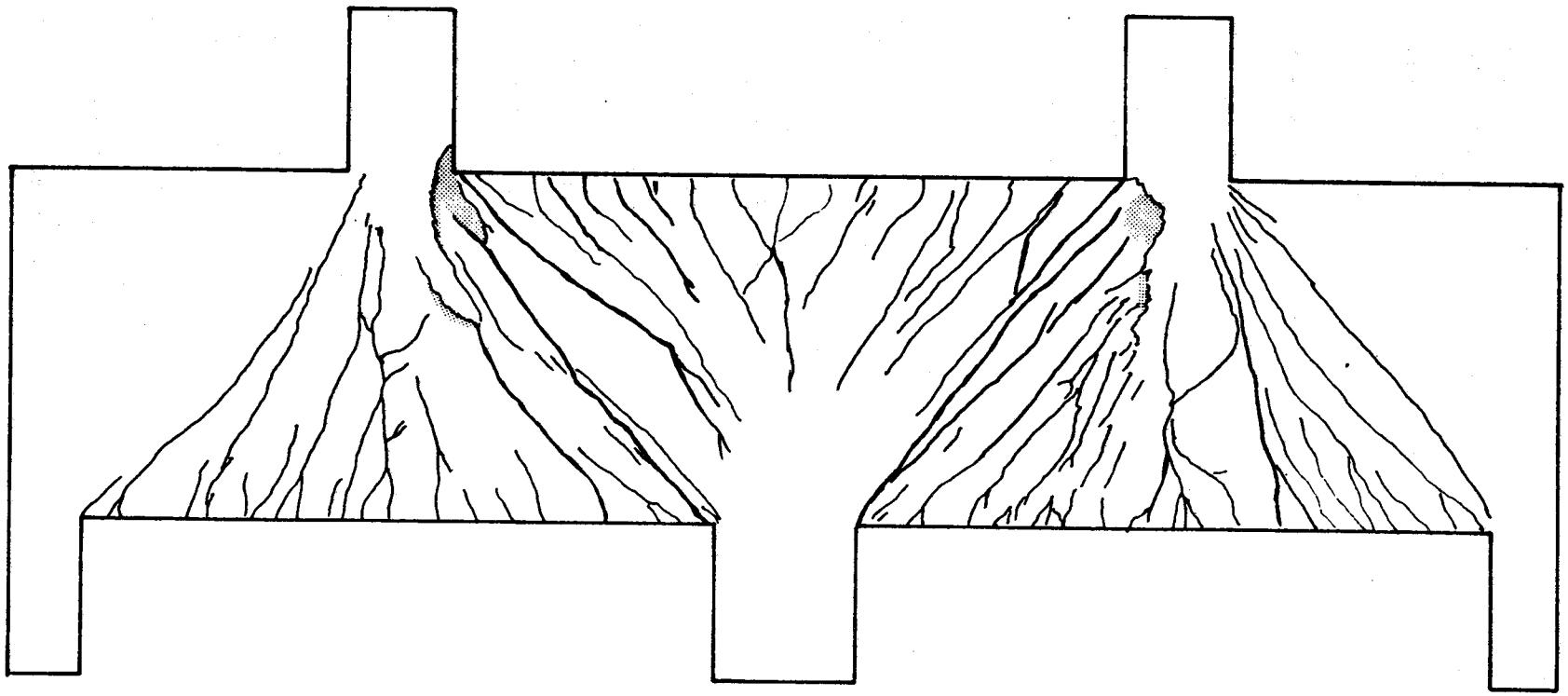

Figure 3.15(a) Beam 5/1.0 Crack Pattern – West Face

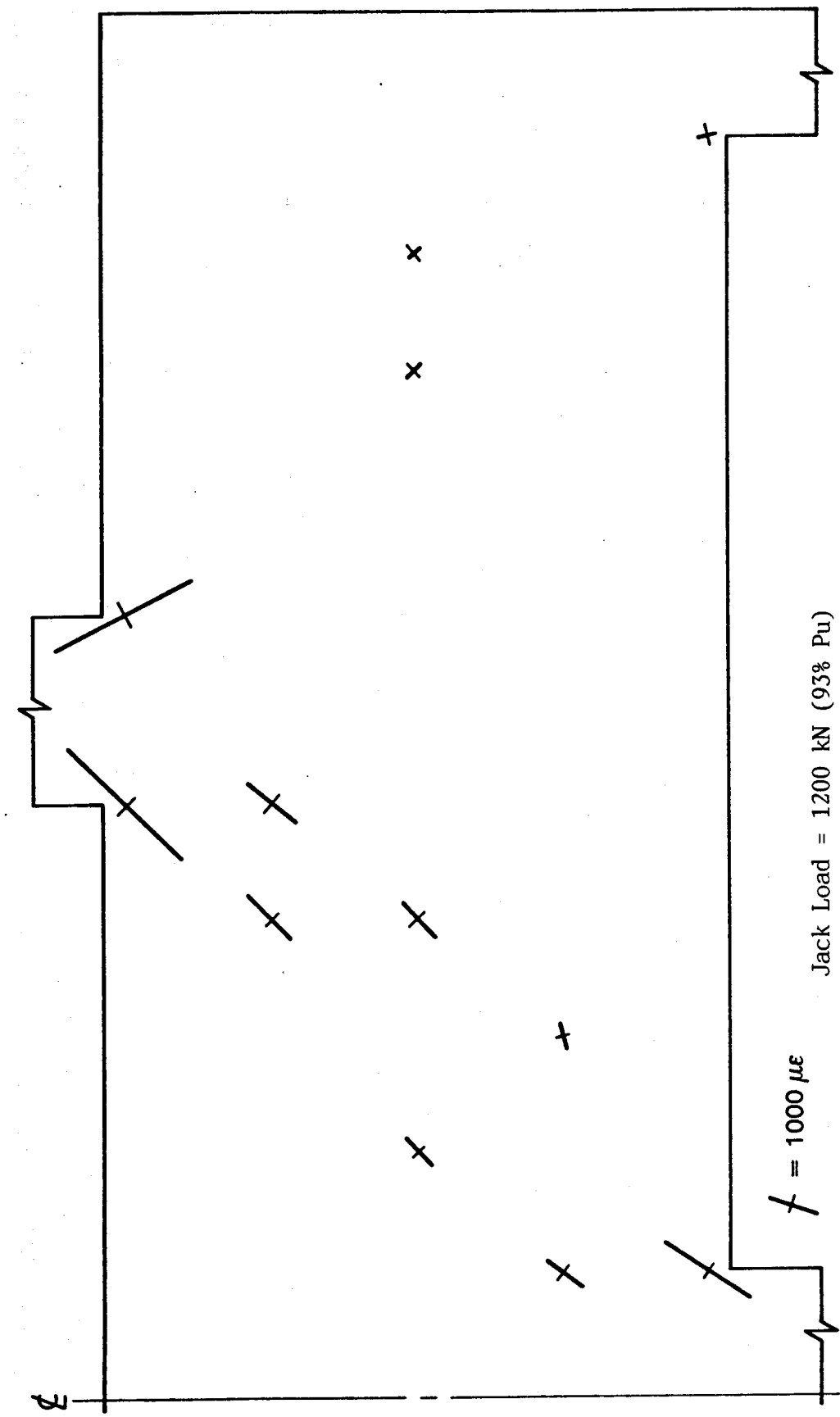

Figure 3.15 (b) Beam 5/1.0 Concrete Compressive Strains

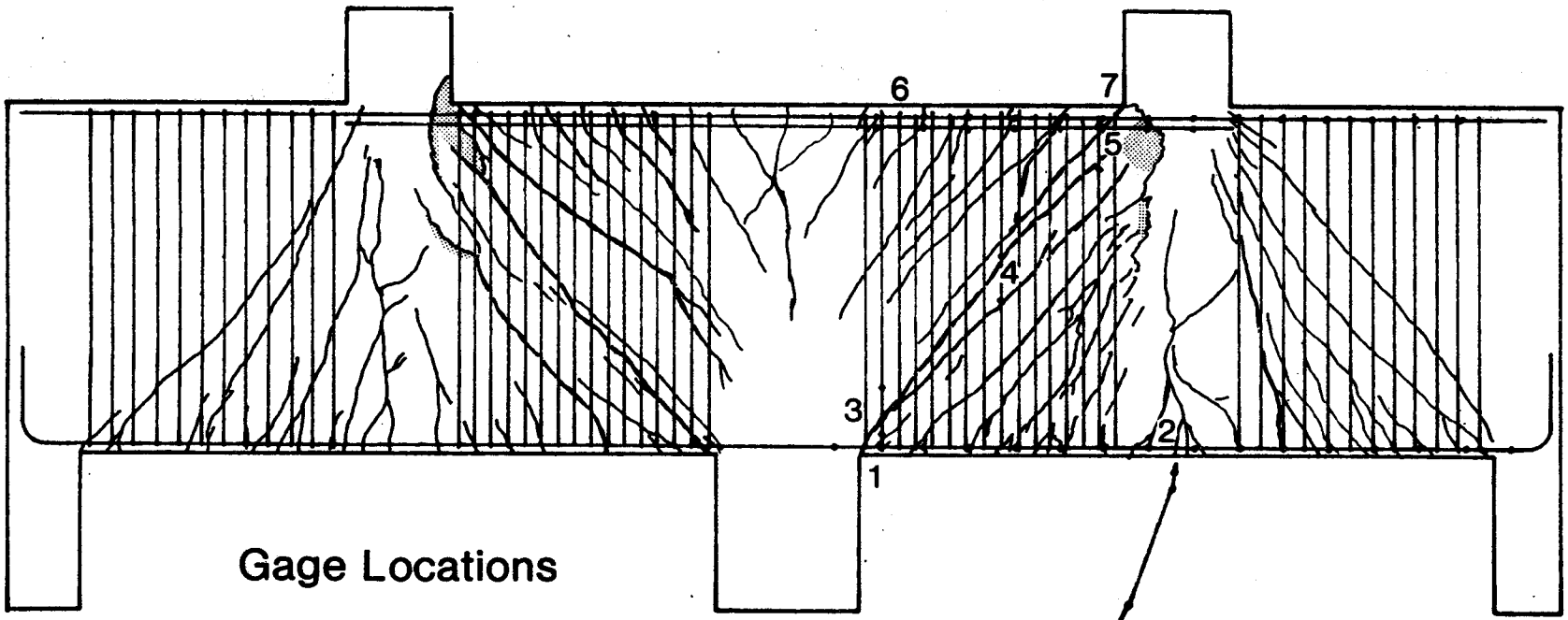

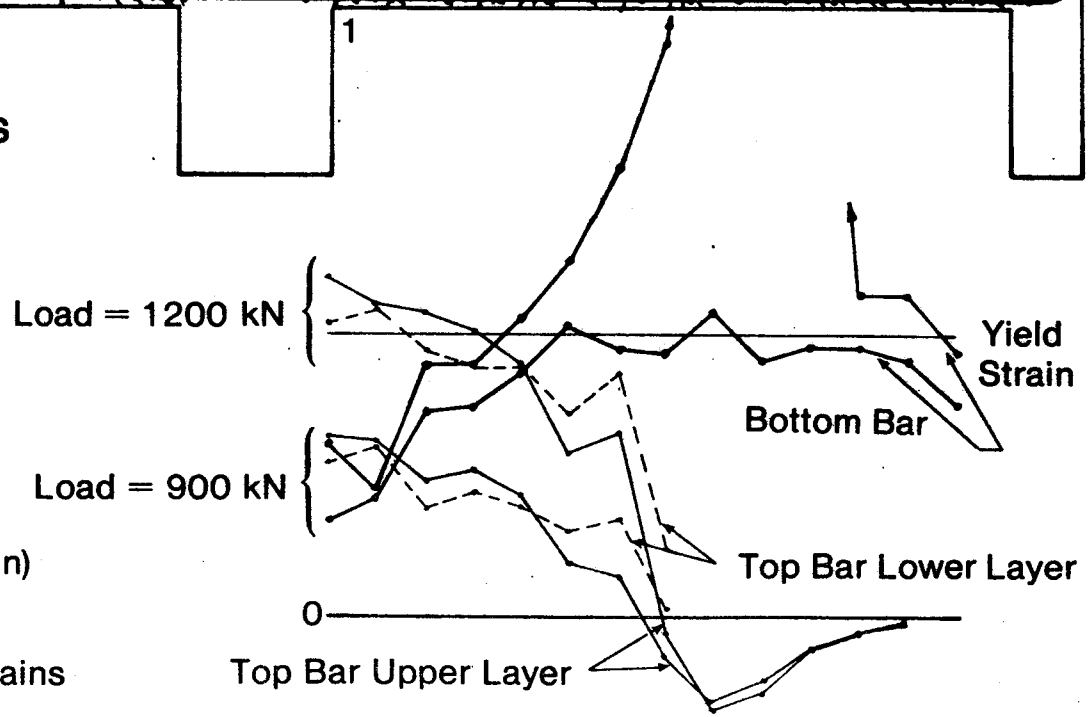

Main Steel Strains

(Strain Scale: 1mm = 50 Micro-Strain)

Figure 3.15(c) Beam 5/1.0 Steel Strains

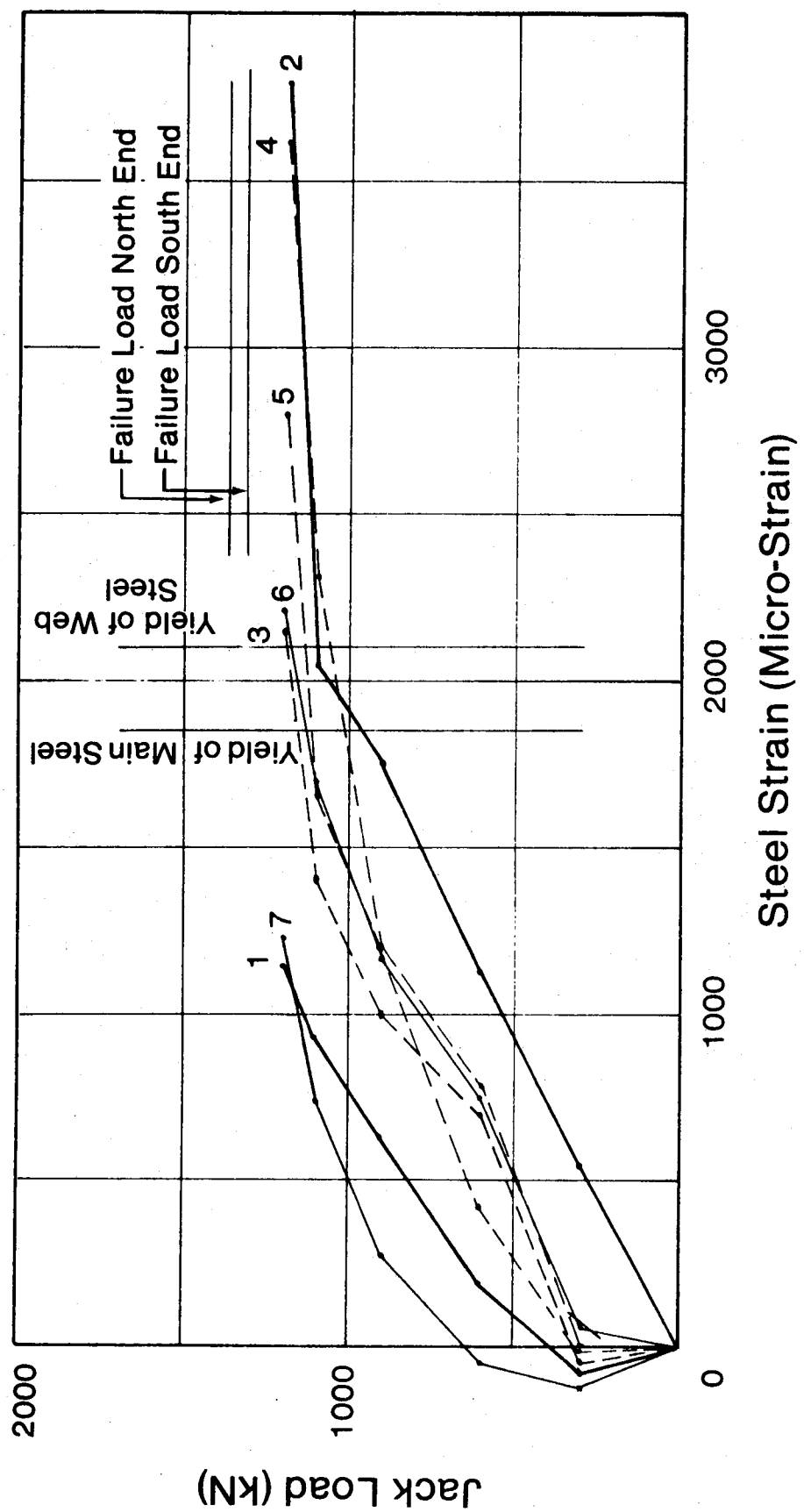

Figure 3.15(d) Beam 5/1.0 Load vs. Steel Strain

as can be seen from the load deflection curves in Fig. 3.7. This was true for all 5/xx beams.

Beam 6/1.0 was typical of a continuous beam without heavy stirrups (Fig. 3.16). There was little difference in behavior for beams with no web reinforcement, minimum stirrups, minimum horizontal web reinforcement, or maximum horizontal web reinforcement. Inclined cracks developed in a sudden manner. The crack fans mentioned above, were not well developed in these beams. The beams did not have a period of significant ductility during which the cracks could develop. In the deeper beams, ultimate failure was by crushing of the compression strut accompanied by opening of the inclined cracks. For the shallower beams (X/2.0) the failures tended to be caused by diagonal tension or opening of the inclined crack. At loads near failure the strain in the longitudinal steel tended to remain constant rather than following the bending moment diagram as shown in Fig. 3.16(c). These beams were brittle, and in many instances, failure occurred before the main steel yielded.

3.4 Summary of Observed Behavior

In summary, two main types of behavior were observed. Beams without stirrups or with minimum stirrups approached tied-arch action at failure. This was true regardless of the amount of horizontal web reinforcement present. These failures were sudden with little or no plastic deformation. On the other hand, beams with large amounts of stirrups failed in a ductile manner.

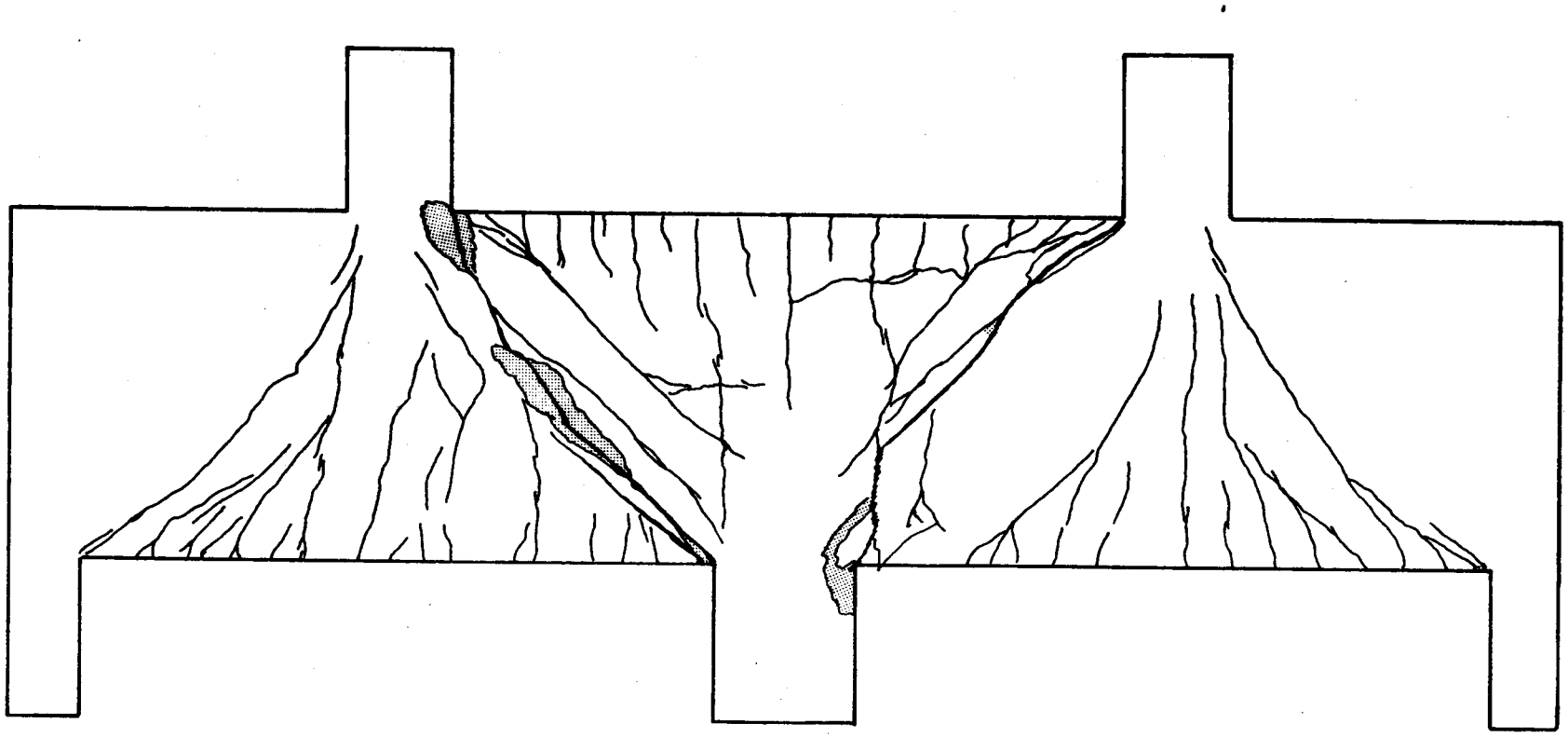

Figure 3.16(a) Beam 6/1.0 Crack Pattern – West Face

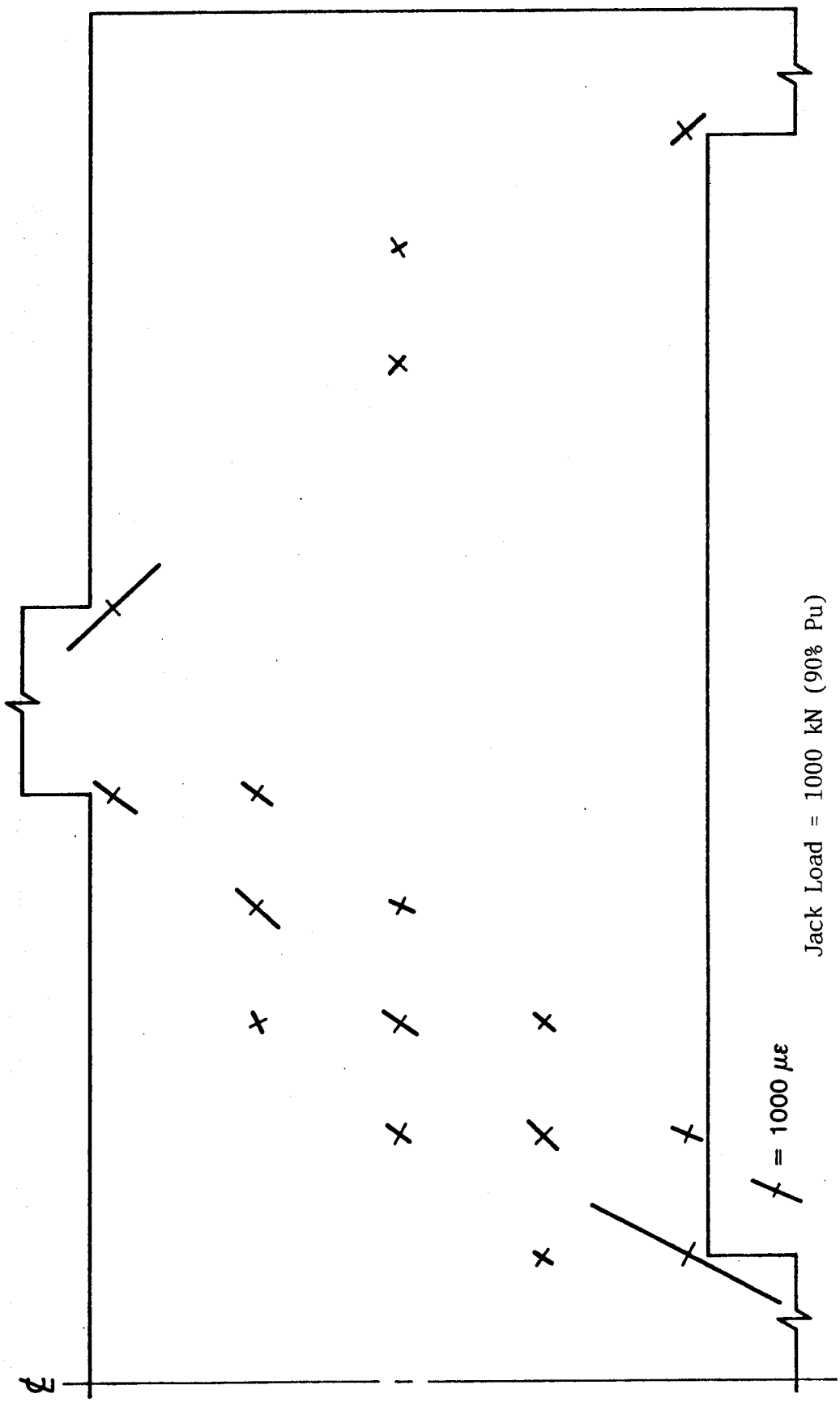

Figure 3.16 (b) Beam 6/1.0 Concrete Compressive Strains

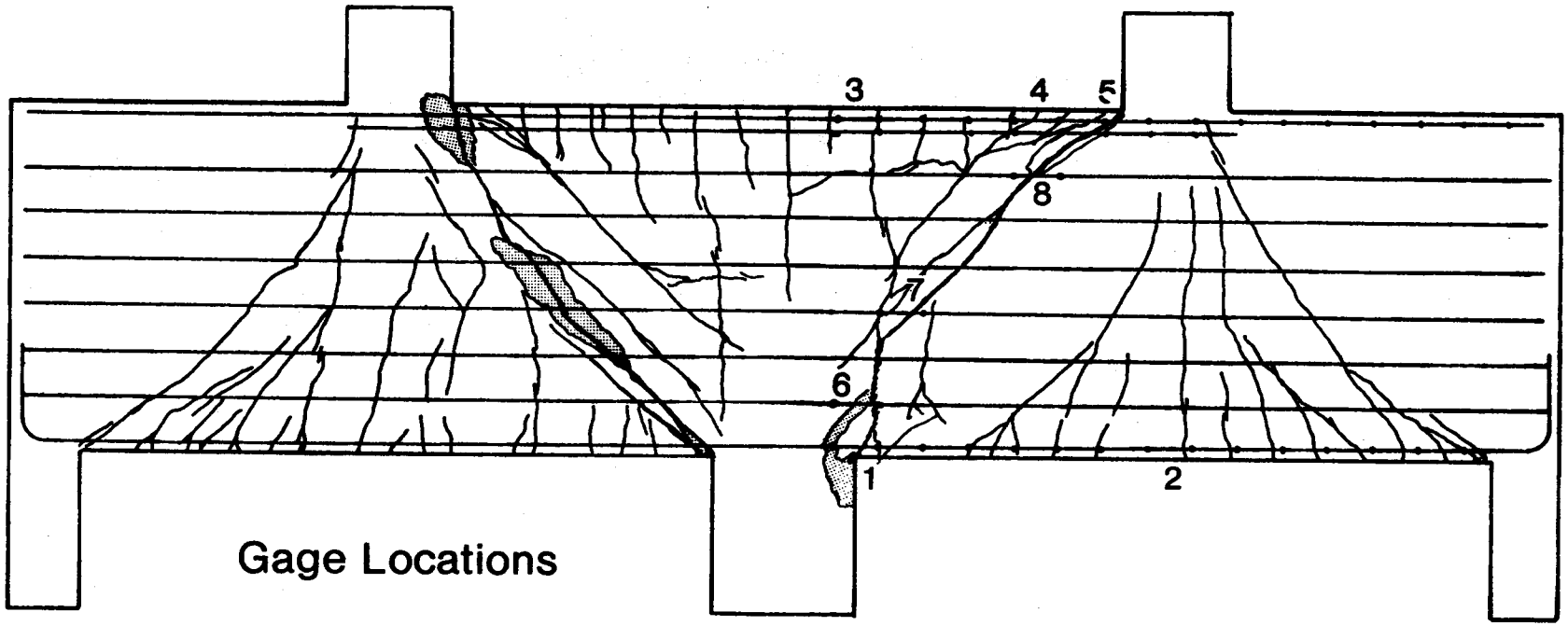

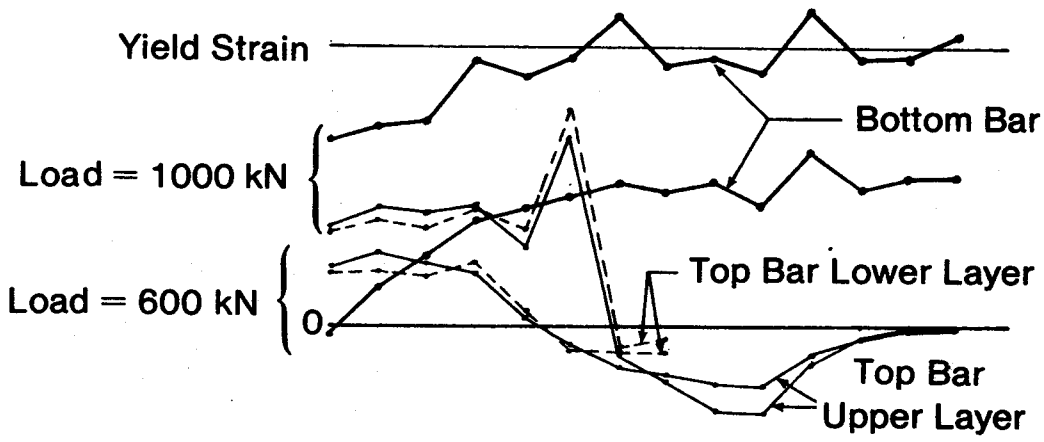

Main Steel Strains

(Strain Scale: 1mm = 50 Micro-Strain)

Figure 3.16(c) Beam 6/1.0 Steel Strains

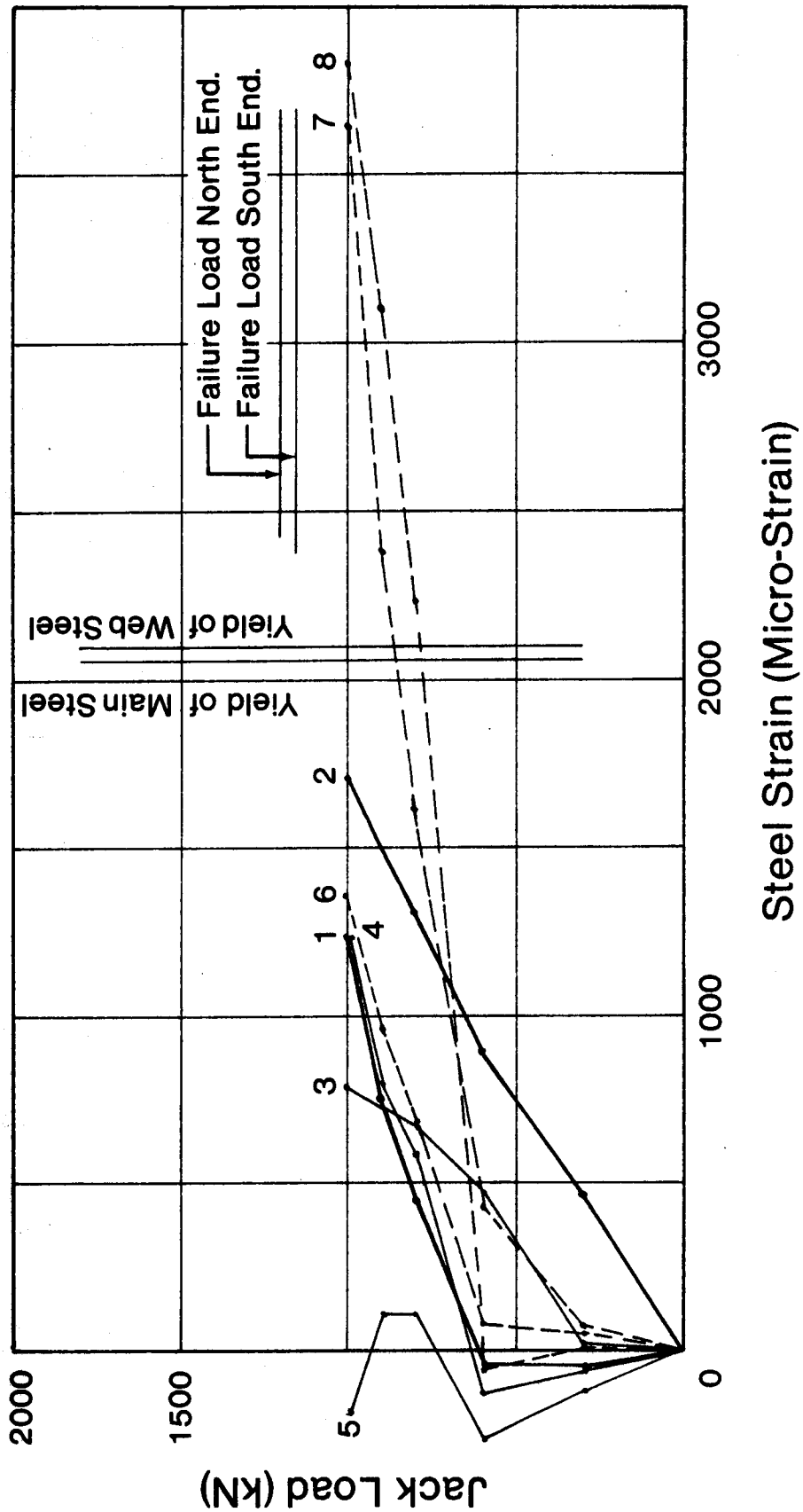

Figure 3.16(d) Beam 6/1.0 Load vs. Steel Strain

4. INTERPRETATION OF RESULTS

4.1 Introduction

This chapter consists of an interpretation of the data and a synthesis of the problem in the light of the data. This results in the proposal of a simple conceptual model of behavior. An overview of this model is presented in this chapter. The model will be developed more fully in the next chapter.

4.2 Evaluation of the Data

The test data will be evaluated by considering a number of different aspects of the deep beam problem. The effects of statical condition; ratio of vertical web reinforcement, ρ_v; ratio of horizontal web reinforcement, ρ_h; shear span to depth ratio, a/d; and concrete strength, f'_c can be examined by considering concrete strains, steel strains, ductility, type of failure, and ultimate shear strength.

First, consider the jack load vs. midspan deflection diagrams shown in Figs. 3.6 to 3.13. A qualitative evaluation of the curves indicates that there is no signficant systematic difference in behavior of the specimens between the virgin test, T1 and the retest, T2. In general, beams without stirrups had very little ductility. Continuous beams with heavy stirrups were ductile while those with light stirrups were fairly brittle. On the other hand, simple span beams with light

stirrups showed some ductility.

Comparison of the load deflection curves for all the continuous beams in each series of a/d, indicate that with the exception of the 5/xx beams which had maximum stirrups, all of the beams had approximately the same strength regardless of the type of web reinforcements. See Fig. 3.9 for example. There are some variations in strength between beams, but these may be due to variations in concrete strength between specimens. In any event, the variations between different specimens is of the same order as variations in strength between the virgin test and the retest of a given specimen. Direct comparison of shear strength between simply supported and continuous beams is not possible from the jack load vs. deflection curves because the maximum shear in a simple beam is 1/2 the jack load while the maximum shear in a continuous beam is approximately 2/3 of the jack load.

Further evaluation of the strength data requires quantitative comparisons which remove the influence of variations in the concrete strength and statical system. These variations can be accounted for by using v_u/f'_c or $v_u/\sqrt{f'_c}$ in comparisons of shear strength at failure. Which parameter should be used is not clear. In shallow beams it is common to correlate the shear stress with $\sqrt{f'_c}$; Smith and Vantsiotis (1982) found that for their deep beams, better correlations were obtained using f'_c. Both $v_u/\sqrt{f'_c}$ and v_u/f'_c are given in Table 3.5. Plots were actually made

using both parameters. Figures 4.1 to 4.,4 are presented for the latter parameter only. It was found that both v_u/f'_c and $v_u/\sqrt{f'_c}$ produced the same general trends except for beam 3/1.5 which had a very low concrete strength of 14.5 MPa. The data for this beam was higher on the diagram when correlated to v_u/f'_c .

Figures 4.1 to 4.4 indicate the influence of the statical system (simple span vs. continuous), a/d, and web reinforcement type. As there are only about 10 data points on each of these figures it is not possible to draw statistically significant conclusions. The data for the simple span beams has been compiled together in Fig. 4.5. There is no distinguishable difference in strength between the various types of web reinforcement. The data for the continuous beams has been compiled in Fig. 4.6. Again, there is no distinguishable difference between specimens except for those with maximum vertical stirrups shown with solid points. For maximum stirrups, the shear strength does not appear to be influenced by a/d. None of the simple span specimens had heavy stirrup reinforcement, so it was uncertain whether a similar insensitivity to a/d occurs in simple spans.

A composite diagram of all the data is presented in Fig. 4.7. The envelopes for simple span and continous span data have been superimposed on the Figure. Simple span beams appear to be stronger than continuous beams for low a/d ratios, while the reverse is true for high a/d ratios.

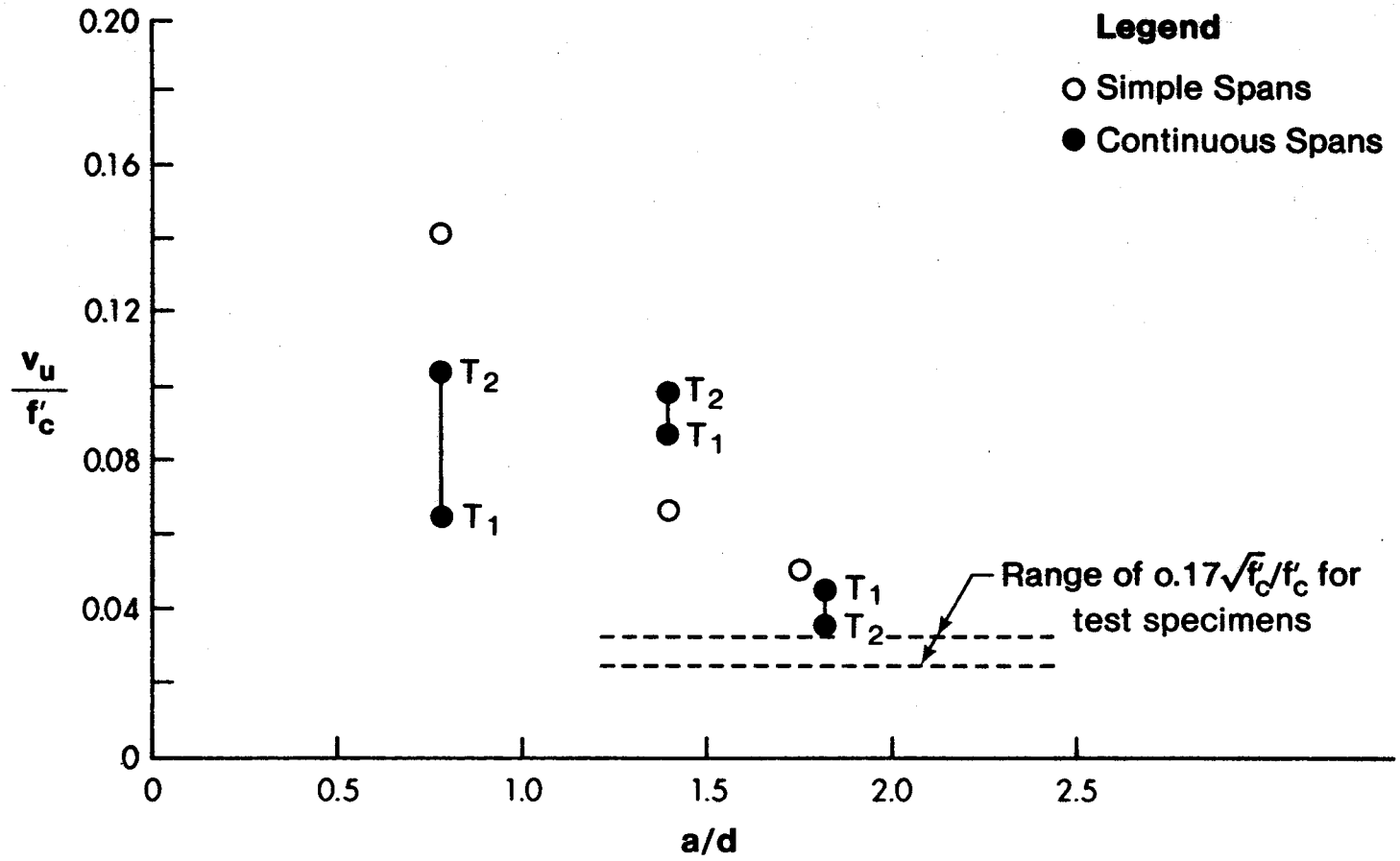

Figure 4.1. Shear Strength For Beams Without Web Reinforcement.

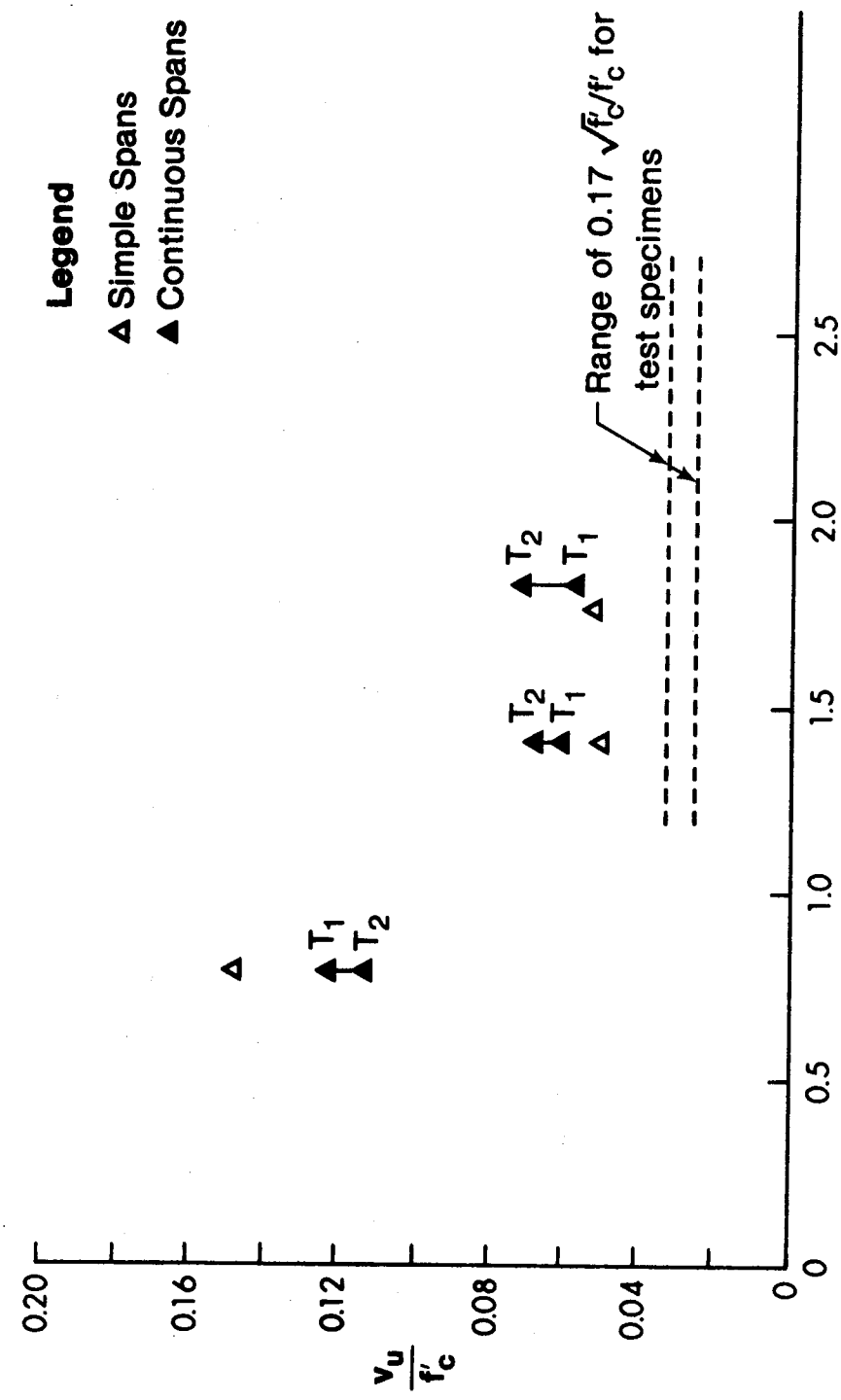

Figure 4.2. Shear Strength For Beams With Minimum Horizontal Web Reinforcement Only.

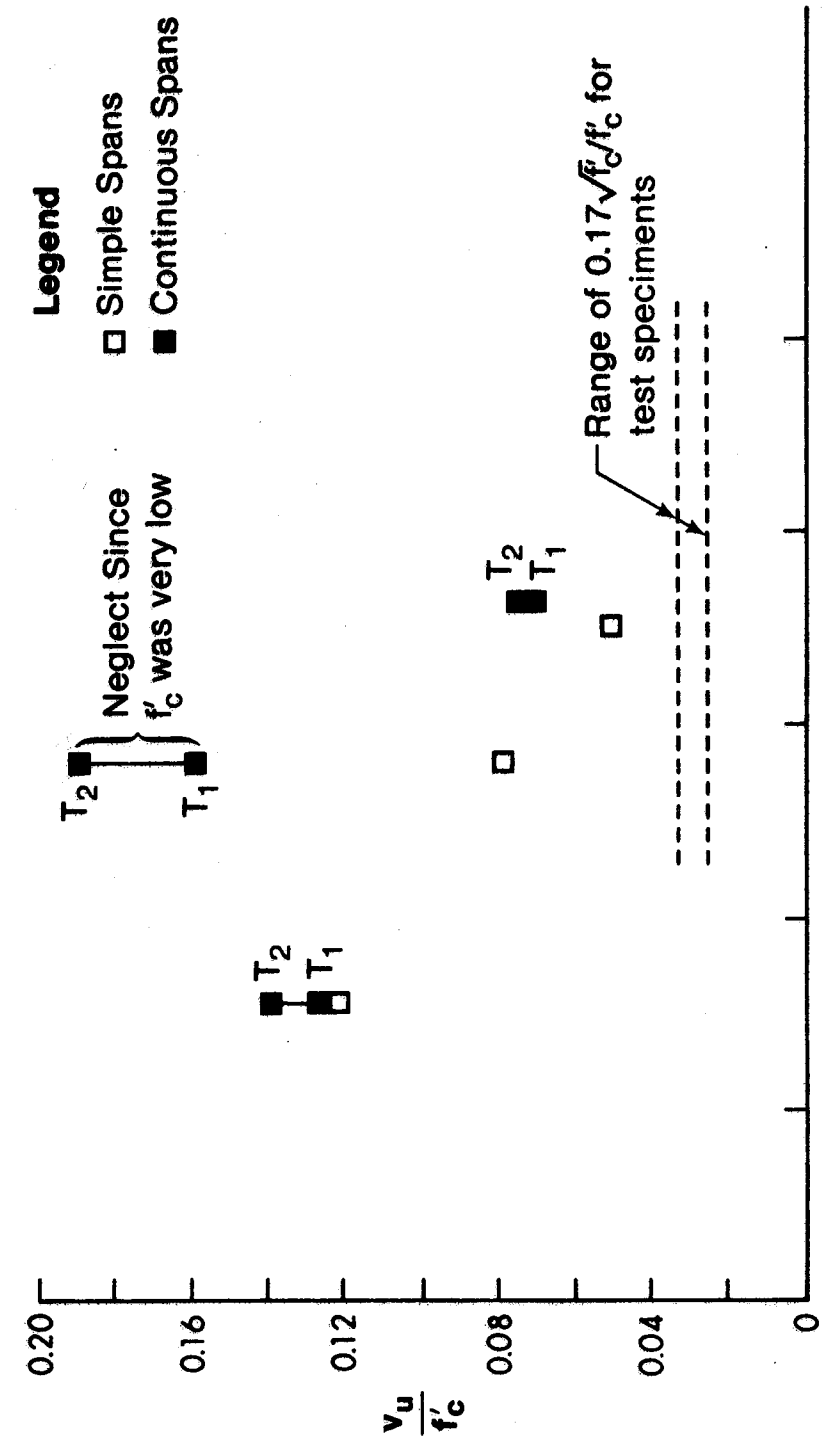

Figure 4.3. Shear Strength For Beams With Minimum Stirrups Only.

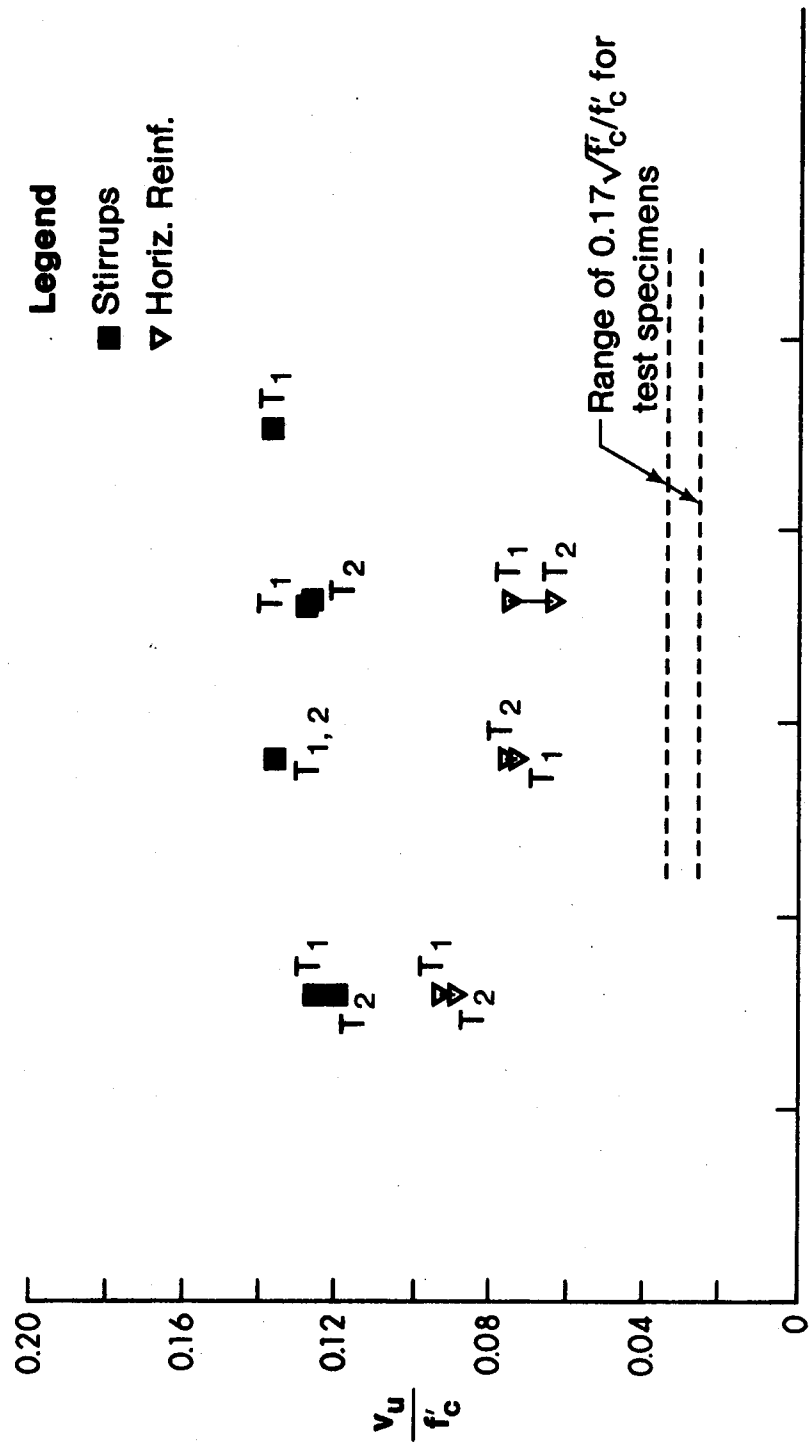

Figure 4.4. Shear Strength For Continuous Beams With Maximum Stirrups or Maximum Horizontal Web Reinforcement.

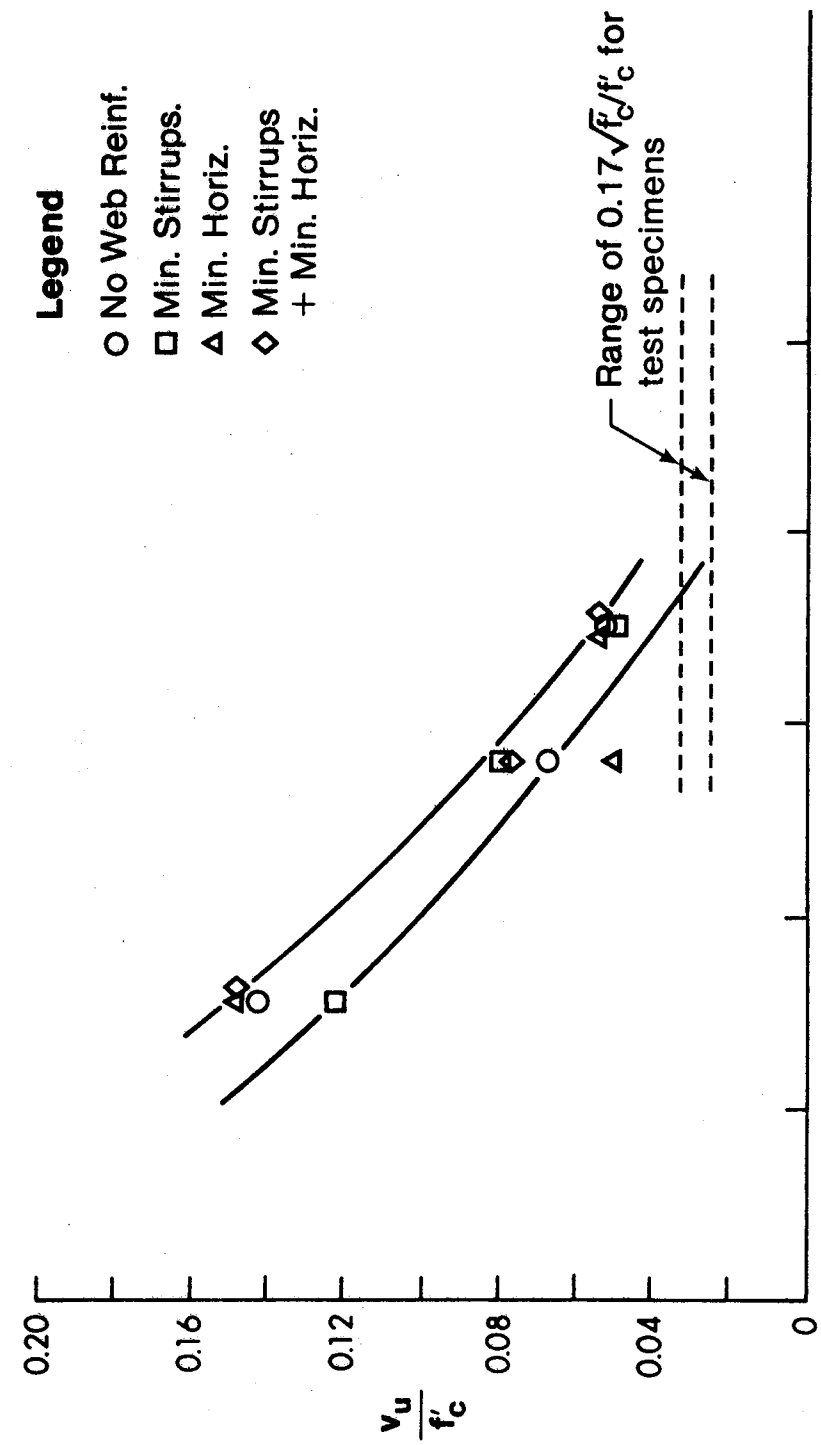

Figure 4.5. Shear Strength For Simple Shear Spans.

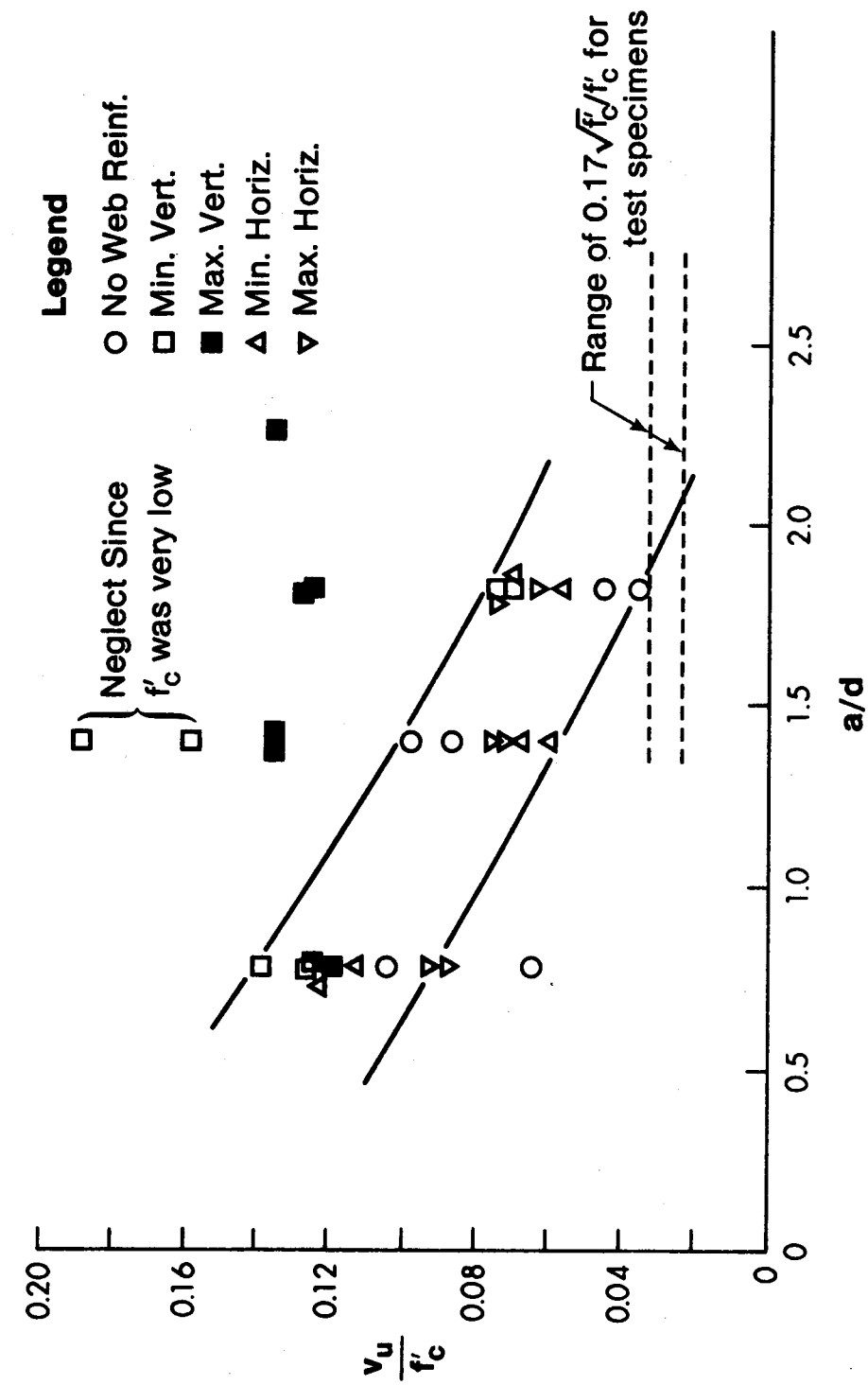

Figure 4.6. Shear Strength For Continuous Shear Spans.

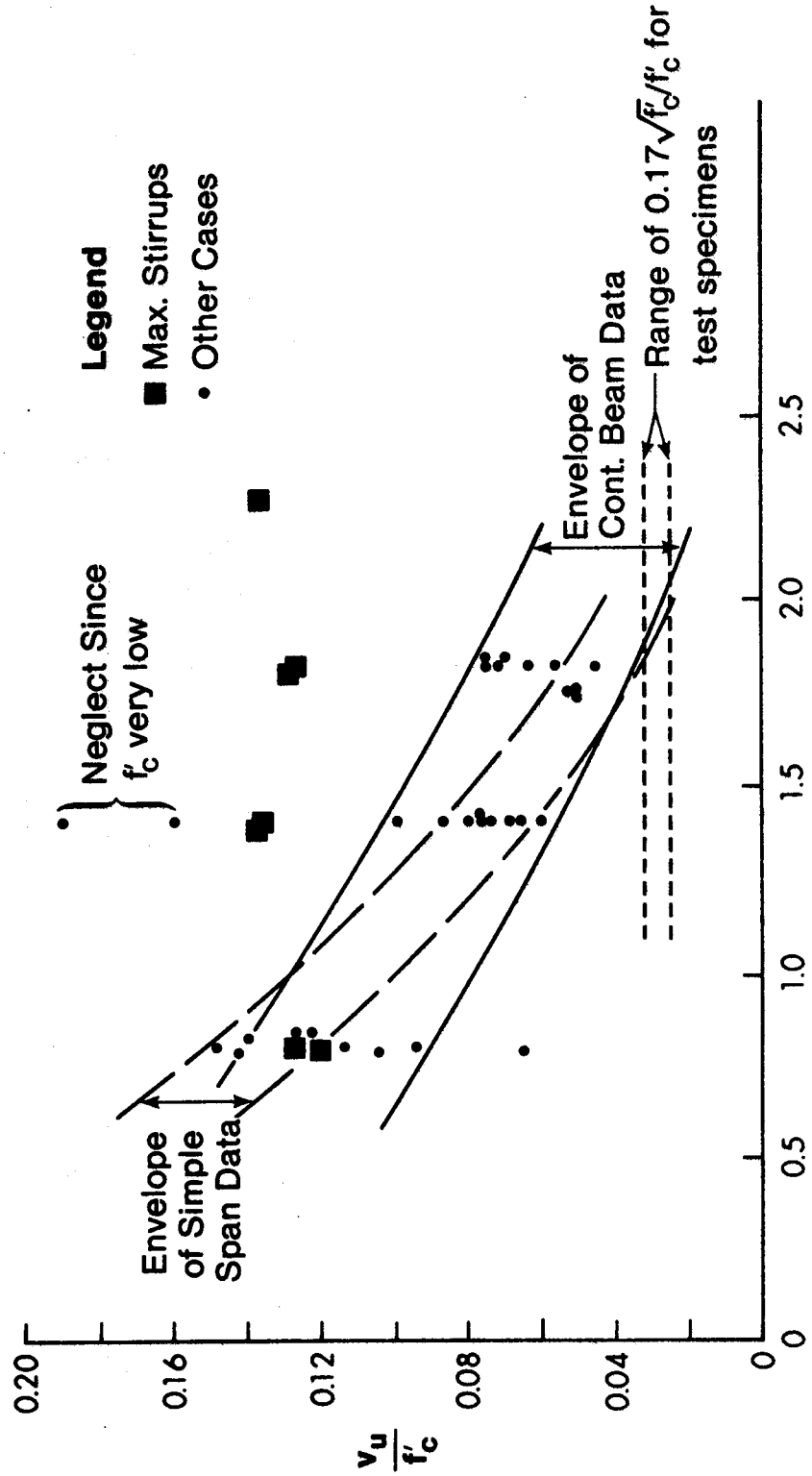

Figure 4.7. Comparison of Shear Strengths For All Test Specimens.

On the other hand, beams with heavy stirrup reinforcement are not affected by the a/d ratio at all.

At an a/d ratio of about 2, the strength of the deep beams has dropped close to $0.17\sqrt{f'_c}$ suggesting that the transition from shallow beam to deep beam behavior occurs near a/d = 2.0.

At this point, it should be re-emphasized that the specimens exhibit two different types of behavior. Beams with heavy stirrups exhibit ductile behavor with very good agreement between the virgin and retest strength. All other beams regardless of the type of web reinforcement had brittle failures. For the continuous beams the virgin and retest strengths varied considerably, but not consistently.. That is, sometimes the beam was weaker in the retest, and sometimes it was stronger. Beams without web reinforcement had the greatest variability (See Beam 7/1.0 for example). Beams with heavy or light horizontal web reinforcement have less, but still significant variability of strength. Beams with light stirrups have even less variability, but still had up to a 15% difference in strength between the virgin test and retest. It appears that while light web reinforcement does not significantly increase the average shear strength of a deep beam, it does lead to more consistent and repeatable results.

4.3 Conceptual Model

The significant experimental observations which a model must explain are:

1) In members without stirrups, the flexural steel strains are constant along the bars between point loads and supports
2) In members without stirrups subjected to point loads, compression struts develop in the concrete which carry the loads directly to the supports. The vertical component of the strut force, and hence the shear capacity is very dependent on a/d.
3) In beams without stirrups, the failures were sudden and were due to crushing of the concrete compression struts.
4) When sufficient stirrups are present, flexural steel strains vary along the bars in approximate accordance with a shifted bending moment diagram. However, the top and bottom steel can have significant tension strain at the face of the load and support columns respectively.
5) When sufficient stirrups are present, crack fans develop under the loads, and over the interior support. These cracks diminish the effective width of any direct compression strut which might develop. The reduction in the amount of shear force carried by direct strut action is indicated by the lack of influence of a/d (the strut slope) on the

total shear capacity.

6) When sufficient stirrups are present, failures were very ductile and were initiated by general yielding of the stirrups.

What physical model explains these observations? The shear friction models of Crist (1971), Kong (1977), etc. reviewed in Chapter 2, do not correctly predict the influence of horizontal and vertical web reinforcement, and do not consider the forces developed along the flexural reinforcement. The truss analogies based on plasticity theory (Fig. 2.5), do predict all 6 observations in a qualitative sense. The question is, "can they also give acceptable quantitative results?" This is considered in Chapter 5.

5. PLASTIC TRUSS MODELS

5.1 Introduction

This chapter deals with the development of plastic truss models. The simple conceptual models of Chapters 2 and 4 will be expanded into detailed computational models, and will be calibrated against the available data. Limits of application for the plastic truss model (PTM) will be examined.

Emphasis in this chapter is on analysis rather than design. The problem in analysis is to determine the strongest plastic truss which fits within, and is compatible with the geometry of the beam. This work is an extension and application of work done by Marti (1978), Müller (1981), Thürlimann (1978), and Nielsen et al. (1978).

5.2 Basic Assumptions

In the application of the plastic truss model one idealizes the beam as a pin jointed truss with concrete acting as compression members and steel acting as tension members. The basic assumptions used are:

1) Equilibrium must be satisfied
2) Elastic strains are negligible compared to the yield strains.
3) The concrete only resists compression and has an effective compressive strength $f_c^* = \nu f_c'$, where $\nu < 1.0$.

4) Steel is required to resist all tensile forces.

5) Failure of the truss analog occurs when it forms a mechanisms due to either a concrete compression member crushing, or a steel tension member yielding.

The basic assumptions lead to several corollaries. They are:

1) The centroid of each truss member and the lines of action of all external loads at a joint must coincide. With a concurrent force system there is no moment in the joint making the assumption of a pinned joint reasonable.

2) Concrete compression struts (shown by light shading in truss diagrams presented later in this chapter) are in uniaxial compression with a uniform stress of f_c^* at the ultimate load. The end faces of a strut are principal stress faces and must be perpendicular to the longitudinal axis of the strut. The values of f_c^* are discussed in Section 5.4.

3) Joints are accommodated by using "hydrostatic stress elements" (shown by dark shading in truss diagrams) in which both principal stresses are equal to f_c^*. While these elements are usually triangular, they may have any polygonal shape, but must have a uniaxial compression stress equal to f_c^* acting on each face or facet of the element within the plane of the beam. (These elements do not have true hydrostatic stress because the stresses on the "free faces" will not be

equal to f_c^*. The Mohr's Circle for the inplane stresses does, however, plot as a point which is characteristic of true hydrostatic stress.)

4) Bearing plates, support conditions and details must be such that local bearing and anchorage failures do not occur.

The assumptions and corollaries given here relate specifically to the plastic truss model. They represent a special case of the more general theory of plasticity in reinforced concrete which is given in Appendix A.

5.3 Analysis of Beams Using the Plastic Truss Model

Use of the plastic truss model will be demonstrated with three hypothetical examples. Beams without web reinforcement, with horizontal web reinforcement, and with vertical stirrups are considered.

The first example consists of a simply supported beam without web reinforcement. The beam is subjected to a point load at midspan. Figure 5.1 illustrates an appropriate truss model for one half of the beam. The concrete which is utilized as part of the truss is shown shaded, with struts (uniaxial compression zones) in light shading and hydrostatic stress elements (biaxial compression zones) in dark shading. The widths of the shaded areas should be drawn to scale, that is, the cross-sectional area of a strut times the effective concrete strength f_c^* should equal the force in the strut. The truss as drawn must, of course, fit

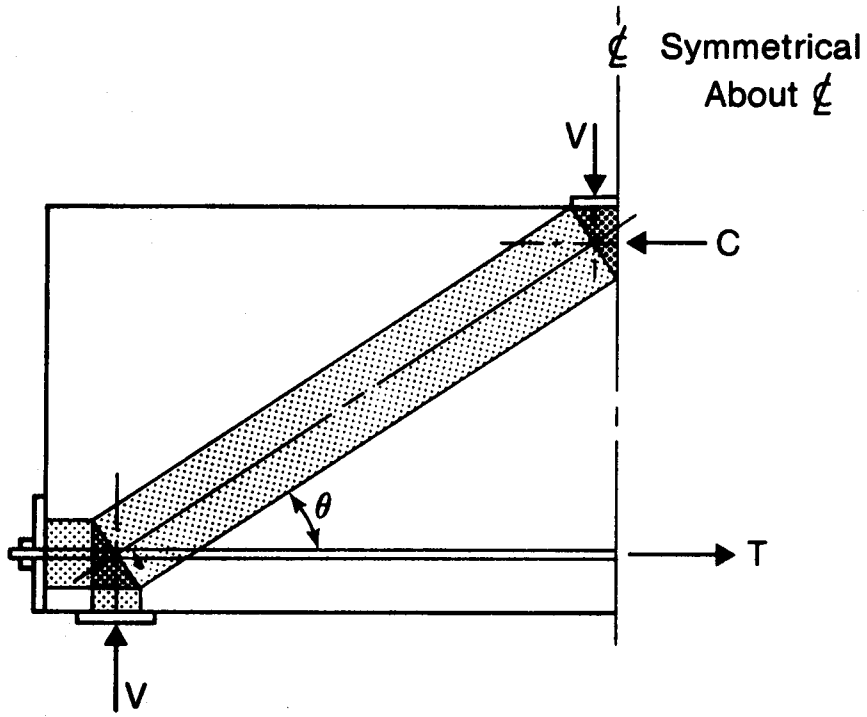

(a) Plastic Truss Model

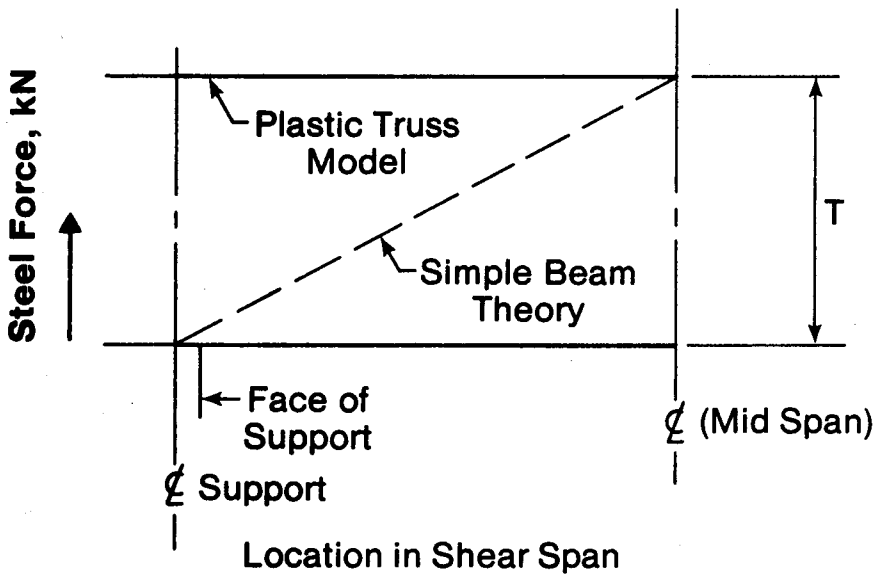

(b) Force in Bottom Steel

Figure 5.1 Plastic Truss Model for Beam Without Web Reiforcement

within the overall beam geometry. The truss in this example is statically determinate, and barring detail failures, the maximum capacity of the truss will be obtained when the tension steel yields, or the compression strut crushes. Generally the latter event will not occur if it is possible to draw a larger strut that satisfies corollary one and still remains within the beam geometry.

Ultimate strength for this member will be obtained when the main steel yields. This is typical of most practical cases one is likely to come across in practice since design codes discourage the use of beams which are over-reinforced in flexure. The starting point in most analyses will be to assume that the steel yields, thus defining the magnitude of T. The effective width of the concrete acting against the anchor plate and the remaining truss geometry can be readily determined. Knowing the slope of the inclined strut, θ, and the horizontal component of the strut force, T, the vertical component, V, is easily found. Figure 5.1(b) illustrates the force in the bottom steel of the beam and shows the significant difference in behavior between a truss model, where the steel force is constant, and simple beam theory where it varies according to the moment diagram.

The second example involves a simply supported beam with flexural steel and one layer of horizontal web reinforcement. Again the beam is subjected to a point load at midspan. As shown in Fig. 5.2 there are really two trusses present, a lower truss utilizing the main steel as

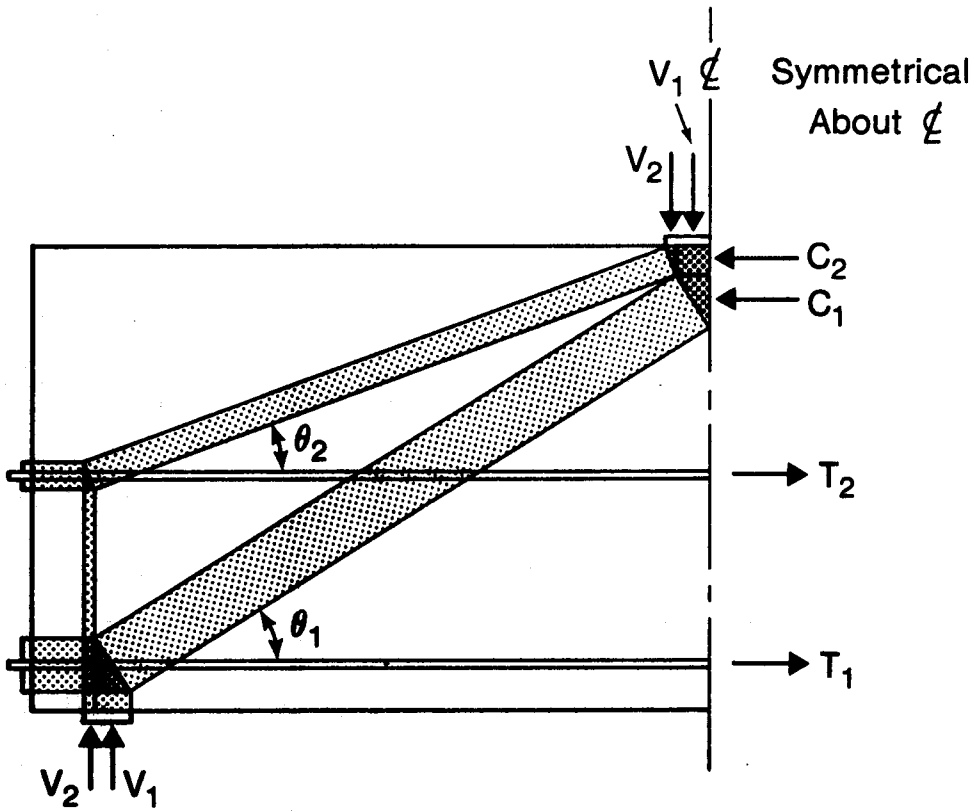

Figure 5.2. Plastic Truss Model for Beam With Horizontal Web Reinforcement

the tension tie, and an upper truss utilizing the web steel as the tension tie. It should be noted that each truss has its own compression strut, tension tie and hydrostatic element. For an ideal plastic material the capacity of the beam would be the capacity of the lower truss plus the capacity of the upper truss. For reinforced concrete, this is not necessarily the case. The kinematics are such that the bottom steel will reach yield before the web reinforcement, hence the lower truss will develop its capacity before the upper truss. The deformations required to yield the web reinforcement and thus develop the upper truss will generally be large enough to destroy the lower truss. The beam strength will thus be equal to or only slightly larger than the strength of the lower truss which utilizes the bottom reinforcement only. Recent tests by Smith and Vantsiotis (1982) on simply supported deep beams indicate that horizontal web reinforcement has little influence on the ultimate strength of such beams. The same is true for the simple span and continuous beams reported in this thesis.

Even if the beams had ideal plasticity, the influence of the horizontal web reinforcement would be small. Usually the amount of web reinforcement will be small in comparison with the main flexural reinforcement, that is $T_2 << T_1$. The shear transferred by the upper truss is the vertical component of the force in the upper strut. The slope of the upper strut, θ_2 will be quite flat. As a result, T_2, the

horizontal component of the upper strut force is small, and V_2, the vertical component of the upper strut force, is even smaller. It would not be overly conservative to ignore the horizontal web reinforcement when determining the ultimate strength of the beams under consideration in this thesis. On the basis of this argument and the experimental results, horizontal web reinforcement will be ignored for strength calculations in the remainder of this work.

The third and final hypothetical example consists of a simple span beam with vertical stirrups, subjected to a concentrated load at midspan. An appropriate truss model is shown in Fig. 5.3. There are really several trusses present. One truss utilizes a direct compression strut running from the load to the support. It carries a shear V_c. The other trusses utilize a stirrup as a vertical tension web member. The left most stirrup cannot be used in such a truss since one cannot draw a compression diagonal from the load point to the stirrup without encroaching on the direct compression strut.

The compression diagonals radiating from the point load intersect the stirrups at the level of the centroid of the bottom steel because the change in the force in the bottom steel is required to equilibrate the horizontal component of the force in the compression diagonal. The bottom steel force is reduced at each stirrup by the horizontal component of the compression diagonal intersecting at that point. This is illustrated in Fig. 5.3(b) where the stepped line

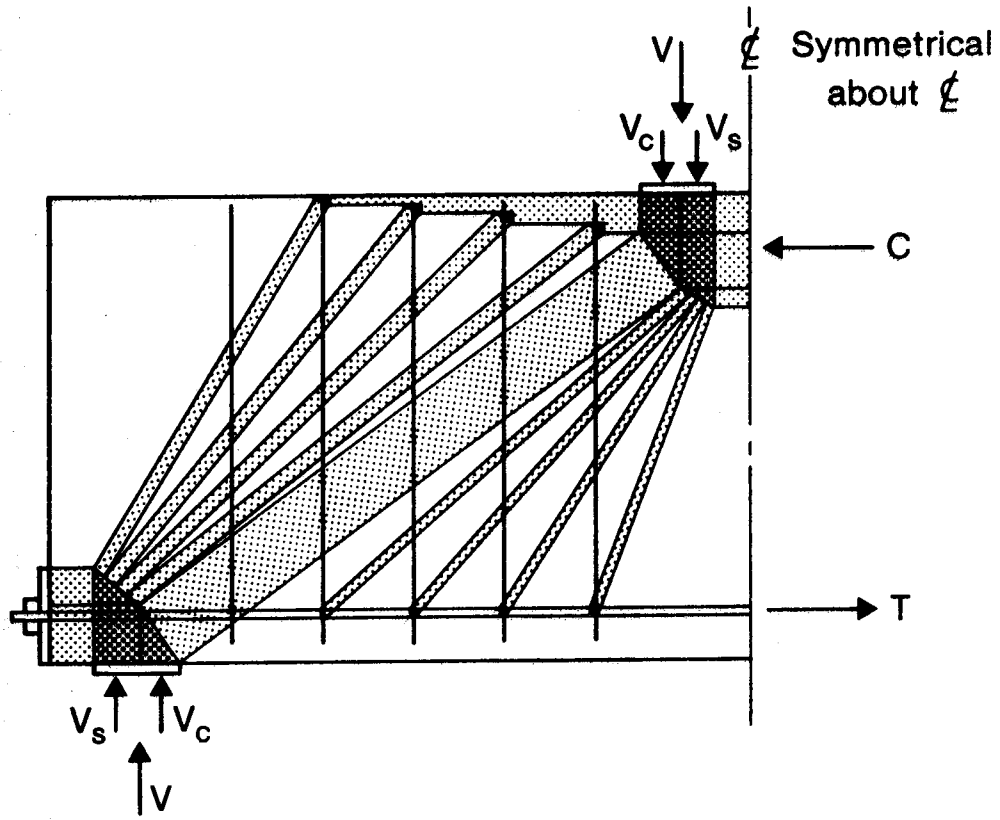

(a) Plastic Truss Model

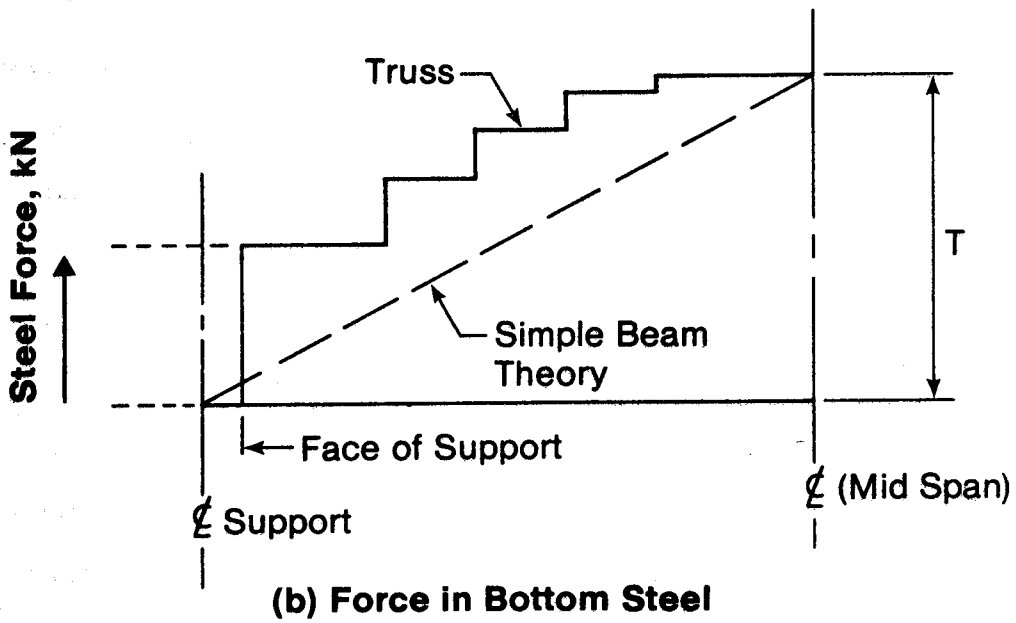

(b) Force in Bottom Steel

Figure 5.3. Plastic Truss Model for Beam With Stirrups

shows the resulting tension force in the bottom steel. The tension force exceeds that calculated from the conventional bending moment diagram throughout the shear span.

The compression diagonals radiating from the support intersect the stirrups at or close to the top of the stirrups. The horizontal component of each diagonal adds to the compression force and hence, the compression zone of the beam. The compression zone builds up as the region of maximum moment is approached. As pointed out earlier the farthest left stirrup is ineffective.

The analysis of this beam begins with a sketch of the plasticity truss from which approximate compression diagonal slopes are obtained. Normally this truss would be statically indeterminate, but in the plastic truss model, plasticity concepts are used to determine the truss member forces in a sufficient number of members to reduce the problem to that of a statically determinate truss.

The bottom steel is assumed to yield at midspan thus providing an estimate for T. The stirrups utilized in the model are assumed to yield, thus providing an estimate of the force they transmit. From the "method of joints" the vertical component of all the compression diagonals acting with the stirrups is equal to the stirrup yield force. The approximate diagonal inclinations are used to obtain the axial force and horizontal force component in each diagonal. As illustrated in Fig. 5.3(b), the horizontal component of force reduces the force in the bottom chord of

the truss (bottom steel). The force remaining in the bottom steel at the support is necessary to equilibrate the compression diagonals radiating to the top of each stirrup (these forces are known), and the direct compression strut. The horizontal and vertical component of the direct compression strut can be readily determined. The support reaction is equilibrated by the sum of the vertical components of the direct compression strut and the compression diagonals radiating from the support.

With this first analysis, all truss member sizes can be checked. The geometry can be adjusted, and the analysis refined. This can be repeated until the desired degree of accuracy is obtained. Two major questions enter into the analysis. First, "What is the effective concrete strength?" This affects the width of the compression struts, the size of the truss joints, and the overall truss geometry. This, in turn, affects the truss member forces and the beam capacity. The second question relates to the model: "What is the 'correct' plastic truss model for a given situation?" This issue has been illustrated to some extent in the last two hypothetical beams. Should the truss model utilize some of the horizontal web reinforcement? Should all of the stirrups be incorporated into the truss model? Will the stirrups and main reinforcement reach yield before beam failure? Are there limits to the slope of the inclined compression members?

The effective concrete strength and the appropriate

truss models will be examined in the following sections. This amounts to "calibration" of the plastic truss model and will be done by comparison with the test data.

5.4 Effective Concrete Strength

In the literature the reliability of solutions obtained with the plastic truss model is thought to be very dependent on the choice of an appropriate effective concrete strength f_c^*. The usual procedure for dealing with this is to introduce a concrete efficiency factor ν such that $f_c^* = \nu f_c'$ where ν is probably less than one. As discussed in Section 2.4, this factor relates to the strain softening behavior of concrete as well as the local complicated stress distributions which are overly simplified in the plasticity model.

The efficiency factor was introduced by the Danish research group under the direction of Nielsen. At present, different ν factors have been suggested for beam shear, punching shear, anchorage etc. For beam shear, ν has been correlated to f_c' (Nielsen et. al., 1978b), with the average value being:

$$\nu = 0.8 - \frac{f_c'}{200} \quad (f_c' \text{ in MPa}) \tag{5.1}$$

and the lower limit to their data being:

$$\nu = 0.7 - \frac{f_c'}{200} \quad (f_c' \text{ in MPa}) \tag{5.2}$$

The current (May 1983) Canadian Concrete Code proposal suggests $\nu = 0.8$ for deep beams while the Swiss group uses $\nu = 1.0$.

The efficiency factor can be back calculated from the test data, and can be bracketed by using upper and lower bound plasticity solutions. These two solutions provide low and high estimates for ν, respectively. Closed form plasticity solutions available in Chen (1982) were used to generate the results presented in Table 5.1 unless otherwise noted. While the plasticity solutions were closed form, they were often nonlinear with respect to ν because the size of the compression struts was a function of ν. This required that the values of ν be obtained by iteration. For the "uncomplicated" test beams the upper and lower bound plasticity solutions used should give the same results in that they are exact solutions. The problem is that finite support widths and concrete cover "complicate" the solutions. While these factors do not enter into the upper bound solution they can have a significant impact on the lower bound solution. Hence, the solutions are not exact, and do not produce the same estimate for ν. The results obtained from lower bound solutions should give high estimates for ν, however, this is not the case when truss geometry is governed by support widths or reinforcement details.

While the results in Table 5.1 are far from complete, they appear to suggest that ν could be approximately 0.3.

This is less than half the value suggested by other authors.

The values of ν in Table 5.1, present two problems: high variability, and low efficiency ν. Both of these problems are not as severe as they first appear since the shear capacity prediction is less than linearly dependent on the concrete efficiency factor. For upper bound solutions, a change in the efficiency factor for concrete changes the internal virtual work done by the concrete. The change in the total internal virtual work done is moderated by the contribution of the internal virtual work done by the steel. Hence, for beams where the steel provides a substantial portion of the internal virtual work, strength predictions will be somewhat insensitive to changes in the concrete efficiency factor. For lower bound solutions, a change in the efficiency factor for the concrete changes the width of the compression struts required to equilibrate the tension tie forces. Even a large change in the width of a compression strut usually produces a very small change in the slope of the strut. Hence the shear capacity, which is the vertical component of the force in the strut, is quite insensitive to changes in the efficiency factor.

Strength predictions based on an assumed efficiency factor of $\nu = 1.0$ are presented in Table 5.2. The specimens have been grouped in this table to emphasize certain trends. The first observation is that while a $\nu = 1.0$ is, in many cases, 3 or 4 times the back-calculated ν given in Table 5.1, the results in Table 5.2 are generally within a

Table 5.1 Concrete Efficiency Factors

Beam	ν	
	Upper-Bound Theorem	Lower-Bound Theorem
1/1.0S	1.15	1.65
2/1.0S	1.00	
4/1.0	0.57	
4/1.0	0.49	
6/1.0	0.37	
6/1.0	0.34	
7/1.0	0.24	0.16*
7/1.0	0.53	0.47*
1/1.5S	0.46	0.67
2/1.5S	0.25	
4/1.5	0.30	
4/1.5	0.34	
6/1.5	0.27	
6/1.5	0.27	
7/1.5	0.35	0.29*
7/1.5	0.54	0.48*
1/2.0S	0.47	1.50
2/2.0S	0.35	
4/2.0	0.36	
4/2.0	0.44	
6/2.0	0.35	
6/2.0	0.26	
7/2.0	0.28	0.25*
7/2.0	0.22	0.21*

* Truss geometry governed by the rebar cover.

Table 5.2 Strength Predictions with $\nu = 1.0$

Remarks	Beam	$\frac{V_{TEST}}{V_{LOWER\ BOUND}}$ ($\nu = 1.0$)	$\frac{V_{TEST}}{V_{UPPER\ BOUND}}$ ($\nu = 1.0$)
Cont. beams with max. vert. web reinf.	5/1.0	0.99	
	5/1.0	0.94	
	5/1.5	1.00	
	5/1.5	1.00	
	5/2.0	1.02	
	5/2.0	1.02	
	5/2.5	1.02	
Simple span beams without stirrups (* ignoring horiz. web steel)	1/1.0S	1.06	1.03
	2/1.0S	1.13 *	1.00
	1/1.5S	0.96	0.82
	2/1.5S	0.72 *	0.54
	1/2.0S	1.00	0.87
	2/2.0S	1.05 *	0.74
Simple span beams with stirrups (* ignoring horiz. web steel)	1/1.0N	0.79	
	2/1.0N	0.99 *	
	1/1.5N	0.88	
	2/1.5N	0.86 *	
	1/2.0N	0.84	
	2/2.0N	0.86 *	
Cont. beams other than those with max. stirrups	3/1.0	0.86	
	3/1.0	0.95	
	4/1.0		0.81
	4/1.0		0.75
	6/1.0		0.64
	6/1.0		0.61
	7/1.0	0.53	0.49
	7/1.0	0.88	0.82
	3/1.5	0.44	
	3/1.5	0.53	
	4/1.5		0.37
	4/1.5		0.42
	6/1.5		0.38
	6/1.5		0.38
	7/1.5	0.54	0.43
	7/1.5	0.85	0.67
	8/1.5		
	8/1.5		
	3/2.0	0.66	
	3/2.0	0.70	
	4/2.0		0.43
	4/2.0		0.57
	6/2.0		0.41
	6/2.0		0.31
	7/2.0	0.70	0.42
	7/2.0	0.57	0.34

factor of 2, and in some beam categories of beams the predictions are almost exact. This supports the statement made earlier that large changes in ν lead to smaller changes in predicted capacity. This implies that the safety of a deep beam is not going to be strongly influenced by the choice of ν.

Each of the four categories of beams listed in Table 5.2 requires a slightly different analogous truss. It appears that reasonable strength predictions are obtained with $\nu = 1.0$ for some categories. It will be shown later in this chapter that in the categories where predictions are not very good, a poor choice of plastic truss was made. This poor choice, while being theoretically acceptable in a pure plasticity sense, requires more plastic deformation than the concrete can accommodate. Rather than accounting for the lack of ductility by using a small value for ν, it is better to use a higher value for ν, perhaps even $\nu = 1.0$, and a more appropriate plastic truss model.

5.5 An Appropriate Plastic Truss Model

The safety of beams designed by the plastic truss analogy is strongly dependent on the choice of an appropriate analogous plastic truss for the beam in question. The most appropriate truss will be one which has a distribution of forces similar to those in the real beam after cracking since this would require little if any plastic redistribution of forces. In simply supported, or

statically determinate beams, there are only a few plausible trusses which can develop to carry the loads applied to the beam. In continuous or statically indeterminate beams, there are several plausible trusses that one could use. Some of these trusses require more ductility from the concrete than it is capable of providing. Hence, these trusses will be unsafe to use, even though they are "lower bound" solutions in the plasticity theory. This section will attempt to identify appropriate plastic trusses for use in various situations.

With an appropriate truss, the lack of significant concrete ductility is not an important issue. This, in conjunction with the fact that the plastic truss solutions are insensitive to changes in ν, suggests that a high value of ν may be appropriate. For the purposes of this discussion, $\nu = 1.0$ will be used. A somewhat smaller value will be proposed for design purposes in Chapter 6. The results for the four beam categories in Table 5.2 will be studied more closely in the following sections in order to identify appropriate plastic truss models.

5.5.1 Continuous Beams with Maximum Vertical Web Reinforcement

The strength predictions for the first beam category, continuous beams with maximum vertical web reinforcement are very good. The ratio of test/predicted strength has a mean of 1.00 and a coefficient of variation of 0.03. This

suggests that the particular plastic truss model used is a good model of the real behavior, and that it is reasonable to use $\nu = 1.0$.

The truss models used in analyzing beams 5/1.0 and 5/2.5 are shown in Figs. 5.4 and 5.5. In these figures, the light shaded areas are major compression struts, the dark shaded areas are hydrostatic elements, the vertical lines are stirrups and the radiating lines represent small compression struts or fans equilibrating the stirrup forces. At the top and bottom of these figures, the predicted and observed forces in the top and bottom steel are compared. The plastic truss model predicts the observed steel forces very well. It predicts the correct chord forces at the top and bottom of the beam at the face of the load and face of the support, along with the very slow change in chord force. Conventional beam theory, on the other hand, would predict a point of inflection near the middle of the shear span with zero chord forces at this point. Conventional theory would certainly not predict tension in the top and bottom of beam at the same cross section as shown in Fig. 5.4. The plastic truss, as crude as it appears to be at first glance, predicts the observed behavior far better than conventional elastic beam theory with all its mathematical elegance.

Most of the shear force in these two beams is transmitted to the interior support by the "fans". A smaller portion of the shear is transmitted by a direct

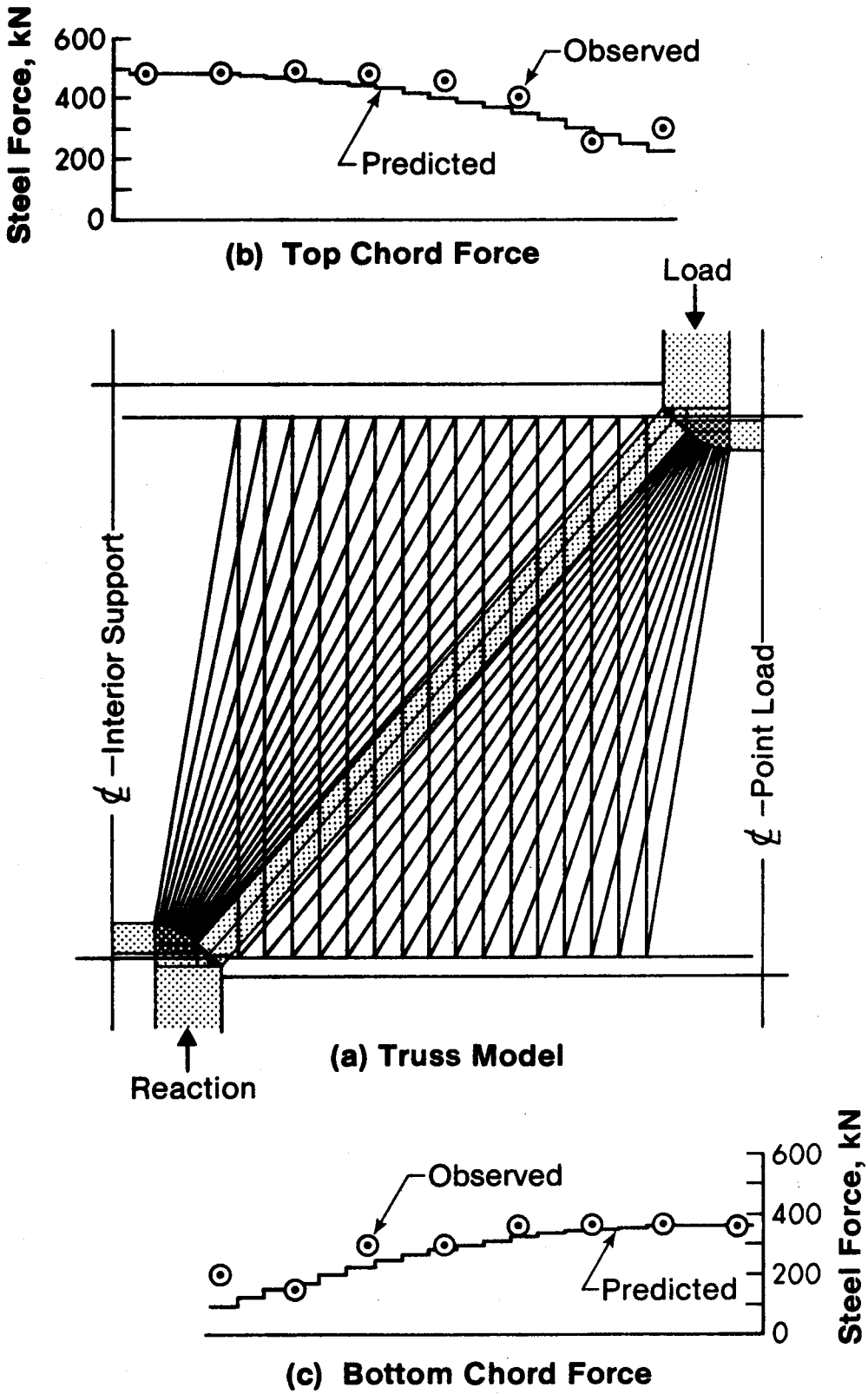

Figure 5.4. Plastic Truss for Beam 5/1.0

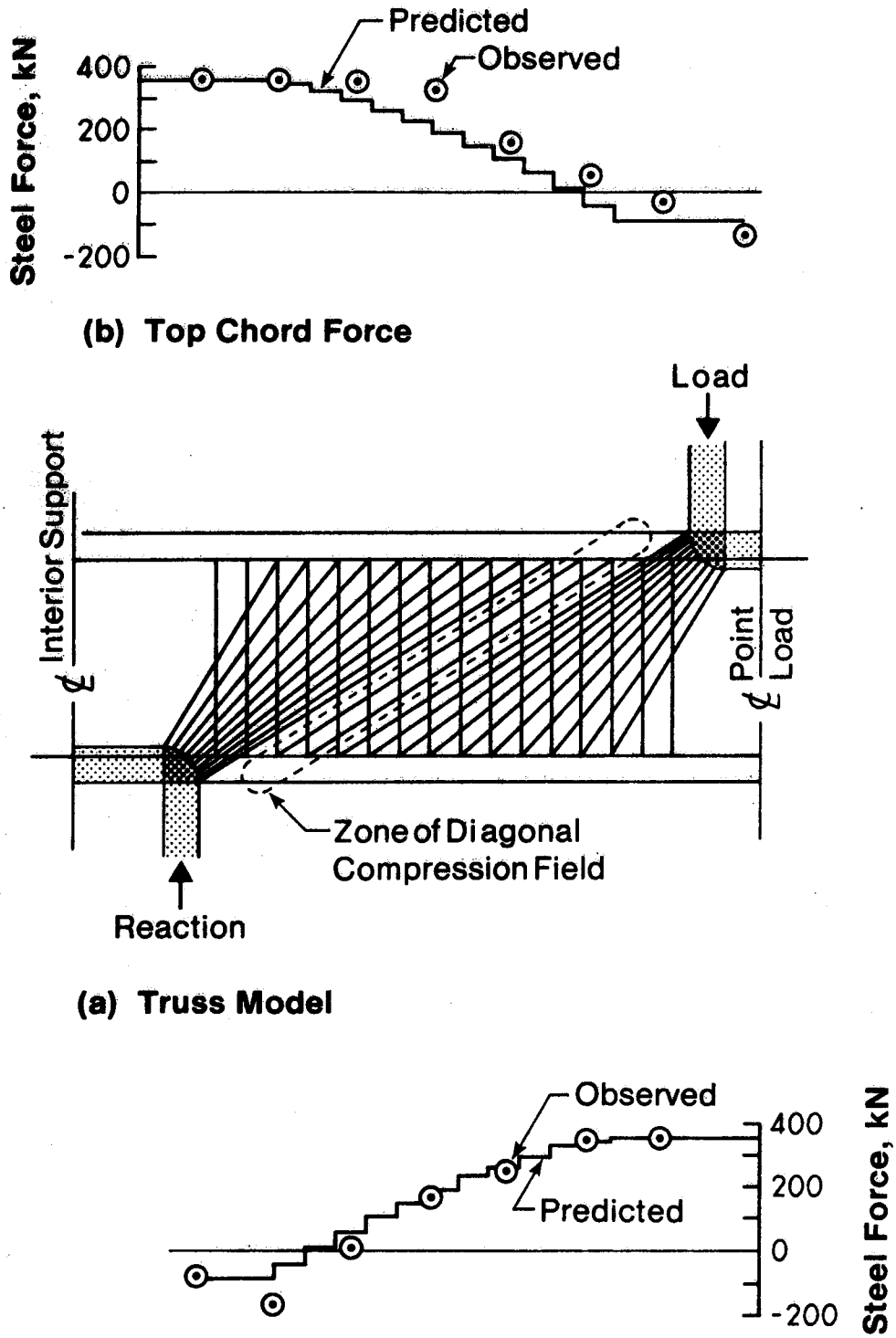

Figure 5.5 Plastic Truss for Beam 5/2.5

compression strut from the load to the support in Fig. 5.4. While the slope of the strut depends approximately on a/d, the geometry of the fans does not. For the range of a/d examined, and for beams with maximum stirrups, the influence of the direct compression strut, and hence the influence of a/d is small. This is clearly demonstrated by the solid points in Fig. 4.7.

In shallower beams, such as beam 5/2.5, no direct compression strut develops at all (Fig. 5.5). (The direct compression strut still carried 5% of the load in beam 5/2.0.) The region between the fans is a zone of "diagonal compression field" as described by Collins and Mitchell (1980). This field is sloped at 32°. For a diagonal compression field sloped at 32° the stirrups will strain more than the longitudinal steel. Assuming a yield strain of 0.002 mm/mm for the steel and peak diagonal compression strain of 0.002 mm/mm, compatibility of strains indicates a stirrup strain of approximately 0.01 mm/mm when the longitudinal steel reaches yield. Based on these strains, Collins and Mitchell's (1980) Eq. 15 gives an effective compression strength of approximately $0.5f'_c$. Although this implies that ν is 0.5, this is of little signficance for this beam. Reducing the concrete strength by 1/2 doubles the width of compression strut required to equilibrate each stirrup. From Fig. 5.5, it is clear that there is sufficient concrete between struts to permit this, hence the geometry and thus the shear capacity of this "diagonal

compression field" zone of the beam will not change. The fact that failure was initiated by general yielding of the steel and not by crushing of the concrete suggests that this is true. One can think of this as an "under-reinforced" beam in which the concrete is of sufficient capacity that it does not fail before the steel yields. Building codes limit web reinforcement to prevent failure due to crushing of the web. The heavy stirrup reinforcement used in this beam is slightly less than the maximum permitted by the ACI Code.

Even though this beam has heavy stirrup reinforcement, it had the desirable ductility characteristics of under-reinforced beams, deflecting 30 mm or 1/60 of the span before failing. The other beams which had fewer stirrups and thus were more under-reinforced in shear did not exhibit this ductile behavior. This apparent contradiction in behavior is due to the form of the plastic truss which was operative in these other beam categories.

5.5.2 Simple Span Beams Without Stirrups

The second category of beams in Table 5.2 consists of simple span beams without stirrups. This includes beams with light horizontal web reinforcement, which was ignored for the lower-bound plastic truss prediction in this table. The failure loads indicated that the horizontal web reinforcement did not significantly change the capacity of these beams when compared to companion specimens without web reinforcement. The strength was predicted with truss models

similar to that shown in Fig. 5.6. The ratio of observed shear capacity to lower bound predicted capacity for this class of beams had a mean value of 0.99 and a coefficient of variation of 0.14 (Table 5.2). Most of this variation was due to specimens with a/d = 1.5. A review of the crack patterns and observations does not provide any indication of why this occurred.

In the lower portion of Fig. 5.6, the predicted and observed force in the bottom steel are compared. The plastic truss model (PTM) predicts the observed steel force very well, while conventional beam theory grossly underestimates the force in the bottom steel at the face of the support.

Beams in this category reached yield of the main steel, but did not display significant ductility before the concrete struts failed. It is believed that the elongation of the main steel after yielding caused the compression struts to rotate slightly. Since the joints of the truss were not in reality pinned, this required plastic deformation of the concrete in or near the truss joints. This local straining of the concrete eventually caused failure of the compression strut at either the top or bottom end. In summary, however, the truss models used for this category produce reasonable predictions for shear strength in spite of the limited ductility of the concrete struts.

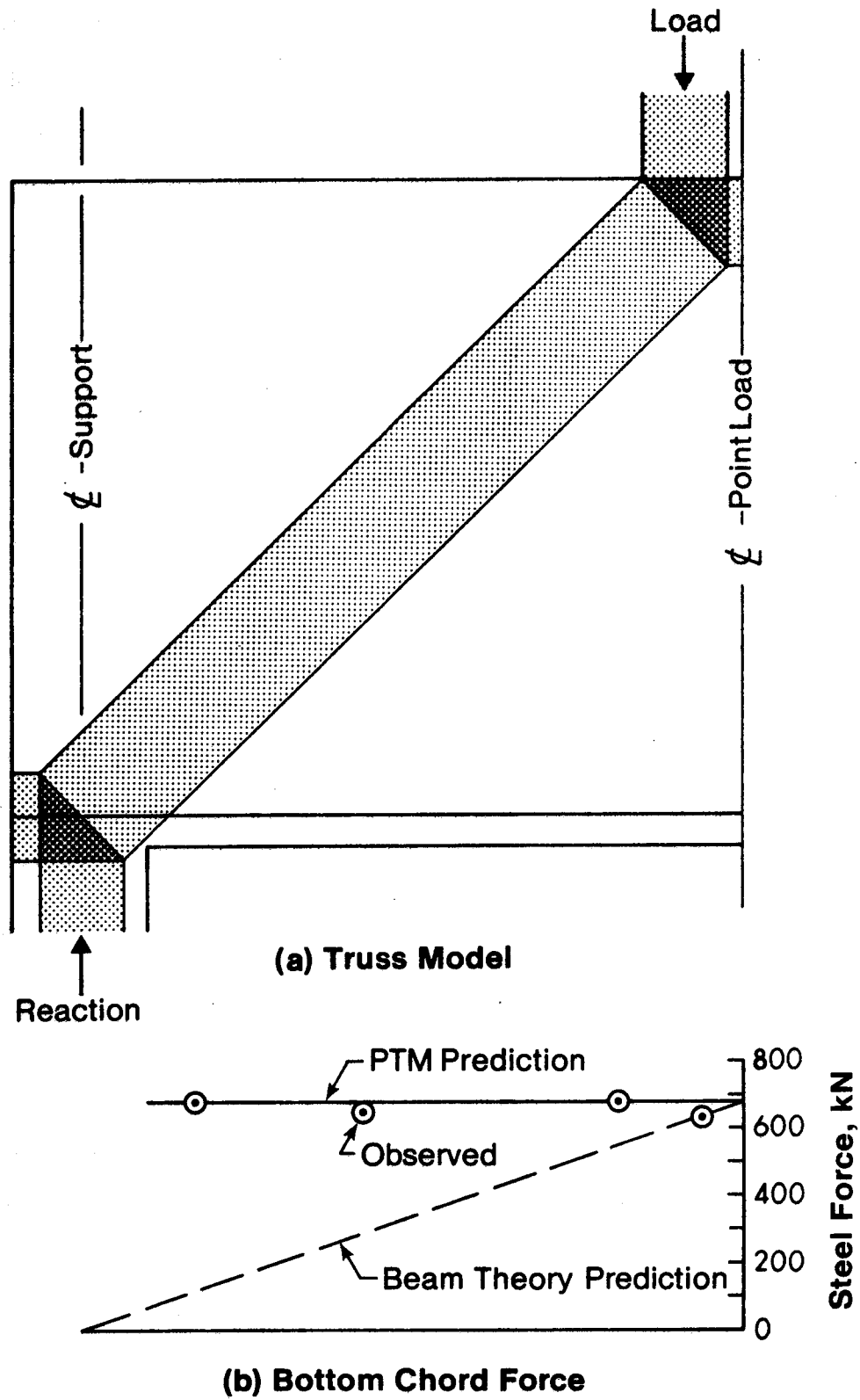

Figure 5.6. Plastic Truss for Beam 1/1.0S

5.5.3 Simple Span Beams With Minimum Stirrups

The third category of beams in Table 5.2 consists of simply supported beams with light stirrups. This includes beams with light horizontal web reinforcement which, as in the previous category was ignored for the lower-bound predictions in this table. The strength was predicted with truss models similar to that shown in Fig. 5.7. The ratio of observed shear capacity to predicted lower bound capacity for this category had a mean value of 0.87 and a coefficient of variation of 0.08. The addition of light stirrups has significantly reduced the variability in the results, but the model now produces slightly unsafe predictions. The predictions are unsafe by about the capacity of one stirrup suggesting that not all of the stirrups have yielded. Examination of the stirrup strain data indicates that the stirrup closest to the point load had less stress than the other stirrups and was probably not yielded at the time of failure, hence the shear force carried by the stirrups was overestimated in the plastic truss model. It is evident from Fig. 5.7 that the upper end of this stirrup passes through the direct compression strut and that large amounts of deformation would be required before this stirrup would yield in tension, unless it was unbonded where it passed through the compression strut.

This rationale cannot be used to explain the results for beam 1/1.0 N which failed at a 14 percent lower load than the opposite end of the beam (1/1.0 S) which had no web

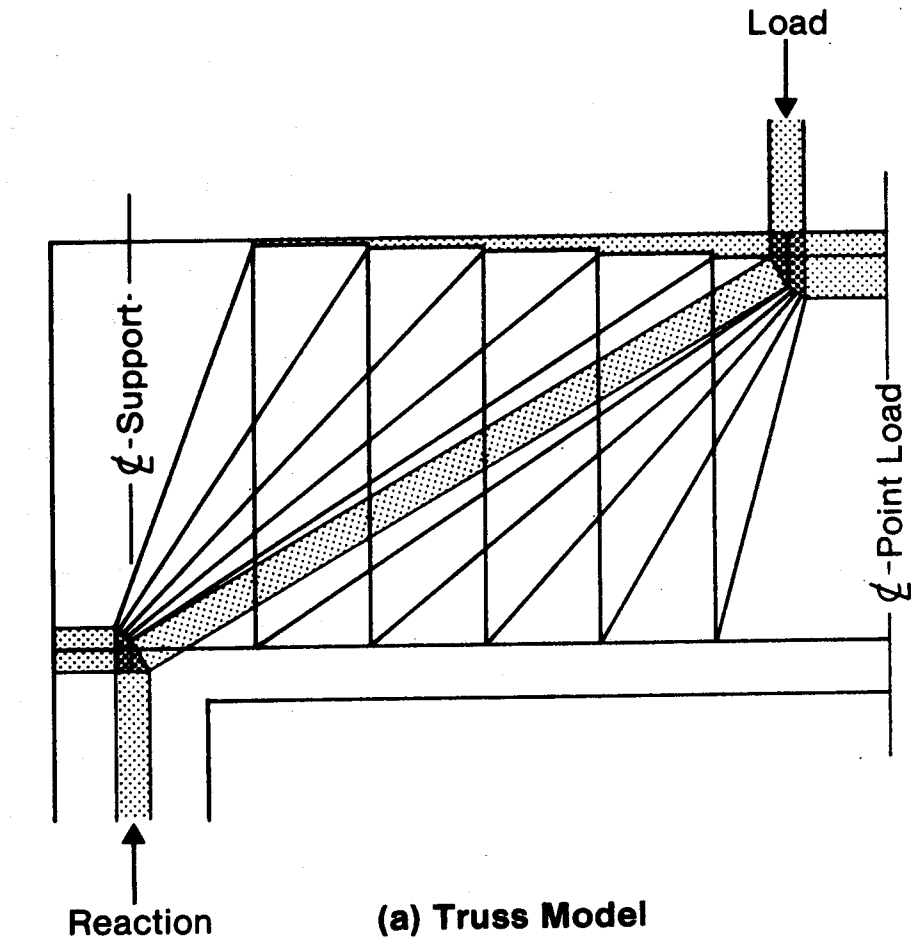

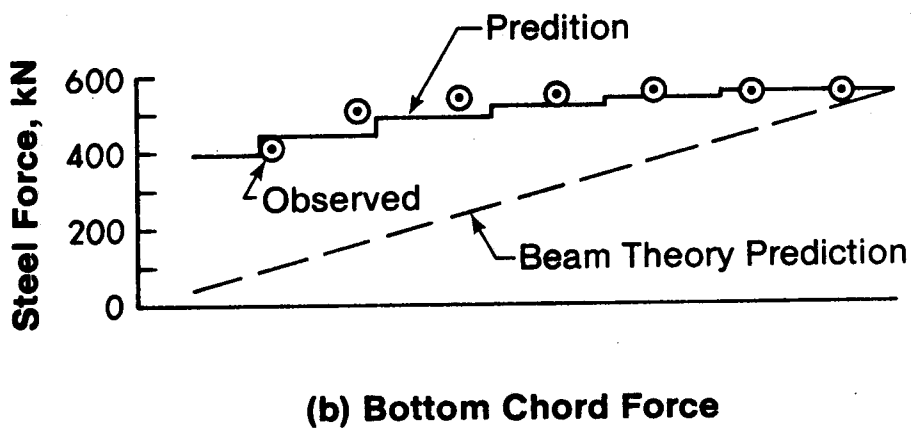

Figure 5.7. Plastic Truss for Beam 1/1.5 N

reinforcement at all. The stirrups appear to have made this beam weaker. For this beam, the shear force carried by the stirrups was quite small and was probably less than the variation in strength of the direct compression strut due to the natural variability of concrete. It is also possible that the stirrups tend to pull the direct compression strut apart reducing its ultimate strength as suggested by Robinson (1965) and others.

The lower portion of Fig. 5.7 compares the observed and predicted force in the bottom reinforcement. Again, the plastic truss model predicts the observed strains very well.

In summary, the truss models used for this beam category produce reasonable predictions for shear strength provided that one recognizes that stirrups which are too close to the point load or support may not be fully effective.

5.5.4 Continuous Deep Beams Without Heavy Stirrups

The final category of beams in Table 5.2 consists of continuous beams other than those with heavy stirrups. For this category the ratio of the observed shear capacity to the predictd lower-bound capacity has a mean value of 0.68 and a coefficient of variation of 0.25. An example of the truss model used for these predictions is shown in Fig. 5.8. The poor predictions of capacity suggest that this truss model requires improvement. Even though this category includes beams with light horizontal, heavy horizontal,

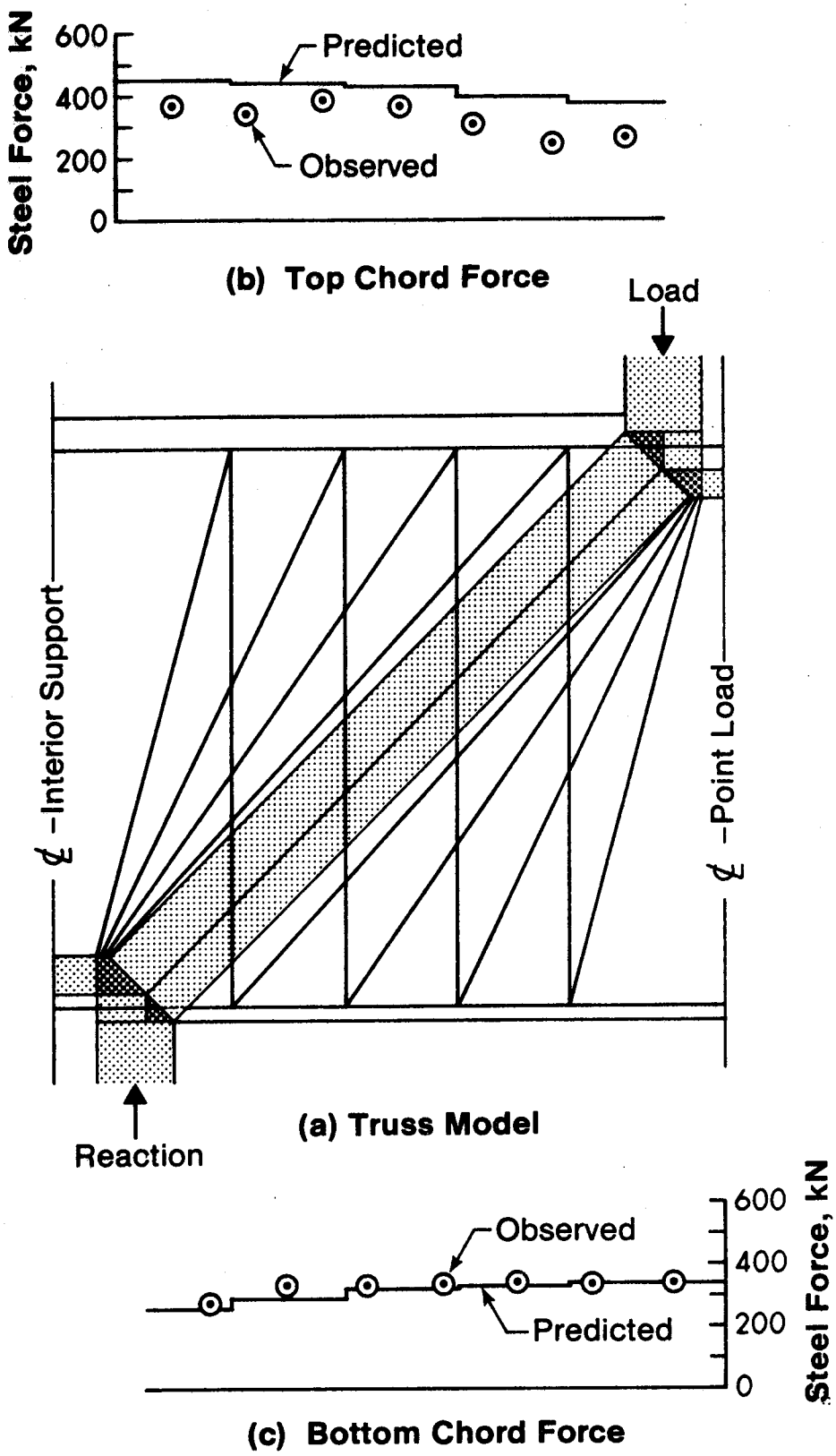

Figure 5.8. Plastic Truss for Beam 3/1.0

light vertical, and no web reinforcement, their strengths are indistinguishable in Fig. 4.6. This implies that the operative plastic truss did not make signficant use of the web steel. If this is so, the behavior of these continuous beams can be studied by analyzing a beam without web reinforcement.

The first problem to address is that of the overestimate of strength with the plastic truss model. These models assume that the top and bottom reinforcement undergo sufficient straining to ensure that both are yielded at or before failure. The experimental observations indicate that this is not true. The observed and predicted forces in the top and bottom steel are compared in the upper and lower portions of Fig. 5.8. The steel strain measurements indicate that although the bottom steel yielded, the top steel had smaller strains than the bottom steel and did not reach yield. In most of the beams in this category the top steel did not reach yield strain before failure.

In a classical elastic continuous beam subjected to midspan point loads, the negative bending moments are larger than the positive bending moments implying that the negative flexural cracks should have formed first. The test specimens, which had flexural reinforcement proportioned approximately in accordance with the elastic distribution of moments, did not behave this way. The negaive moments were smaller and positive moments were larger than predicted.

This agrees with the pattern of crack development in which positive moment flexural cracks developed at midspan before negative moment flexural cracks developed over the interior support.

A third corroborating observation relates to the proportion or distribution of support reactions. For continuous deep beams without heavy stirrups the observed interior support reaction had a mean value of 62% of the total applied load with a coefficient of variation of 0.04. The theoretical interior support reaction for an elastic uncracked beam considering shear deformation effects ranges from 64% to 68% of the total applied load for beams x/1.0 and x/2.5 respectively. The variation in the theoretical value reflects the influence of shear deformations which are more significant in the deeper specimens.

The measured steel strains, the cracking patterns, and the distribution of support reactions all indicate that the behavior of these specimens was somewhere between that of a two span continuous beam, and two adjacent simple span beams, for which the interior support reaction would be 50% of the total applied load.

There are two explanations for this behavior. Some of the reduction in top steel force results from relative "settlement" of the interior support which was typically about 0.25 mm but ranged as high as about 0.75 mm. SFRAME (1982), a linearly elastic frame analysis computer program

incorporating shearing displacements was used to examine the possible effects of support settlement. The results summarized in Table 5.3 indicate that for the magnitudes of load and settlement experienced, settlement is not likely to reduce the magnitude of the negative moment below the maximum positive moment except in the deepest beam series. Even in the deepest beams, support settlement effects may not be as significant as Table 5.3 suggests since their influence has been overestimated in the analysis by the use of an uncracked flexural stiffness.

The second source of reduction in the top steel force relates to the specimen behaving as a two span truss. The constant steel strains along the bottom longitudinal reinforcement and almost constant strains in the top steel (Fig. 5.8) imply that it acts as a tension tie in a truss rather than as flexural reinforcement in a conventional beam. Two plausible elastic trusses and the resulting member forces are illustrated in Fig. 5.9. The relative stiffness of the interior web members in the truss in Fig. 5.9(b) are twice as stiff as those in the truss in Fig. 5.9(a). The reactions from the two truss models bracket the observed support reactions, which implies that the member forces also bracket the equivalent member forces. Hence, if the continuous beam acts as a truss, the top chord force will be less than the bottom chord force unless the interior web members are very stiff. For the two trusses shown in Fig. 5.9, a linear combination of 58% of

Table 5.3 Analysis of Continuous Beams for Support Settlement

a/d	1000 kN Point Loads 0 mm Support Settlement (Load Case 1)			0 kN Point Loads 1 mm Support Settlement (Load Case 2)			1000 kN Point Loads 0.25 mm Support Settlement (Case 1) + (0.25 x Case 2)		
	Interior Support Reaction (kN)	Midspan Moment (kNm)	Interior Support Moment (kNm)	Interior Support Reaction (kN)	Midspan Moment (kNm)	Interior Support Moment (kNm)	Interior Support Reaction (kN)	Midspan Moment (kNm)	Interior Support Moment (kNm)
1.0	1282	359	-347	-240	120	251	1222	389	-284
1.5	1320	340	-386	-58	29	61	1306	347	-371
2.0	1346	327	-413	-34	17	36	1338	331	-404
2.5	1356	322	-424	-18	9	19	1352	324	-419

- Based on gross uncracked EI with increased EI for finite support widths.
- Includes shear deformation effects.

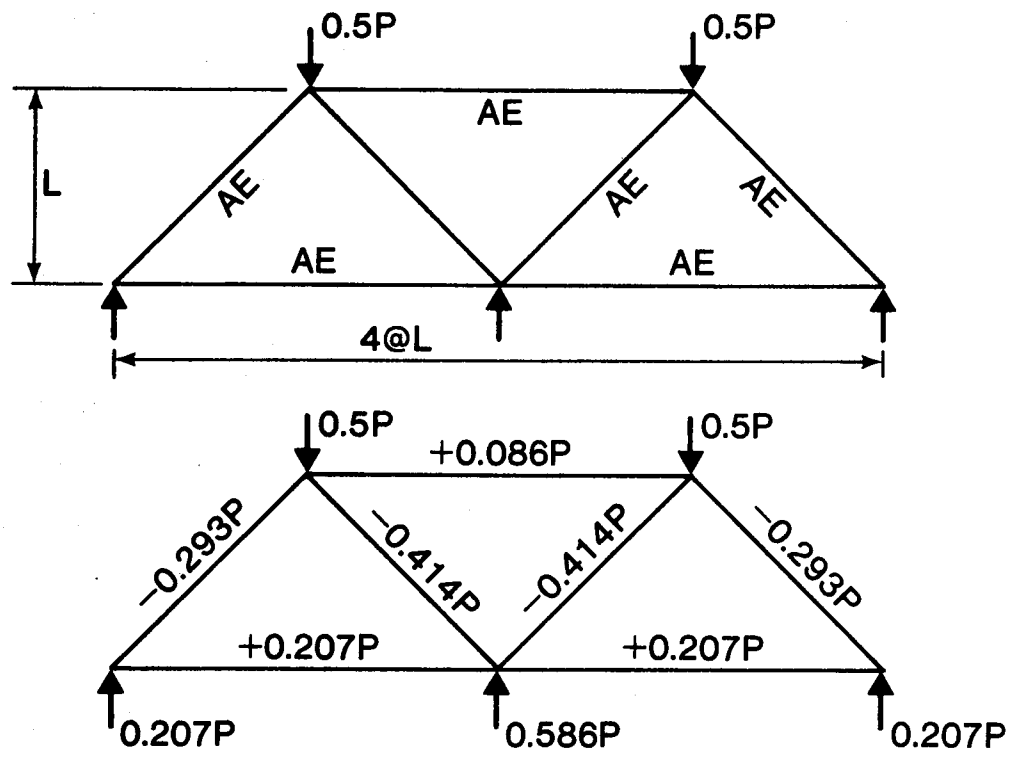

(a) Uniform Member of Stiffness

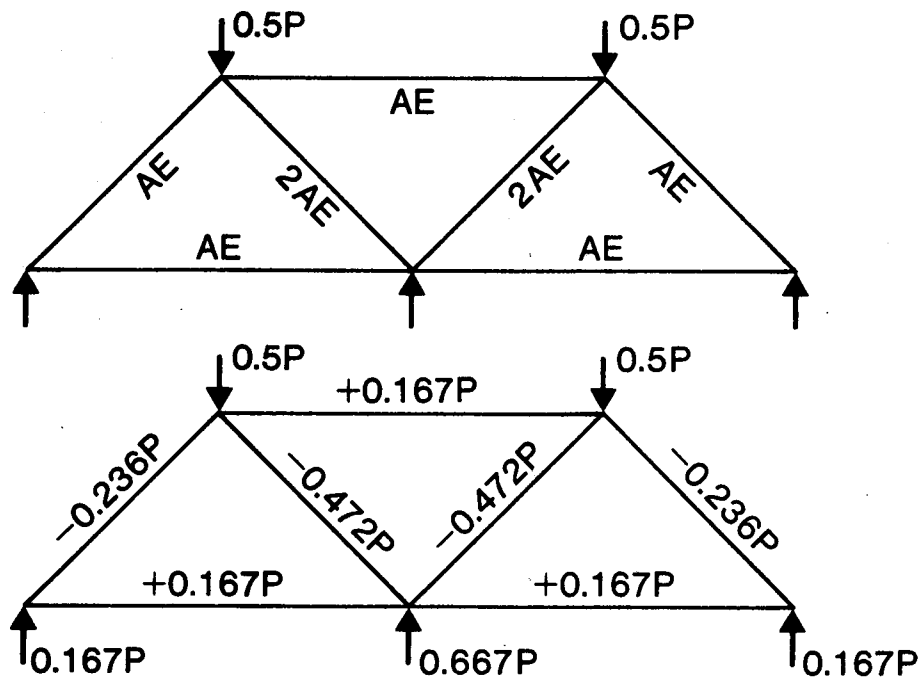

(b) Stiffer Interior Web Members

Figure 5.9. Two Span Truss Behavior

the first truss plus 42% of the second truss produces the observed distribution of support reactions. This also produces a ratio of top chord force to bottom chord force of 0.63. Recalculating the results in Table 5.2 for this beam category using a top chord force equal to 63% of the yield force of the bottom chord significantly improves the strength predictions. For beam 3/1.5, for example, the ratio of average test to calculated shear strength changes from 0.48 to 0.90. The agreement is particularly good in view of the fact that this beam had an abnormally low concrete strength f'_c = 14.5 MPa.

In summary, continuous beams without heavy stirrup reinforcement do not possess sufficient ductility to undergo complete redistribution. A plasticity truss with top and bottom chord forces assigned arbitrarily will not generally lead to safe predictions of beam capacity. The most appropriate truss will be one which produces the expected distribution of support reactions. For the beams tested, it was found that the interior support reaction had a mean value of 62% of the total applied load. This is smaller than predicted by elastic beam theory, and has a significant effect on the distribution of shears and moments in the continuous beam. The plastic truss model can account for this by utilizing a top chord force equal to approximately 60% of the bottom chord yield force.

5.6 What is a Deep Beam?

The previous section attempted to identify appropriate plastic truss models for deep beams. The question now is, "What is a deep beam?" The following definition is proposed:

> A deep beam is any beam in which a substantial portion of the load is transferred to the support by a direct compression strut.

This is a statical rather than a geometrical definition. By this definition a deep beam will be one which exhibits an increase in shear strength with a decrease in shear span to depth ratio. It obviously excludes indirectly loaded beams (unless specially detailed), and beams which are too shallow or have loads too far away from the support to permit the development of struts with significant vertical components. The test data and truss models presented previously suggest that top loaded, bottom supported beams have the potential for developing deep beam action if a/d is less than about 2.0. This is less than the value implied by the ACI Code which for shear calculations defines deep beams as those having a clear span to depth ratio ℓ_n/d less than 5. The CEB Model Code defines deep beams as those having ℓ_o/d less than 2 where ℓ_o is the distance to the point of contraflexure.

The real behavior of a deep reinforced concrete beam is very similar to that of a truss, hence the beam can be idealized as a platic truss in order to obtain a

quantitative distribution of the forces. Whether or not a beam will actually develop deep beam action depends on the design truss used. For example, the statical definition of a deep beam may exclude short shear spans with heavy stirrup reinforcement. Heavy stirrups acting in conjunction with the minor struts can reduce the chord forces such that no significant horizontal force exists which can equilibrate a direct compression strut. This is shown in Fig. 5.4 where the direct compression strut is small, and in Fig. 5.5 where there is no direct compression strut at all. Thus, in Fig. 4.6 the strength of beams with heavy stirrups was independent of a/d while the strength of beams of similar geometry but different web reinforcement was highly dependent on a/d. This suggests the beams with heavy stirrups did not fit the statical definition of a deep beam presented earlier.

There does not appear to be an upper limit to the slope of the direct compression strut, hence corbels and brackets of practical proportions fall into the category of deep beams by the proposed definition. Hagberg (1983) has proposed a truss model for the design of corbels and brackets with $0.5 < a/d < 1.0$. His model is very similar but less rigorous than the plastic truss models previously presented in this thesis. The models are compared in Fig. 5.10. The similarity suggests that the more rigorous model is also applicable down to values of a/d equal to about 0.15. Analysis of the corbel test data obtained by Kriz and

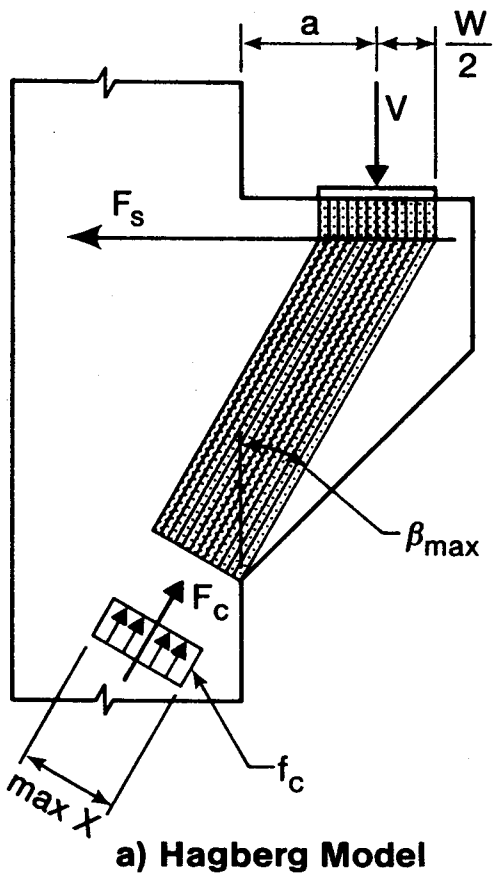

a) Hagberg Model

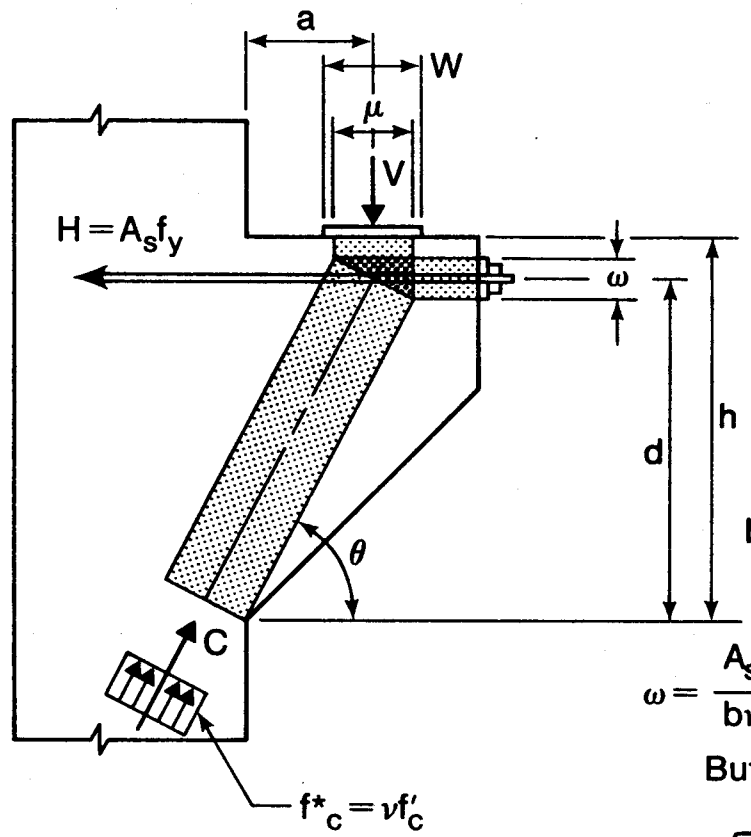

b) Plastic Truss Model

$$\omega = \frac{A_s f_y}{b \nu f'_c} \qquad (1)$$

But $\geq 2(h-d)$

$$\mu = \sqrt{a^2 - \omega^2 + 2\omega d} - a \qquad (2)$$

But $\geq W$

$$V = \mu b \nu f'_c \qquad (3)$$

$$v_u = \frac{V}{bd} \qquad (4)$$

Figure 5.10. Corbel Models

Raths (1965) was performed using the plastic truss model and associated equations assuming $\nu = 1.0$. The results presented in Fig. 5.11 indicate that the plastic truss model is suitable and slightly conservative for corbels with a/d ratios as low as 0.15. Thus, corbels are merely deep beam cantilevers.

5.7 Effectiveness of Horizontal Reinforcement

The effectiveness of horizontal reinforcement has been a matter of considerable debate in the literature. For the simple span and continuous beams tested, horizontal reinforcement had no measureable effect on behavior as shown by Figs. 4.5 and 4.6. Beams with minimum or maximum horizontal web reinforcement behaved essentially the same as beams without web reinforcement. Recent data published by Smith and Vantsiotis (1982) also supports this conclusion. This is in contrast to the ACI Code which indicates that horizontal web reinforcement is more effective than vertical web reinforcement in deep beams.

The plastic truss model shown in Fig. 5.2 suggests that horizontal web reinforcement will not significantly increase the strength of the plastic truss, unless the beam is very deep, and has substantial horizontal web reinforcement as in the case of some corbels. In using the plastic truss it would not be prudent to assume that all of the horizontal web reinforcement yields at failure. Kong (1977) after testing numerous simply supported deep beams with a/d ratios

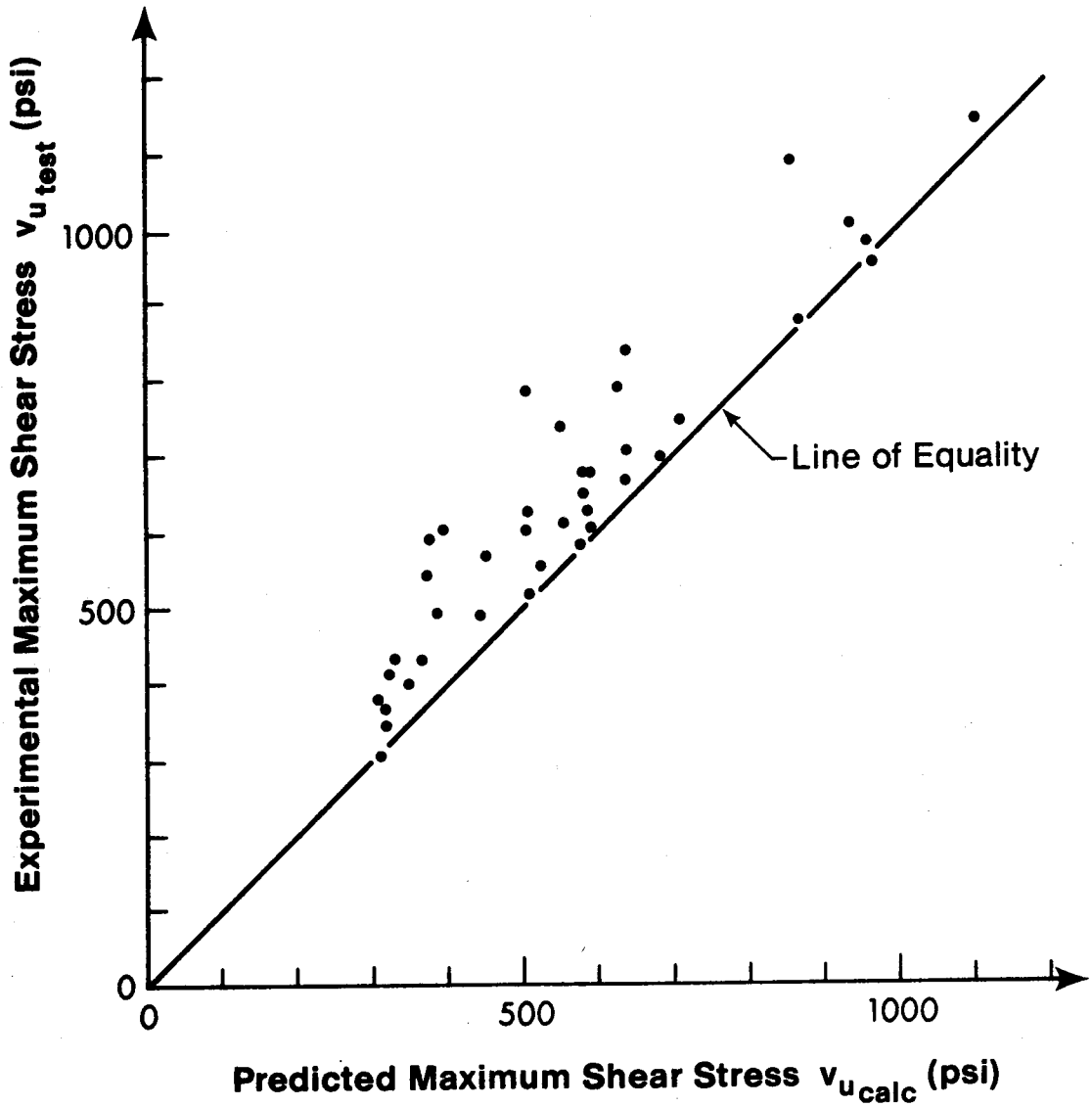

Figure 5.11. Plastic Truss Model Predictions of Corbel Strengh (Kriz and Rath (1965) data)

between approximately 0.3 and 0.7 suggests an equation with a form such that the stress in a horizontal web bar is proportional to its relative depth within the beam. That is, a horizontal web bar adjacent to the main steel would yield along with the main steel while a horizontal web bar at mid-depth of the beam would have only half the yield stress. This is in sharp contrast to ACI which assumes that all of the reinforcement is at yield.

5.8 Minimum Web Reinforcement Requirements

Some minimum amount of web reinforcement should be used in deep beams. While this reinforcement does not influence the mean shear resistance significantly, it does significantly reduce the variability of the test results. For continuous beams without web reinforcement the ratio of retest to virgin test shear strength had a coefficient of variation of 35%. The same ratio for beams with web reinforcement had a coefficient of variation of 14%. Beams with maximum and minimum stirrups had variabilities (COV) of 3% and 6% respectively while beams with maximum and minimum horizontal web reinforcement had variabilities of 14% and 15%.

The minimum amount of web reinforcement one might choose to use depends upon the amount of variability one is willing to tolerate. It would appear that minimum vertical stirrups as used in this thesis (approximately the same as ACI minimum stirrups) are able to reduce the variability to

the level typical of other applications of reinforced concrete.

5.9 Relationship With Compression Field Theory

The plastic truss model (PTM) is a special case of the more general theory of plasticity in reinforced concrete (See Appendix A). As a lower-bound solution, it is compatible with other lower-bound solutions such as the compression field theory of Collins and Mitchell (1980). Beam 5/2.5 shown in Fig. 5.5 illustrates how these two theories compliment each other in a slender beam. The compression field theory deals with zones of the beam which have a uniform stress field of constant inclination. The failure criteria for the concrete was empirically obtained from test panels with completely uniform stress field. The theory works best in such situations. It is uncertain whether the compression field theory is applicable to the direct compression struts or to the "fan" zones under the load and over the interior support. It, for example, would not predict that the first stirrup or two at each end of the shear span would be ineffective as indicated in Fig. 5.5. The plastic truss model deals with these fan zones. It also deals with the case of short shear spans where the fans intersect permitting a direct compression strut.

There are some differences between the plastic truss model and compression field theory. The plastic truss model uses a very simple failure criteria for the concrete but

deals with the question of an appropriate model in detail. That is, it considers questions like: how many stirrups are effective, what are the chord forces in indeterminate beams, is there sufficient room for the truss "joints" and "members"? The compression field theory on the other hand uses a simple model of uniform diagonal compression and sophisticated constitutive law for the concrete.

Perhaps in the future it will be possible to marry the two theories. At present the two theories can be coupled as in Fig. 5.5 to produce solutions. The solutions may not be legitimate not because the parents are not yet married but because of minor inconsistencies in the effective concrete strength used in the two theories.

5.10 Summary

In summary, this chapter has dealt with an examination of the plastic truss model as an analytical tool for predicting the ultimate strength of deep beams. The current literature suggests that the effective concrete strength, as expressed through the concrete efficiency factor ν, is an important parameter. Analysis of the test data showed that ν is highly variable because it reflects both concrete behavior and, more importantly, whether the plastic truss model used was good or bad. It was found that good predictions or strength could be obtained with $\nu = 1.0$, provided that an appropriate plastic truss model was used. An examination of models for the beams in this thesis

indicated that:

- horizontal web reinforcement was ineffective,
- the first one or two stirrups at each end of the shear span may be ineffective due to finite truss member and joint sizes
- for indeterminate beams the forces developed in the top and bottom bars may vary significantly from those predicted by simple beam theory

It was found that once these factors were recognized, it was possible to draw appropriate plastic truss models which predicted the strength for each of the specimens. At the transition between deep beams and slender beams, the plastic truss models were compatible with the compression field theory, while the truss models were found to be directly applicable to very deep beams, i.e. corbels, with a/d as low as 0.15.

6. DESIGN BY PLASTIC TRUSS

6.1 Introduction

This chapter deals with design procedures utilizing plastic truss models. Design presents a somewhat different problem than analysis. In analysis, one tries to find the strongest plastic truss which fits the beam geometry while in design one starts with a truss of the required strength and fits the beam around it.

In design, one must account for the possibility of:

- adverse loading and environmental conditions
- understrength materials
- inaccuracies or uncertanties in the design model

This can be done through the introduction of three sets of factors. Load factors are used to increase the specified loads to some extreme value in order to account for overloads. Material performance factors ϕ_c and ϕ_s are used to reduce the specified concrete and steel strengths in order to account for under-strength material. And finally, a model performance factor ϕ_m may be used to reduce the strength predicted by the plastic truss utilizing factored material properties to account for uncertainties in the design model.

The design process consists of drawing a design truss capable of resisting the factored loads. The design truss would utilize factored material strengths and would have its overall strength factored. Reinforcement would be provided

and anchored to resist the required tensile forces. Auxilliary reinforcement for serviceability or other conditions would be added as required. The beam dimensions would then be chosen so that they encompass or enclose the design truss with adequate cover.

6.2 Performance Factors

In design, the possibility of overloads, understrength materials, and uncertainty with regard to overall structural response, are accounted for by load and performance factors. The load factors proposed for use are those given in the National Building Code of Canada (1977) which are 1.25 and 1.5 for dead and live loads respectively. These are identical to the load factors used in the Canadian steel design standard S16.1-M78, and similar to those used in the European concrete design standard (CEB, 1978), but slightly smaller than those used in the American Concrete Institute design standard ACI 318-77.

The ratio of load factors to performance factors is a measure of safety. The performance factors may be obtained from statistical studies but in this work they will be obtained from calibration with existing code requirements. Once the load factors have been set, the performance factors can be determined to maintain approximately the same level of safety as in existing codes.

It is proposed that a separate performance factor be used for each material - concrete and steel, rather than a

single performance factor for the overall beam strength as currently used in shear or flexure. This is done because the plastic truss does not fail in "shear" or "flexure", rather, the tension members or compression members in the truss fail. Hence, it seems reasonable to use separate performance factors (partial safety factors), as used in CEB-FIP Model Code for Concrete Structures (CEB, 1978).

For dead and live load factors of 1.25 and 1.5, the concrete performance factor ϕ_c may be taken as 0.67. The effective concrete strength for design purposes is taken as $f_c^* = \phi_c \times 0.85 \times f'_c$. The factor 0.85 relates the strength of the concrete in the member to the specified 28 day cylinder strength f'_c. The selected value for ϕ_c is the same as that currently used in the Canadian steel design standard and the European concrete design standard.

The steel performance factor ϕ_s may be taken as 0.85. The effective steel yield strength is taken as $f_y^* = \phi_s \times f_y$. The value of ϕ_s is slightly smaller than that used for structural steel in S16.1. The variability of yield strength is greater in reinforcing bars than in structural steel, hence a more conservative ϕ_s was chosen.

The performance factors for the individual materials do not account for the variability of the combined system or uncertainty in the design model. This may be dealt with in at least two ways. The first proposal is that once the design truss has been analyzed with reduced material strengths, the truss strength would be further reduced by a

model performance factor ϕ_m = 0.95. While this parameter deals in part with tolerances in beam dimensions and the locations of bars, it deals mainly with variations in the truss model. Since the problem is solved semi-graphically, in that strut interferences and slopes are determined by scaling the truss diagrams, there may be variations in solutions obtained for the same problem by different individuals. The principal difference likely to occur would be the exclusion of one or two stirrups from the plastic truss model as discussed in Chapter 5. The use of model performance factor less than 1.0 is academically acceptable, but awkward in practice. It also has the effect of "smearing" the uncertainty over the whole truss model. An alternative and superior approach would be to use the full theoretical truss capacity (i.e. ϕ_m = 1.0) and be more cautious in the development of the plastic truss. Important details should be dealt with conservatively. This results in putting extra safety into the critical details - where it will do the most good.

6.3 Application of Model

The purpose of the design truss is to provide a plausible and consistent "flow of forces" through the beam. The plastic truss is one of many possible lower bound plastic solutions. As such, the truss must be in equilibrium, and the members and joints must not be stressed to failure. For design purposes, the effective material

strengths as determined in Section 6.2 are used in the model.

The plastic design truss consists of a pin-jointed truss with steel tension members and concrete compression members. The centroids of the members must coincide at a joint. The joint is accommodated by the use of concrete "hydrostatic" stress zones. The stresses in the struts and joints will then be the maximum principal stress and are taken equal to the effective concrete strength.

The design procedure consists of drawing to scale, a plastic truss subjected to the factored design loads. Truss member forces and stresses are then determined and compared to the permissible values. Truss members are modified as required.

This procedure may require some iteration as the force in each member depends on the truss geometry which, in turn, depends on the width of the compression struts and the size of the joints which, in turn, are determined from the member forces. One can start with a simple preliminary design truss which is drawn approximately to scale. Slopes for each compression member may be measured from this figure, and used in the analysis of the truss. Once the truss member forces have been approximately determined, the member sizes are computed using the design material strengths. A more accurate plastic truss model may be drawn using this information. This model would be analyzed, and member sizes determined again. The process is repeated until the truss

member forces and geometry have converged to the desired level of accuracy. Convergence is usually very rapid and one or two iterations will usually be adequate.

Once a satisfactory plastic truss is obtained, the beam is detailed in a manner consistent with the assumed plastic truss. Beam dimensions should be chosen so that the plastic truss fits entirely within the beam and is provided with adequate cover. Auxilliary reinforcement may be added for serviceability or other conditions.

The following thoughts may be useful in establishing the preliminary design truss:

1. If stirrups are used, one may assume that all are yielded and fully effective in the plastic truss model.

2. Unless the beam is shallow ($a/d > 2$) or large amounts of stirrup reinforcement are used, the stirrups will not add significant capacity to the beam. In this case, the stirrups would be ignored in the design truss.

3. The main flexural steel requirement may be estimated from the maximum bending moments. As with other trusses, the chord force may be estimated by dividing the maximum bending moment by the internal lever arm of about 70% to 80% of the beam depth.

4. In continuous or statically indeterminate beams, one must arrive at a truss which produces the desired distribution of support reactions. This is done by adjusting the ratio of top steel to bottom steel.

5. The solution for member forces in what would

normally be an indeterminate truss is simplified by assuming yielding (at the effective yield stress f_y^*) of at least some of the reinforcement, so that the plastic truss becomes statically determinate. The question of which reinforcement should be assumed to yield was discussed in Chapter 5.

6.4 Reinforcement Details

The detailing of the reinforcement must be consistent with the assumed plastic truss. Adequate anchorage of the main steel is most important. Deep beams require significantly higher bar forces at anchorage locations than indicated by the bending moment diagram. This is illustrated in Figs. 5.1 to 5.5. Hence, bars must not be cut off in accordance with the bending moment diagram. They should be anchored to develop the forces required in the plastic truss model. The truss drawing will indicate the desired location of the centroid of the tensile reinforcement, so that members meet at joints, as well as the zone over which the reinforcement may be distributed.

Some minimum amount of vertical web reinforcement should be used to reduce the variability in the strength of the member. The test data indicate that the current ACI minimum web reinforcement requirement is not enough to significantly increase the average strength, but it will bring the weakest fractile much closer to the average strength.

Even though horizontal web reinforcement does not

increase the ultimate strength of a deep beam, it would be prudent to use some horizontal reinforcement so that the crack widths are minimized at service loads. Serviceability requirements were not considered in this study. Franz and Breen (1980) discuss minimum face steel requirements.

In addition to the vertical and horizontal web reinforcement already described, one may also require auxilliary reinforcement in the region of loads and supports. This reinforcement is used to handle the bursting stresses produced by heavily loaded bearing plates. The situation and hence the solution is similar to the anchorage point of a prestressing cable. For beams supported and loaded in this way, the recommendations of CEB (1970) or CIRIA (1977) may be followed for proportioning this reinforcement as these recommendations were based on tests in which the beams were loaded and supported by steel bearing plates. A real beam however, is likely to be loaded and supported by concrete columns. All of the specimens in this study were loaded and supported by reinforced concrete columns with the vertical column reinforcement and ties extending at least a compression development length into the beam. No additional auxilliary reinforcement was used, and apparently none was required as no bursting failures were observed. If for some reason, the columns were very highly stressed, the bursting stresses should be checked.

6.5 Design Strategies

This section deals with several philosophical questions one may address during the design of a deep beam. Should the beam be simple span or continuous? How can one account for support movements? Can one utilize the enhanced shear strength of a deep beam and still have a reasonably ductile member? All of these questions revolve around the issue of safety.

Both simple span and continuous beams may be designed with the plastic truss analogy. There are, however, some differences in the design strategy. The abundance of experimental data for simple span beams coupled with only a few plausible plastic trusses, permits one to design simple span deep beams with confidence. Closed form equations can be developed for specific reinforcement and geometric conditions. On the other hand, the experimental data that has been obtained for continuous beams indicates that it is very important that one use an appropriate truss model in the design of such a beam. The model must produce the expected support reactions. If this is not the case, very unsafe predictions may be obtained with the plastic truss model. The perceived increase in safety due to redundancy in a continuous beam may be more than offset by the difficulty of safely predicting the strength of a continuous beam.

Two major difficulties in the design of continuous deep beams result from shear deformation effects and support

movements. In the tests, support movements were kept very small so that only shear deformations were significant. In real beams, however, larger support movements are possible making them relatively more important. The support movements may be due to foundation movements or temperature, creep, and differential strain effects between interior and exterior columns. Support movements can drastically change the distribution of reactions in continuous deep beams making it difficult to establish an appropriate plastic truss. One solution would be to account for the uncertainty of the plastic truss model by the use of a reduced model performance factor ϕ_m. A better solution would be to estimate the range of support reactions and design plastic trusses for each limiting case (i.e. maximum and minimum exterior reactions). This is by no means unimportant. De Jong (1970) measured and predicted foundation movements for several high rise buildings founded on a stiff till. Using these movements he analyzed the structures and found that foundation loads (support reactions) changed by up to 40%. Simple span deep beams would of course not be sensitive to support movements.

The last question to be addressed relates to ductility. A design utilizing heavy stirrup reinforcement will be more ductile and more accommodating of variations in support reactions. The stirrups permit the development of crack fans which gradually reduce the tension forces in the main reinforcement. With adequate stirrups, the tension is

eventually eliminated so that no horizontal force exists to equilibrate a direct compression strut. While stirrups provide some ductility because of their confining effect on the concrete, in deep beams, most of the ductility is due to the elimination of the brittle direct compression strut. In eliminating the direct compression strut, the strength enhancement associated with low a/d ratios is lost. In order to reach this state, the number of stirrups must be such that the strength of the beam will be greater than that obtained with a direct compression strut. The contribution of extra stirrups to increased ductility is more important than the increase in strength when viewed from an overall safety point of view. In continuous deep beams with uncertain support reactions, consideration should be given to a more ductile and forgiving design with heavy stirrups.

6.6 Summary of Design Procedures

As with all structural analysis problems there are three essential ingredients in the solution of the plastic truss:equilibrium, kinematics, and constitutive laws.

a) Constitutive Laws

Rigid-plastic material or constitutive laws are used for design. The effective steel and concrete strengths are taken as:

$$f_y^* = \phi_s \times f_y \qquad \text{where } \phi_s = 0.85$$

$$f_c^* = \phi_c \times 0.85 \times f'_c \qquad \text{where } \phi_c = 0.67$$

These strengths are compatible with dead and live load factors of 1.25 and 1.5 respectively.

b) Kinematics

The kinematics or geometry should be that of a pin jointed truss. The centroids of all members framing into a joint should coincide. While steel is used to resist tension forces, concrete is used to resist compression forces. The dimensions of compression members should be determined from the member force and the effective concrete strength. Truss joints are accommodated by hydrostatic stress elements. The plastic truss should be drawn to scale.

c) Equilibrium

Static equilibrium must always be satisfied in the analysis of the plastic truss. The solution for member forces in what might normally be an indeterminate truss is simplified by assuming yielding (at the effective yield stress) of at least some of the reinforcement, so that the plastic truss becomes statically determinate.

The kinematics and statics are solved or satisfied in an iterative manner. One starts by drawing a rough sketch of a truss with approximate kinematics. This is analyzed to

determine member forces which are used to refine the kinematics. This process is repeated until convergence is achieved.

Once a satisfactory plastic truss is obtained, the beam must be detailed in a manner consistent with this model. Additional reinforcement may be required for ductility, serviceability or other conditions.

7. SUMMARY AND CONCLUSIONS

7.1 Experimental Observations

Tests were conducted on simply supported and continuous deep beams with various depth to span ratios and various amounts and types of web reinforcement. Two categories of behavior were observed. Beams with heavy stirrup reinforcement exhibited considerable ductility. The strengths obtained for each end of symmetrical specimens were very consistent. The beams in this category did not exhibit the characteristic change in shear strength with changes in a/d which is normally associated with deep beam behavior. All other test specimens, that is, those beams without significant vertical web reinforcement fell into a second behavioral category. These beams were brittle and somewhat inconsistent in strength unless minimum stirrups were present. The a/d ratio had a very significant influence on the shear strength of beams in the second category.

A comparison of the results for simple span beams and continuous beams indicates that both types of members had similar shear strengths with simple span beams being slightly stronger than continuous beams at low a/d ratios (a/d = 1.0).

The beams developed distinctive inclined cracks running from the support to the point load. These cracks formed well below failure load. This was especially true for the

deeper beams in which inclined cracks developed at loads as low as 1/4 to 1/3 of the ultimate load. Crack formation was sudden, complete, and was accompanied with a bang. The inclined cracks were widest at mid depth of the beam. Web reinforcement did not prevent the formation of these cracks. Flexural cracks, on the other hand, formed quietly and grew slowly in length as the load was increased.

The specimens with light or no web reinforcement generally behaved as trusses after cracking developed. Cracks often defined concrete compression struts running from the loads to the supports. Concrete strain measurements implied that struts (narrow zones of high uniaxial compression) exist in deep beams even if not specifically outlined by cracks. Steel strain measurements indicated constant steel strains along tension members in the truss rather than the variation in strains expected from the bending moment diagram. Significant steel strains were observed in the main reinforcement at locations of zero bending moment. These were as high as the yield strain in some cases.

The specimens with heavy stirrup reinforcement developed crack fans over the interior support and under the point loads, thus reducing the influence of a direct compression strut from load to support. The observed variations in the concrete and steel strains were similar to those predicted by the plastic truss analogy.

Horizontal web reinforcement was found to have no

influence on the strength of the specimens tested. The behavior of beams with minimum or maximum horizontal web reinforcement was indistinguishable from that of beams without web reinforcement.

7.2 Plastic Truss Hypothesis

The truss analogy for shear strength is not new. It dates back to the early days of reinforced concrete design (Ritter, 1899; Mörsh, 1902). Truss models based on plasticity were introduced about 1970 (Lampert and Thürlimann, 1971). The plastic truss model explains the results observed in this series of tests, and correctly predicts the influence of each of the important parameters on the behavior of deep beams. It provides a rational basis for design and detailing provided that the correct model is used.

The plastic truss analogy has been tuned against the experimental behavior. Using the correct truss model is far more important than selecting values of the effective concrete strength, unless the beam is over reinforced in shear. A beam over reinforced in shear is one which has so much vertical web reinforcement that the concrete web crushes before the reinforcement yields. Current design codes avoid this situation by limiting the amount of stirrup reinforcement one can use so that over reinforced webs will not occur in practice. Since web crushing will not occur in beams designed using such codes, the concrete strength is

not overly signficant. Good strength predictions were obtained for the test specimens even when the full concrete strength was utilized provided that an appropriate truss model was used in the analysis.

The selection of appropriate truss models was considered in detail in Chapter 5. One must find a truss model which:

- is in equilibrium with the external loads and reactions.
- when drawn to scale with truss members of finite width has their centroids coincident at each truss joint.
- has concrete compression members, steel tension members and "hydrostatic" stress joints subjected to the maximum permissible stresses.

Appropriate truss models for simple span beams are relatively easy to obtain. The relatively few plausible models coupled with numerous test results permit one to design simple span beams by the plastic truss method with confidence.

Appropriate truss models for continuous beams are more difficult to obtain. It is possible to visualize several different truss models for a continuous deep beam. The safety of a continuous deep beam is very dependent on the model used in the design. The tests indicated that unless the beam has heavy stirrup reinforcement, it will have limited ductility. If the design model is significantly different from the natural behavior of the beam, the beam

may not have sufficient plastic redistribution capacity to develop the assumed distribution of forces, and hence will have less strength than predicted in the design.

The best truss model for a continuous beam will be one which produces support reactions identical to those experienced in the real structure. Due to creep, shrinkage, support movements etc. there may be several possible distributions of reactions during the life of the structure. A suitable truss model for each possibility must be found, and the overall beam design must permit each of these plastic truss models to develop. For continuous deep beams without heavy stirrups, the reliability of the strength predictions can be no better than the reliability of the prediction of support reactions. When the distribution of support reactions is in doubt, one should resort to a design utilizing heavy stirrup reinforcement. The increased ductility of such a design will make the beam less sensitive to support movements.

An important aspect of design utilizing the plastic truss analogy is that a consistent model is used for "shear" and "flexure" design. It is recommended that in designing a deep beam, one draw the truss in detail, and then detail the reinforcement in a manner consistent with the drawing.

An engineer can only accept responsibility for a new design if he can (to use Westergaard's expression) "feel in his bones" how the structure will carry the load. Drawing a picture of the structure in action will provide the designer

with such a feeling. Hardy-Cross (1952) has said:

> "Students should be encouraged more to draw pictures of what they are thinking about. They should draw pictures of deformed structures, pictures of structural failure, pictures of stress distribution. To try to draw them raises, or should raise, hundreds of questions. If men can't draw them they don't know what they are talking about and the degree of detail shows the amount of familiarity with the subject. To try to draw a picture, ... will frequently answer or invalidate a question."

The plastic truss model is a simple application of this advice. It provides a rational qualitative and quantitative explanation for the behavior of deep reinforced concrete beams.

REFERENCES

ACI Committee 318, *Building Code Requirements for Reinforced Concrete (ACI 318-77)*, American Concrete Institute, Detroit, Mich., 1977.

ACI-ASCE Committee 426, *The Shear Strength of Reinforced Concrete Members*, Journal of the Structural Division ASCE Vol. 99, No. ST6, June, 1973.

ACI Committee 426, *Suggested Revisions to Shear Provisions for Building Codes*, ACI Journal, Vol. 74, No. 9, 1977.

Barton, N., *Review of New Shear-Strength Criterion for Rock Joints*, Engineering Geology, Vol. 7, 1973.

Bresler, B., Pister, K.S., *Strength of Concrete Under Combined Stresses*, ACI Journal, Vol. 55, No. 3, 1958.

Chana, P.S., *Some Aspects of Modelling the Behaviour of Reinforced Concrete Under Shear Loading*, Cement and Concrete Association Technical Report No. 543, July 1981.

Chen, W.F., *Plasticity in Reinforced Concrete*, McGraw-Hill Book Company, New York, 1982.

Chow, L., Conway, H.D., and Winter, G., *Stresses in Deep Beams*, Trans. ASCE Vol. 118, Paper No. 2557, 1953.

CIRIA, *The Design of Deep Beams in Reinforced Concrete*, Guide 2, Construction Industry Research and Information Association, London, January, 1977.

Collins, M.P. and Mitchel, D., *Shear and Torsion Design of Prestressed and Non-Prestressed Concrete Beams*, PCI Journal, September-October, 1980.

Comite Europeen du Beton, *International Recommendations for the Design and Construction of Deep Beams*, Information Bulletin No. 73, Paris, France, June, 1970.

CEB-FIP *Model Code for Concrete Structures*, Information Bulletin No. 124/125E, Paris, France, 1978

Crist, R.A., *Static and Dynamic Shear Behavior of Uniformly Loaded Reinforced Concrete Deep Beams*, Ph.D. Thesis, University of New Mexico, Albuquerque, New Mexico, 1971.

Cross, Hardy, *Engineers and Ivory Towers*, McGraw-Hill Book Company, New York, 1958.

CSA Standard, *CAN3-A23.3-1977, Code for the Design of Concrete Structures for Buildings*, Canadian Standards Association, Rexdale, Ontario, 1977.

CSA Standard, *CAN3-S16.1-1978, Steel Structures for Buildings - Limit States Design*, Canadian Standards Association, Rexdale, Ontario, 1978.

de Paiva, H.A.R., and Siess, C.P., *Strength and Behavior of Deep Beams in Shear*, Journal of the Structural Division, ASCE, Vol. 91, No. ST5, October, 1965.

Dischinger, F., *Contribution to the Theory of Wall-Like Girders*, International Association for Bridge and Structural Engineering, I, 1932, pp. 69-93.

Exner, H., *On the Effectiveness Factor in Plastic Analysis of Concrete*, Colloquium on Plasticity in Reinforced Concrete, IABSE Reports of the Working Commissions, Vol. 29, Copenhagen, 1979.

Franz, G.C., Breen, J.E., *Design Proposal for Side Face Crack Control Reinforcement for Large Reinforced Concrete Beams*, Concrete International: Design & Construction, Vol. 2, No. 10, 1980.

Geer, E., *Stresses in Deep Beams*, Journal of the American Concrete Institute, Vol. 56, January, 1960.

Hagberg, T., *Design of Concrete Brackets: On the Application of the Truss Analogy*, ACI Journal, Vol. 80, No. 1, 1983.

Jensen, B.C., *Reinforced Concrete Corbels - Some Exact Solutions*, Colloquium on Plasticity in Reinforced Concrete, IABSE Reports of the Working Commissions, Vol. 29, Copenhagen, 1979.

Johansen, K.W., *Failure Criteria of Concrete and Rock*, Bygningsstat. Medd., Vol. 29, No. 2, 1958.

Kong, F.K., Robins, P.J., and Sharp, G.R., *Design of Reinforced Concrete Deep Beams in Current Practice*, The Structural Engineer, Vol. 53, No. 4, April, 1975.

Kriz, L.B., and Raths, C.H., *Connections in Precast Concrete Structures - Strength of Corbels*, PCI Journal, Vol. 10, No. 1, 1965.

Kumar, P., *Collapse Load of Deep Reinforced Concrete Beams*, Magazine of Concrete Research, Vol. 28, No. 94, March 1976.

Kupfer, H., Hilsdorf, H.K., and Rusch, H., *Behavior of Concrete Under Biaxial Stresses*, ACI Journal, Vol. 66, No. 8, 1969.

Lampert, P., Thurlimann, B., *Ultimate Strength and Design of Reinforced Concrete Beams in Torsion and Bending*, Publications No. 31-I, IABSE, Zurich, 1971.

Leonhardt, F., and Walther, R., *Wandartige Trager*, Deutscher Ausschuss fur Stahlbeton, Vol. 178, Wilhelm Ernst und Sohn, Berlin, West Germany, 1966.

MacGregor, J.G., and Hawkins, N.M., *Suggested Revisions to ACI Building Code Clauses Dealing with Shear Friction and Shear in Deep Beams and Corbels*, ACI Journal, Vol. 74, No. 11, 1977.

Manuel, R.F., *Failure of Deep Beams*, Shear in Reinforced Concrete, ACI Special Publication SP-42, Vol. 2, Detroit, Mich., 1974.

Marti, P., *Plastic Analysis of Reinforced Concrete Shear Walls*, Bericht Nr. 87, Institut fur Baustatik und Konstruktion, Zurich, November, 1978.

Morsch, E., *Concrete-Steel Construction*, English Translation by E.P. Goodrich, McGraw-Hill Book Company, New York, 1909, (Translation from third edition of *Der Eisenbetonbay*, first edition, 1902).

Mueller, P., *Plastic Analysis of Torsion and Shear in Reinforced Concrete*, Colloquium on Plasticity in Reinforced Concrete, IABSE Reports of the Working Commissions, Vol. 29, Copenhagen, 1979.

National Building Code of Canada 1980, Associate Committee on the National Building Code, National Research Council of Canada, Ottawa, 1980.

Nielsen, M.P., Braestrup, M.W., Jensen, B.C. and Finn Bach, *Concrete Plasticity, Beam Shear - Shear in Joints - Punching Shear*, Special Publication of the Danish Society For Structural Science and Engineering, Technical University of Denmark, Lyngby/Copenhagen, 1978.

Ong, S.Y., *Effect of Web Reinforcement on Deep Beams*, M.Sc. Thesis, University of Alberta, Edmonton, Alberta, 1982.

Paulay, T., *The Coupling of Shear Walls*, Ph.D. Thesis, University of Canterbury, Christchurch, New Zealand, 1969.

Portland Cement Association, *Design of Deep Girders*, Publication ISO79.01D, Skokie, Illinois, 1980.

Richart, F.E., Brandtzaeg, A., and Brown, R.L., *A Study of the Failure of Concrete Under Combined Compressive Stresses*, University of Illinois, Engineering Experimental Station Bull. 185, 1928.

Ritter, W., *Die Bauweise Hennebique*, Schweizerische Bauzeitung, Zurich, February, 1899.

Robinson, J. R., *Influence of Transverse Reinforcement on Shear and Bond Strength*, ACI Journal, Vol. 62, Mar., 1965.

Rogowsky, D.M., MacGregor,J.G., and Ong, S.Y., *Tests of Reinforced Concrete Deep Beams*, Structural Engineering Report No. 109, Dept. of Civil Engineering, University of Alberta, Edmonton, Alberta, 1983.

SFRAME, Computer Program Coded by R.B. Pinkney, Dept. of Civil Engineering, University of Manitoba, Winnipeg, Manitoba, updated 1982.

SIA Schweizerischer Ingenieur - und Architekten - Verein, *SIA Code 162 - Concrete, Reinforced Concrete and Prestressed Concrete*, Zurich, 1976.

Smith, K.N., and Vantsiotis, A.S., *Shear Strength of Deep Beams*, ACI Journal, Vol. 79, No. 3, 1982.

Thurlimann, B., *Plastic Analysis of Reinforced Concrete Beams*, Bericht Nr. 86, Institut fur Baustatik und Kondstruktion, Zurich, November, 1978.

Thurlimann, B., *Discussion in Session 2*, Colloquium on Plasticity in Reinforced Concrete, IABSE Reports of Working Commissions, Vol. 29, Copenhagen, 1979.

APPENDIX A

Plasticity in Reinforced Concrete

During the last two decades the literature of plasticity in reinforced concrete has grown extensively. 'Limit-analysis' techniques have been used to predict upper and lower bounds for the carrying capacity of beams in shear. These techniques are based on the basic theorems of plasticity which for the purposes of this thesis are: (Chen, 1982)

I: Lower-Bound Theorem

If an equilibrium distribution of stress can be found which balances the applied load and is everywhere below yield or at yield, the structure will not collapse or will just be at the point of collapse. Since the structure can carry at least this applied load, it is a lower-bound to the load carrying capacity of the structure.

II: Upper-Bound Theorem

The structure will collapse if there is any compatible pattern of plastic deformation for which the rate at which the external forces do work exceeds the rate of internal dissipation. Since the structure will fail under these external forces by this kinematic mechanism, this load represents an upper-bound to the load carrying capacity of the structure.

These theorems assume or require that:

1) The material exhibits perfect or ideal plasticity. That is, strain hardening of the steel and strain softening of concrete are ignored.
2) A failure or yield criterion for the material is required. It is convenient to assume a convex yield surface from which plastic-strain rates are derivable through the associated flow rule. This implies that the principal plastic strains occur in the same direction as the principal stresses and that the resulting internal work done is positive.
3) Changes in geometry of the structure that occur at the collapse load are insignificant, hence the equilibrium equations can be formulated with the original geometry.

The plasticity solutions to be examined use these theorems and assumptions, but they differ in the rigor with which the theorems are applied. A discussion of the assumptions is in order. All solutions make use of assumption 3 which effectively limits the application of this approach to problems in which second order geometric effects are negligible.

Most of the solutions use a "Modified Mohr-Coulomb" failure criterion. A family of Mohr's Circles at failure for various states of biaxial stress are illustrated in Fig. A.1 (Bresler and Pister, 1958). An idealized, Modified Mohr-Coulomb failure envelope for biaxial stress is

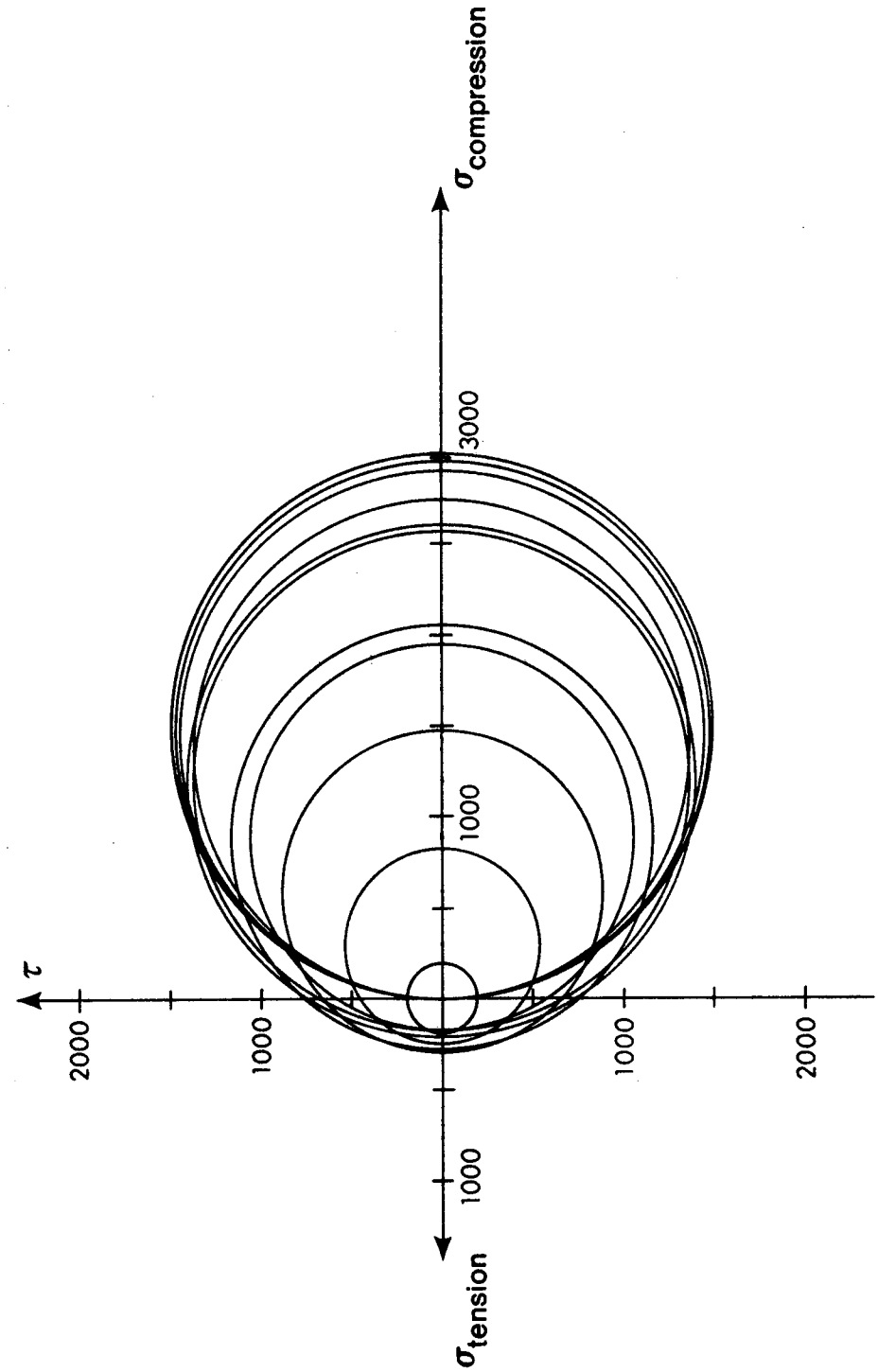

Fig. A 1. Mohr's Failure Circles for 3000 psi Nominal Concrete.

illustrated in Fig. A.2. This envelope passes through the uniaxial tensile strength of concrete at A and the uniaxial compressive strength at D. The arc CD and FD is a part of the Mohr's Circle for uniaxial compression. The portions BC and EF have the equation $\tau = c + \sigma \tan \phi$.

This envelope appears to be a good first estimate of the actual experimental behavior plotted in Fig. A.1. The Coulomb parameters c and ϕ have been determined experimentally for concrete (Johansen 1958; Richart et al. 1928). The apparent cohesion c is approximately $f'_c/4$ and the internal-friction angle ϕ is approximately 37°. This envelope can be expressed in terms of principal stresses and is illustrated in Fig. A.3(a). The slope, m, of the inclined portion in this figure is derivable from Fig. A.2 and is 4.0. The terms σ_1, σ_2 and σ_3 represent the three principal stresses shown in Fig. A.3(b). In the biaxial stress state or plane stress state $\sigma_2 = 0$.

Figure A.3(b) compares this failure envelope with experimental data obtained by Kupfer, Hilsdorf and Rusch (1969). The modified Mohr-Coulomb failure criteria appears to be a good, slightly conservative first estimate for the actual experimental failure envelope except in the vicinity of points B and E.

For lower-bound solutions the state of stress must lie within or on the failure envelope. For upper bound solutions, one makes use of the associated flow rule which defines the plastic strain directions from the failure

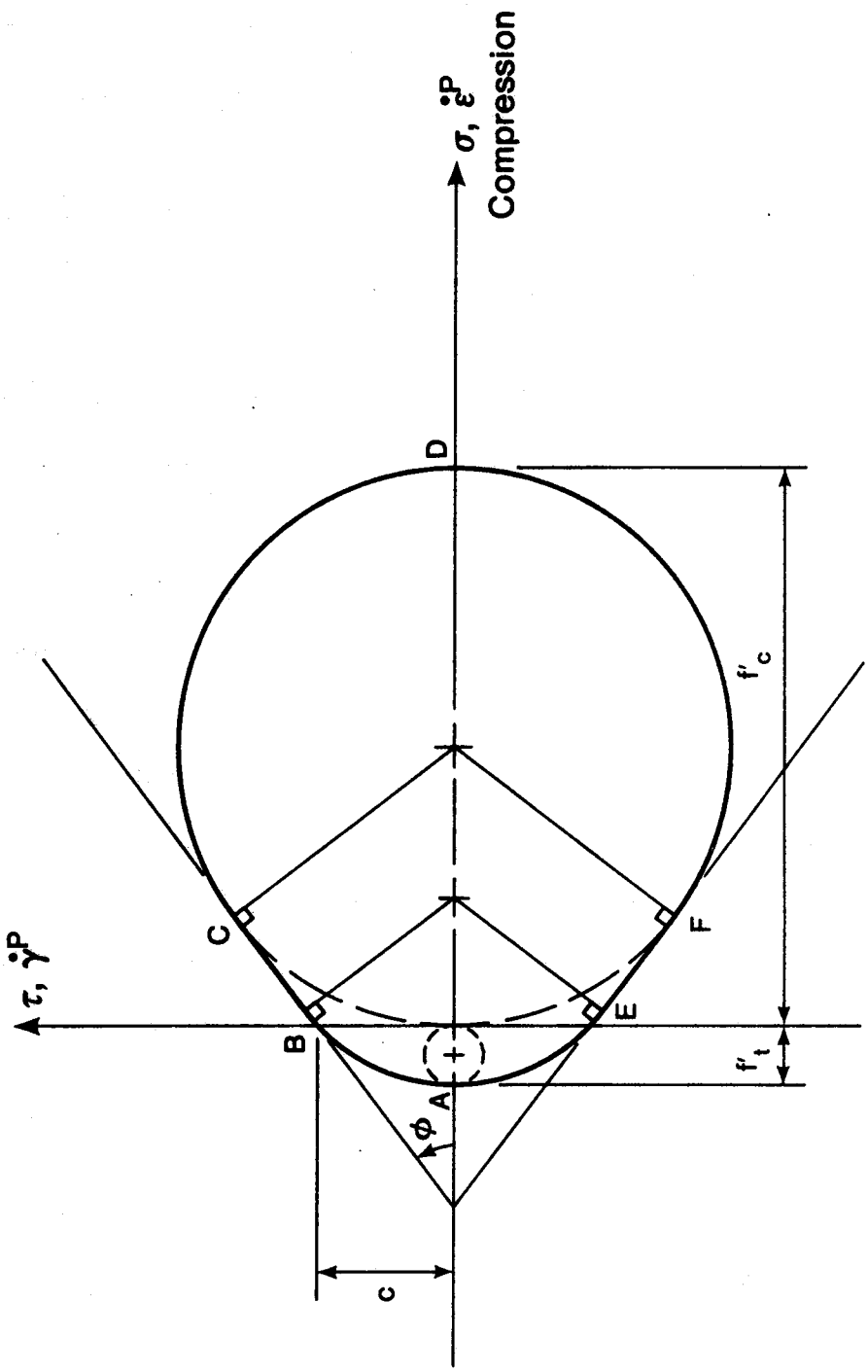

Fig A 2. Modified Mohr-Coulomb Failure Envelope

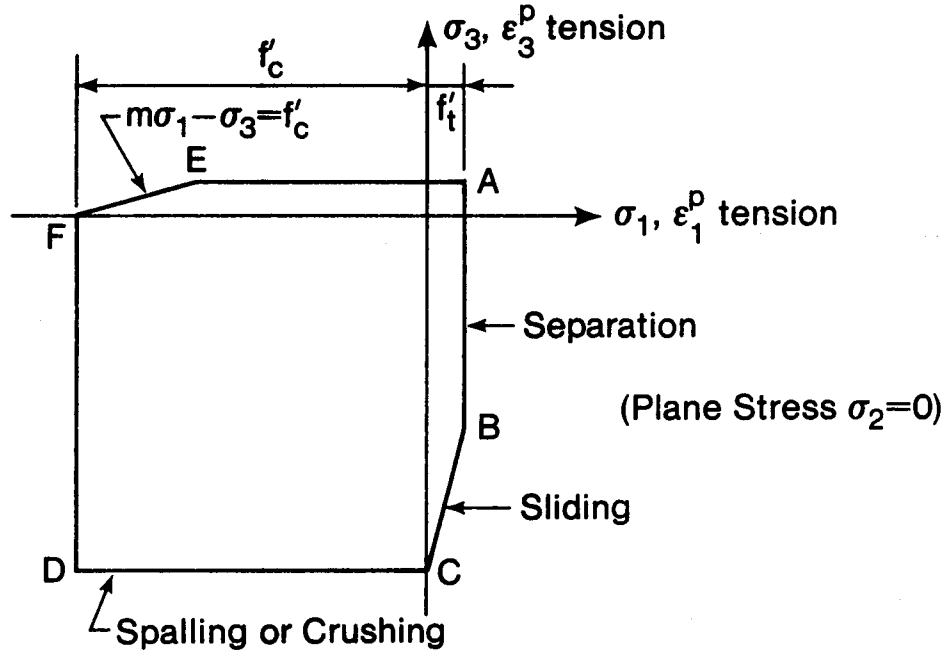

a) Failure Criterion on $\sigma_1 - \sigma_3$ Space.

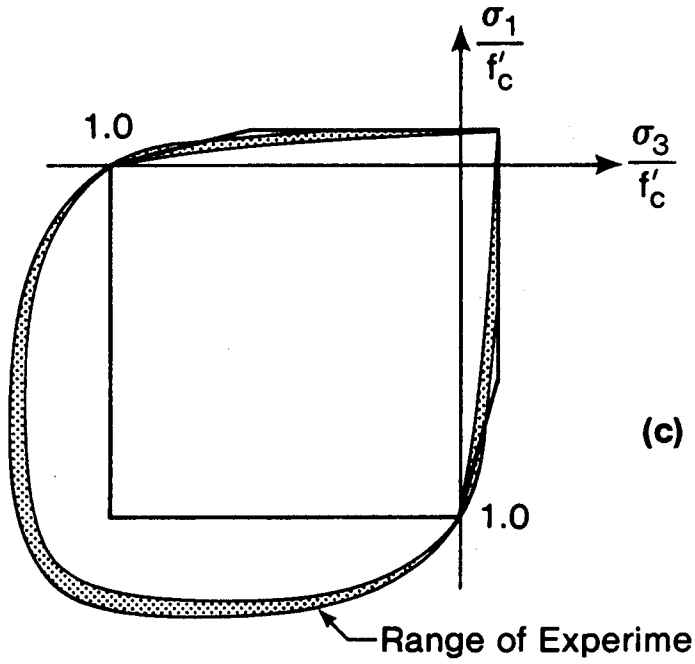

b) Modified Mohr-Coulomb Failure Envelope and K.H.R. Biaxial Stress Data.

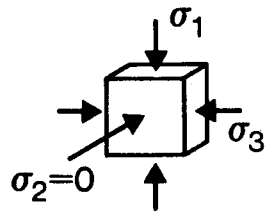

(c) Stress Directions.

Figure A.3. Failure Criterion in Terms of Principle Stresses.

envelope. Between A and B in Figures A.2 and A.3(a), cracking occurs perpendicular to the direction of the principal tension stress. The virtual deformation δ, is normal or 90° to the crack, hence W_i, the virtual internal work per unit of crack, is:

$$W_i = f'_t \delta \tag{A.1}$$

Along BC, a sliding failure occurs with the virtual deformation δ acting at an angle of ϕ to the crack. The resulting internal virtual work per unit area of crack is:

$$W_i = \left(\frac{1 - \sin \phi}{2}\right) f^*_c \delta \tag{A.2}$$

At point B, the virtual displacement δ can take place at an angle α to the crack such that:

$$\phi \leq \alpha \leq 90^0$$

and

$$W_i = \left[\left(\frac{1 - \sin \alpha}{2}\right) f^*_c + \left(\frac{\sin \alpha - \sin \phi}{1 - \sin \phi}\right) f'_t\right] \delta \tag{A.3}$$

Along CD, a simple crushing failure takes place with the virtual deformation acting at -90° to the plane of crushing. The resulting internal virtual work per unit area of the plane of crushing is:

$$W_i = f_c^* \delta \qquad (A.4)$$

It should be noted that for the biaxial plane stress condition ($\sigma_2 = 0$) along CD, it is the $\sigma_3 \cdot \sigma_2$ Mohr's Circle which contacts the failure envelope rather than the $\sigma_1 \cdot \sigma_3$ circle. The failure is out of the plane of the member and could more properly be called a spalling failure. This behavior is observable in the photographs presented by Kupter et al. (1969). Equations A.1 to A.4 are used in developing upper-bound solutions.

The assumption of perfect or ideal plasticity is questionable. While it is generally safe to neglect the strain hardening of the steel, it is usually unsafe to neglect strain softening of the concrete. Often, some portions of the concrete along the rupture face will be stressed beyond peak strength and begin to soften before other portions of the concrete mobilize their full strength. Hence, one cannot rely on mobilizing the full strength of the concrete over the entire section, and only part of the rupture face is effective. This leads to the introduction of an 'efficiency factor' $\nu < 1.0$ by which f_c' must be multiplied in order to get an equivalent strength f_c^* over the whole rupture surface. The efficiency factor is back calculated from test data, and depends upon the plasticity model used in predicting the member capacity. Because of the manner in which it is empirically obtained,

ν also compensates for errors in the plasticity model.

If the same failure envelope is used to develop upper and lower-bound solutions, the solutions will bracket the 'exact' plasticity solution. The 'exact' solution is obtained when upper and lower-bound solutions give the same failure load. Most of the closed form plasticity solutions published in the literature are exact solutions.

To illustrate the use of the plasticity models the deep beam shown in Fig. A.4 will be analyzed using both the upper bound and lower bound methods. Referring back to the Lower Bound Theorem presented earlier, a lower-bound solution involves finding a pattern of internal stresses that:

(a) is in equilibrium with the loads, and

(b) at no place exceeds the strength of the material.

The truss shown in Fig. A.5 satisfies these requirements. The diagonal members are "compression struts", the horizontal member is the reinforcement and the shaded regions are "hydrostatic elements" chosen so that the 3 forces meeting at A or B or C are concurrent. This geometry can be obtained graphically by trial, or analytically through simple algebra, using the principles outlined in Section 2.4. In this solution the concrete resists compression only (i.e. $f'_t = 0$) and shall be assumed to have an efficiency factor $\nu = 1.0$. The lower-bound shear capacity V_L calculated using Eq. 2.16 is:

$$V_L = 684 \ (\tan 42.4^0) = 625 \text{ kN}$$

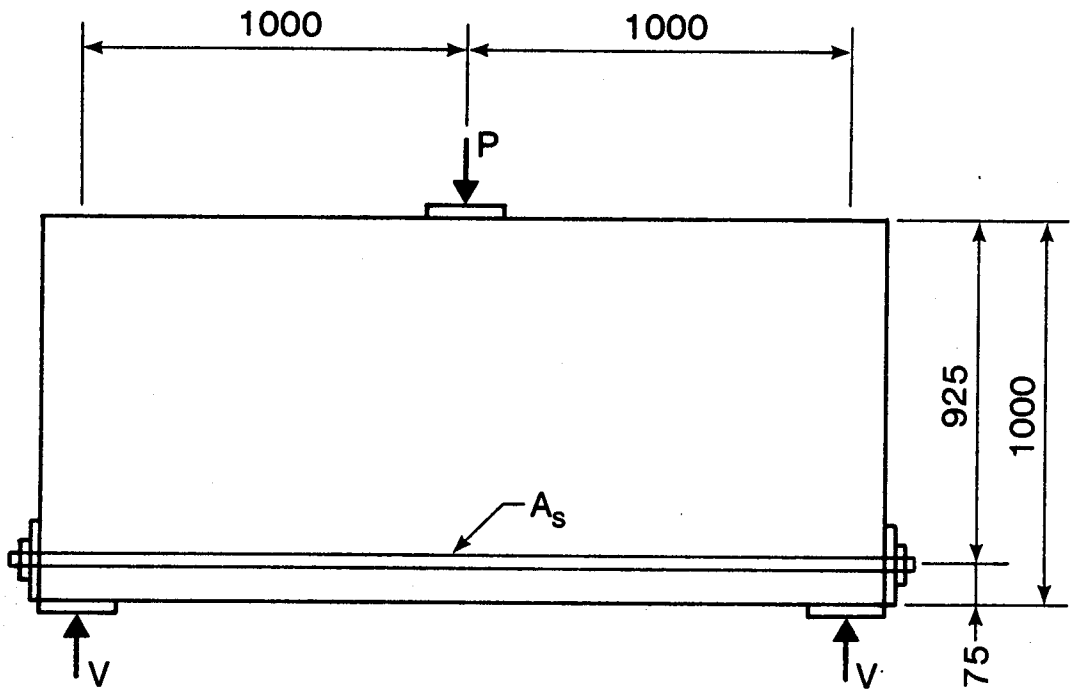

b = 200
f'_c = 26.1 MPa
$A_s fy$ = 684 kN

Figure A.4. Example Problem

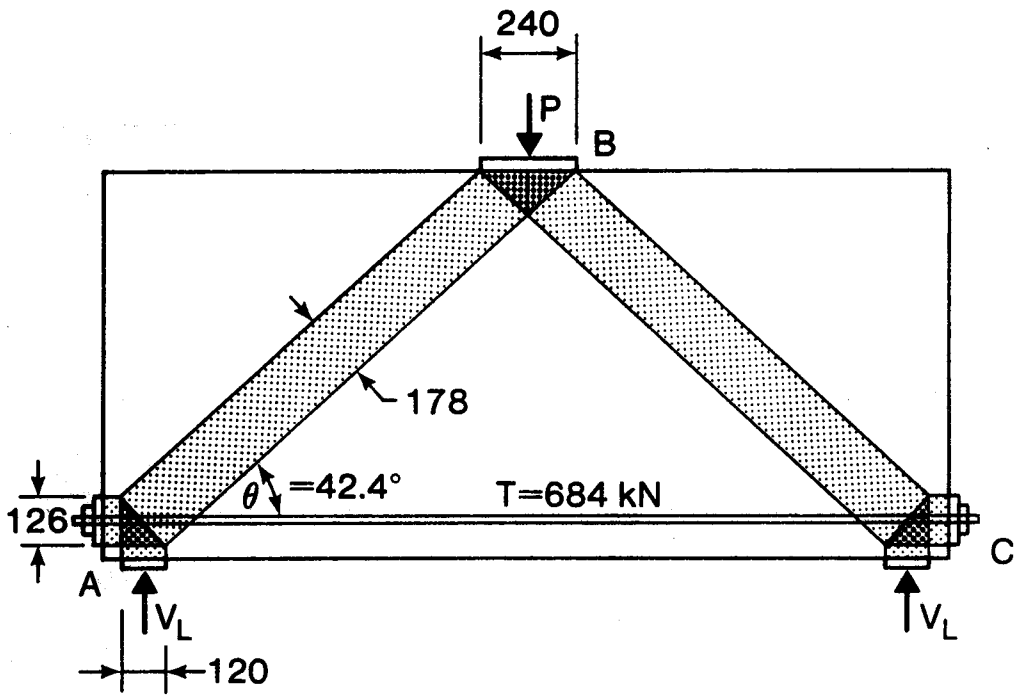

Figure A.5. Lower Bound Solution

It should be pointed out that in arriving at the truss geometry, the horizontal length of the support bearing is V_L/bf_c^*, similarly the vertical height of the anchorage plate is $A_s f_y/bf_c^*$. The dimensions shown in Fig. A.5 satisfy these conditions.

Using the bearing plate lengths shown in Fig. A.5, one can obtain an upper bound solution by postulating failure by vertical opening of a tension crack running corner to corner as illustrated in Fig. A.6. Using the same assumptions as in the lower bound solution, i.e. $\nu = 1.0$ and $f_t' = 0$ and Eq. A.3, the internal virtual work done during the virtual displacement δ is:

$$V_I = \left(\frac{(1 - \sin 39.4)}{2} 26.1\right)(200 \times 1293)\ \delta = 1235 \times 10^3\ \delta$$

The external virtual work for this virtual displacement is:

$$W_E = V_U\ \delta$$

Since $W_E = W_I$, an upper-bound to the shear strength is:

$$V_U = 1235\ \text{kN}$$

Hence:

$$V_L < V < V_U$$

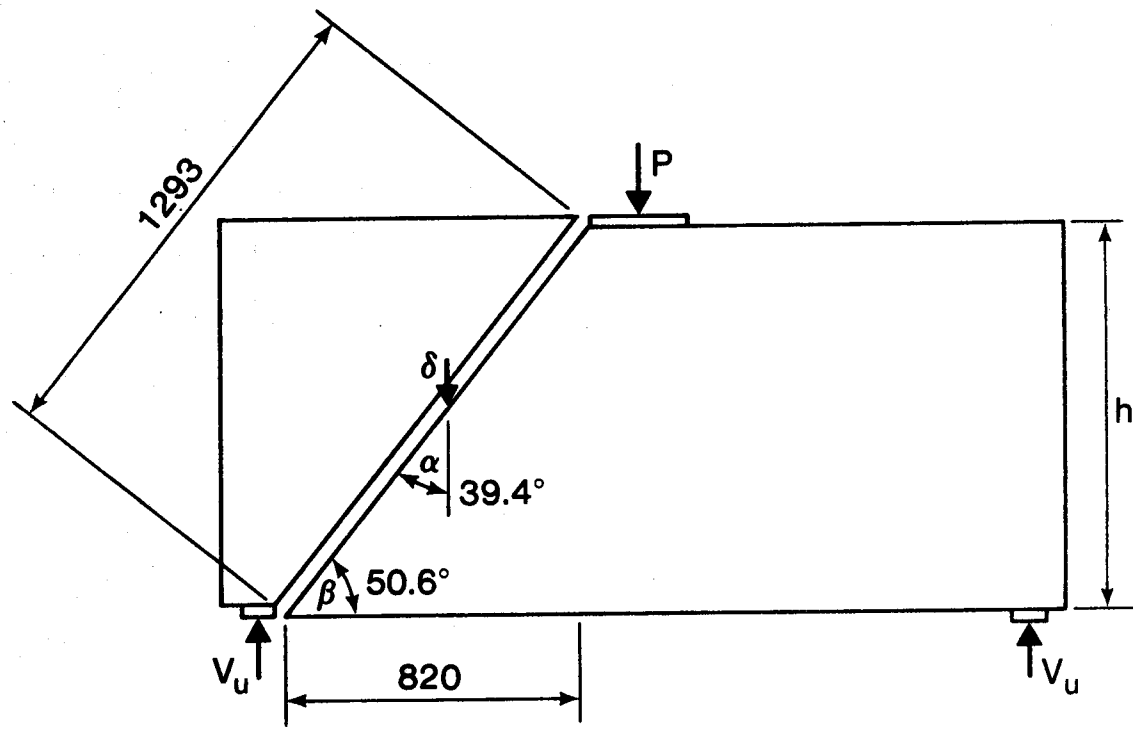

Figure A.6. Upper Bound Failure Mechanism

$$625 \text{ kN} < V < 1235 \text{ kN}$$

In this example, there is a significant difference between the upper and lower-bound solutions. The problem in this instance is that the upper-bound solution is not very good. It has been assumed that the crack opens vertically, that is $\alpha = 39.4°$. Other angles are possible, the angles which give the least upper-bound is the correct angle. For a virtual displacement δ acting at a general angle α to crack inclined at an angle β the internal virtual work is:

$$W_I = \left[\frac{1}{2} f_c^*(1 - \sin\alpha) \frac{bh}{\sin\beta} - A_s f_y \cos(\alpha + \beta)\right] \delta \quad (A.5)$$

The external virtual work is:

$$W_E = V_u \sin(\alpha + \beta)\, \delta \quad (A.6)$$

This gives:

$$V_U = \frac{\frac{(1 - \sin\alpha)}{2} \frac{bh}{\sin\beta} f_c^* - A_s f_y \cos(\alpha + \beta)}{\sin(\alpha + \beta)} \quad (A.7)$$

For $\beta = 50.6°$, V_U has a minimum value = 631.6 kN when $\alpha = 74.1°$. Now it can be said that:

$$V_L < V < V_U$$

$$625 < V < 632 \text{ kN}$$

The problem has been bounded to within 1%. Other failure mechanisms need not be considered as this is accurate enough. The problem specifications make it similar to test specimen 1/1.0 which had failure strengths of 602 and 699 kN in the two shear spans. The angle of crack displacement near failure corresponded to $\alpha = 70°$.

APPENDIX B

Design Example

Transfer Girder

Design a 36 ft long transfer girder which is continuous at one end to support the loads shown in Fig. B.1. For simplicity in this example only one load case is considered. Normally one would also investigate the effects of support settlement. Use f'_c = 5000 psi and f_y = 60000 psi.

Try a design truss with a width of 2 ft and an effective depth of 10.5 ft. The overall beam depth will be approximately to scale in Fig. B.2. Factored or effective material strengths are f^*_c = 2850 psi and f^*_y = 51000 psi. Use a model performance factor ϕ_m = 1.0.

Left Shear Span

At the left end of the beam, a direct compression strut carries a significant portion of the point load directly to the support. The uniformly distributed load to the left of the point load is carried directly to the exterior support by a fan of minor compression struts. The plastic truss analysis for this shear span is presented in Table B.1. The uniformly distributed load of $8.05^{k/l}$ has been modeled as 8.05^k point loads at 1 ft centres, hence the vertical force component in each of the minor struts is 8.05^k. The horizontal force component is calculated from the vertical component and measured strut slope. The vertical component

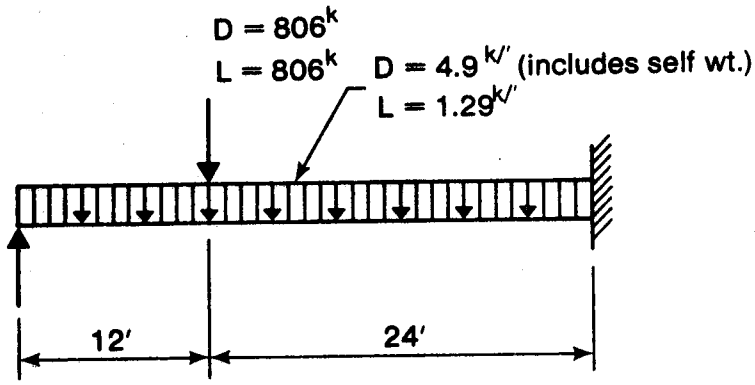

a) Service Loads

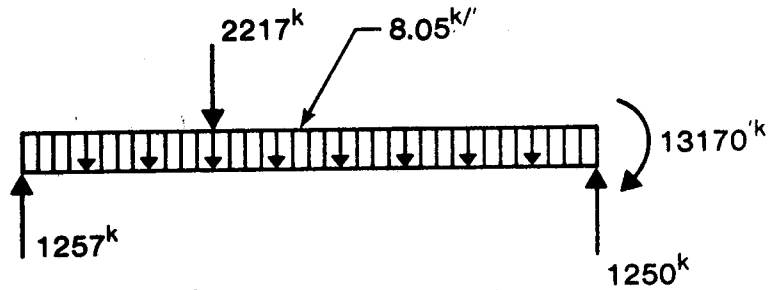

b) Ultimate Loads and Reactions

Fig. B 1. Transfer Girder Loads

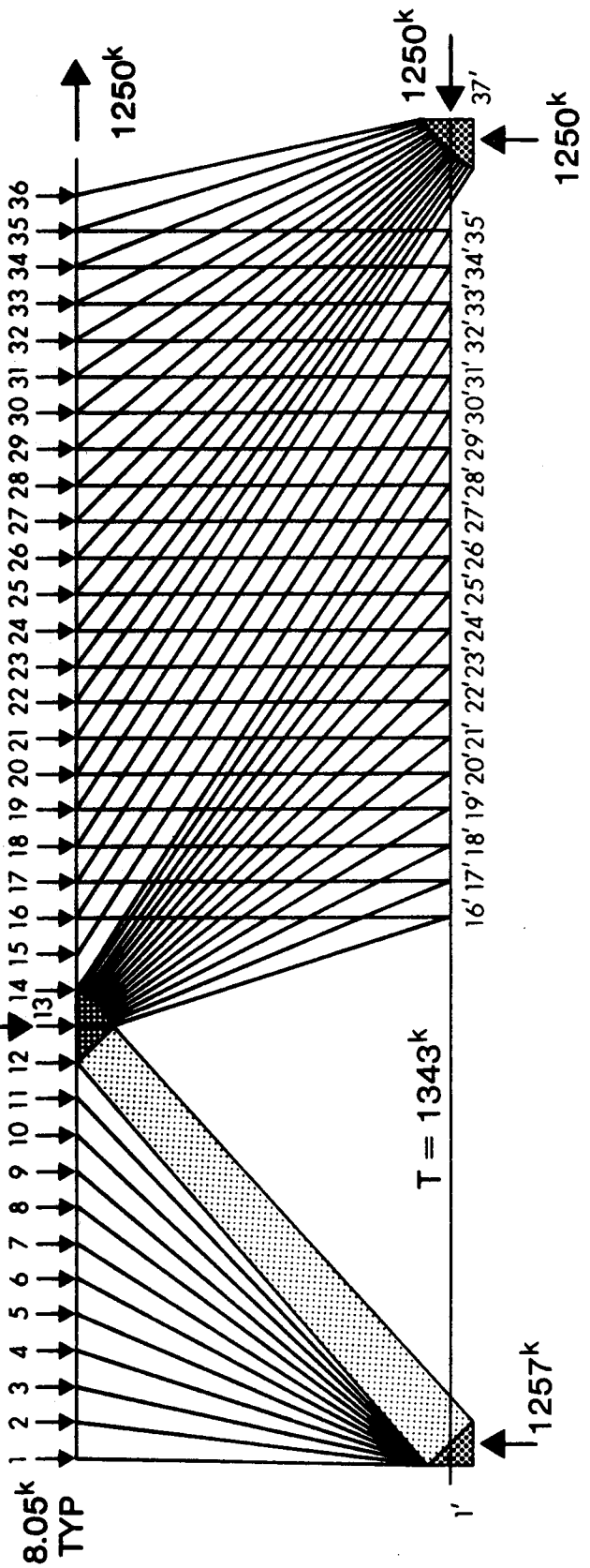

Fig. B 2. Design Truss

Table B.1 Analysis of Left Shear Span

Strut No.	Slope θ (Degrees)	Force Components	
		V^k	H^k
1-1'	88	8.05	0.3
2-1'	83	8.05	1.0
3-1'	78	8.05	1.7
4-1'	72	8.05	2.6
5-1'	67	8.05	3.4
6-1'	63	8.05	3.4
7-1'	58	8.05	5.0
8-1'	55	8.05	5.6
9-1'	51	8.05	6.5
10-1'	48	8.05	7.2
11-1'	45	8.05	8.0
12-1'	42	8.05	8.9
13-1'	42	1160	1289
	Summations	1257	1343

of the major direct compression strut (strut number 13-1') is chosen so that the desired support reaction of 1257^k is obtained. The total tension force required in the bottom chord is 1343^k. Tension reinforcement consisting of 28 #9 bars stressed at f_y^* will be adequate. The #9 bars were chosen instead of larger bars to reduce the anchorage problems. It is essential that all 28 #9 bars which extend into the left support be anchored to develop their full strength. The dimensions for the compression struts should be checked. The major direct compression strut carries a total force of 1735^k. The required cross sectional area is 1735/2.850 = 608 sq in. and the required dimensions are 24 in. x 25.4 in. This confirms that the member was drawn approximately to scale in Fig. B.2.

While web reinforcement is not required for strength, some reinforcement should be provided for serviceability. ACI minimum requirements (Sections 11.8.8 and 11.8.9) are satisfied with #4 @ 11" o/c vertical each face and #5 @ 10" o/c horizontal each face.

Right Shear Span

At the right end of the beam, a major direct compression strut is not appropriate. It would have a slope of about 25° which is too flat. The design truss shown in Fig. B.2 utilizes a fan of minor struts from the point load. The vertical force is (due to the assumption of plasticity) distributed equally to 15 stirrups. For simplicity, the stirrups have been assumed at 1 ft

centres. Each stirrup carries a load of 71.5^k. Some conservatism is introduced into the truss model in that stirrups near the point load are neglected and the fan is not permitted to get flatter than 33°. For simplicity, the stirrups have been assumed at 1 ft centres. The final design may utilize other stirrup spacings with an equivalent capacity per lineal ft of beam. A similar fan of minor compression struts occurs at the interior support. The stirrup forces in this fan are slightly larger than in the stirrups near midspan due to the uniformly distributed load. The stirrup force required per for of span is 71.5 + 8.05 = 79.5^k. This is satisfied by #7 @ 9" o/c vertical each face, which for simplicity will be used throughout this shear span. The vertical bars must be lap spliced with U bars at the top and bottom of the beam to form closed stirrups. The truss analysis of the right shear span is given in Table B.2. The variation in chord forces has been calculated. The bottom chord force of 1343^k under the point load is obtained from the analysis of the left shear span. The top chord force of 1250^k at the support is obtained by dividing the support moment by the effective truss depth. The variation in chord forces has been plotted in Fig. B.3(a) and (c). These diagrams were used to determine cutoff points. The reinforcement should extend a development length beyond these points. The final beam design is shown in Fig. B.3(b).

Table B.2 Analysis of Right Shear Span

Strut No.	Slope θ (Degrees)	Force Components		Chord Force Remaining	
		V^k	H^k	Bottom Chord^k	Top Chord^k
				1343	
14-16'	72	71.5	23	1320	
14-17'	62	71.5	29	1291	
14-18'	64	71.5	35	1256	
14-19'	60	71.5	41	1215	
14-20'	56	71.5	48	1166	
14-21'	52	71.5	56	1111	
14-22'	49	71.5	62	1048	
14-23'	46	71.5	69	979	
14-24'	44	71.5	74	905	
14-25'	41	71.5	82	823	
14-26'	39	71.5	88	735	
14-27'	37	71.5	95	640	
14-28'	36	71.5	98	541	
14-29'	34	71.5	106	435	
14-30'	33	71.5	110	325	
15-31'	33	8.05	12	313	
16-32'	33	79.5	123	190	
17-33'	33	79.5	123	68	
18-34'	33	79.5	123	-55	
19-35'	33	79.5	123	-177	
36-37'	76	8.05	2		1250
35-37'	71	87.6	30		1248
34-37'	66	87.6	39		1179
33-37'	62	87.6	47		1132
32-37'	58	87.6	55		1077
31-37'	55	16.1	11		1066
30-37'	53	79.5	60		1006
29-37'	49	79.5	69		937
28-37'	47	79.5	74		863
27-37'	44	79.5	82		780
26-37'	42	79.5	88		692
25-37'	41	79.5	92		601
24-37'	39	79.5	98		502
23-37'	37	79.5	106		397
22-37'	36	79.5	110		287
21-37'	34	79.5	118		169
20-37'	33	79.5	123		47
19-35'	33	79.5	123		-76
18-34'	33	79.5	123		-198
17-33'	33	79.5	123		-321
16-32'	33	79.5	123		-444

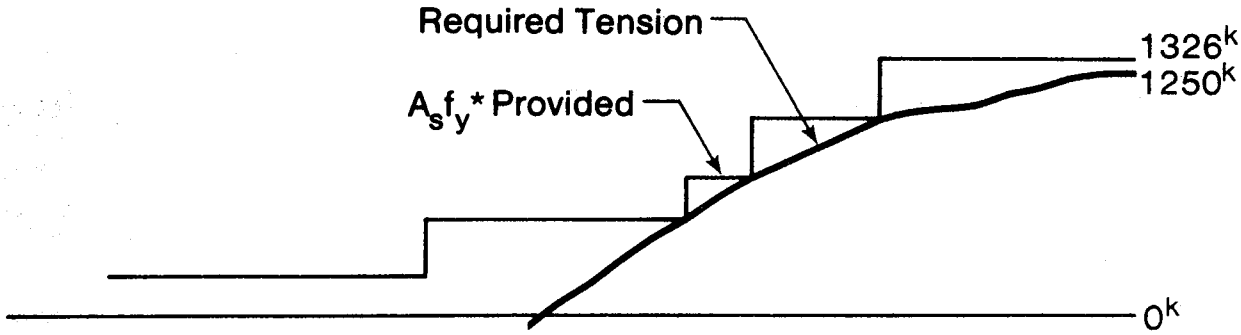

a) Top Chord Tension Force

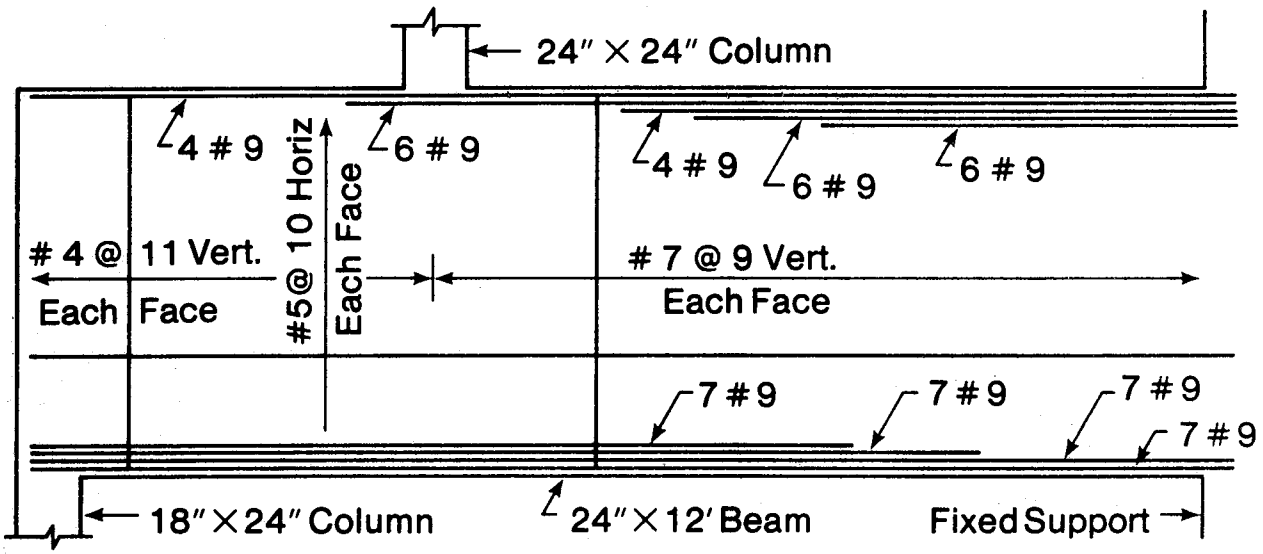

b) Elevation

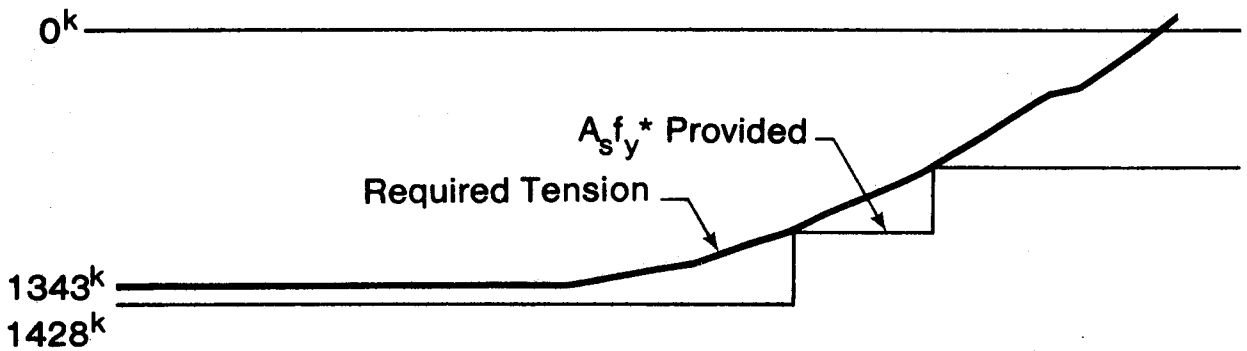

c) Bottom Chord Tension Force

Fig B 3. Design of a Deep Beam

Comparison with Other Methods

This example has been contrived to be directly comparable to that given by MacGregor and Hawkins (1977). The service loads are equivalent (for service live load = service dead load), and the dimensions are identical. The flexural reinforcement is the same in both designs with minor variations in cutoff points. The web reinforcement is somewhat different. In the left shear span, the proposed design and ACI 318 both use minimum web reinforcement. The design of MacGregor and Hawkins which was based on the proposed code revisions of ACI-ASCE Committee 426 (1977) requires significantly more web reinforcement, #7 @ 12" o/c vertical and horizontal each face. In the right shear span, the vertical web reinforcement is the same in the proposed design and the design done by MacGregor and Hawkins. ACI 318 would require considerably less vertical web reinforcement (#5 @ 15" o/c E.F. vs. #7 @ 9" o/c E.F.). The (minimum) horizontal web reinforcement used (0.25%) in this example is 2/3 more (0.25% vs 0.15%) than used by MacGregor and Hawkins but less than suggested by Franz and Breen (1980) (0.25% vs 0.53%).

The plastic truss design model provides a consistent model for flexure and shear design. In this example, it produced a design for the exterior shear span similar to that which would be obtained using ACI 318. For the interior shear span the plastic truss required more than three times as much vertical web reinforcement as ACI 318.

The flexural reinforcement required was the same for the plastic truss model and ACI 318. However, the truss model provides detailed information on the cut-off points.

94. *Plastic Design of Reinforced Concrete Slabs* by D.M. Rogowsky and S.H. Simmonds, November 1980.

95. *Local Buckling of W Shapes Used as Columns, Beams, and Beam-Columns* by J.L. Dawe and G.L. Kulak, March 1981.

96. *Dynamic Response of Bridge Piers to Ice Forces* by E.W. Gordon and C.J. Montgomery, May 1981.

97. *Full-Scale Test of a Composite Truss* by R. Bjorhovde, June 1981.

98. *Design Methods for Steel Box-Girder Support Diaphragms* by R.J. Ramsay and R. Bjorhovde, July 1981.

99. *Behavior of Restrained Masonry Beams* by R. Lee, J. Longworth and J. Warwaruk, October 1981.

100. *Stiffened Plate Analysis by the Hybrid Stress Finite Element Method* by M.M. Hrabok and T.M. Hrudey, October 1981.

101. *Hybslab - A Finite Element Program for Stiffened Plate Analysis* by M.M. Hrabok and T.M. Hrudey, November 1981.

102. *Fatigue Strength of Trusses Made From Rectangular Hollow Sections* by R.B. Ogle and G.L. Kulak, November 1981.

103. *Local Buckling of Thin-Walled Tubular Steel Members* by M.J. Stephens, G.L. Kulak and C.J. Montgomery, February 1982.

104. *Test Methods for Evaluating Mechanical Properties of Waferboard: A Preliminary Study* by M. MacIntosh and J. Longworth, May 1982.

105. *Fatique Strength of Two Steel Details* by K.A. Baker and G.L. Kulak, October 1982.

106. *Designing Floor Systems for Dynamic Response* by C.M. Matthews, C.J. Montgomery and D.W. Murray, October 1982.

107. *Analysis of Steel Plate Shear Walls* by L. Jane Thorburn, G.L. Kulak, and C.J. Montgomery, May 1983.

108. *Analysis of Shells of Revolution* by N. Hernandez and S.H. Simmonds, August 1983.

109. *Tests of Reinforced Concrete Deep Beams* by D.M. Rogowsky, J.G. MacGregor and S.Y. Ong, September 1983.

110. *Shear Strength of Deep Reinforced Concrete Continuous Beams* by D.M. Rogowsky and J.G. MacGregor, September 1983.